

TECHNICAL REPORT STANDARD PAGE

1. Report No. FHWA/LA.09/440		2. Government Accession No.	3. Recipient's Catalog No.
4. Title and Subtitle Field Verification for the Effectiveness of Continuity Diaphragms for Skewed Continuous P/C P/S Concrete Girder Bridges		5. Report Date October 2009	
		6. Performing Organization Code	
7. Author(s) Aziz Saber Ph.D., P.E.		8. Performing Organization Report No.	
9. Performing Organization Name and Address Civil Engineering Program Louisiana Tech University Ruston, LA 71272		10. Work Unit No.	
		11. Contract or Grant No. LTRC Project No. 06-3ST State Project No. 736-99-1373	
12. Sponsoring Agency Name and Address Louisiana Department of Transportation and Development P.O. Box 94245 Baton Rouge, LA 70804-9245		13. Type of Report and Period Covered Final Report April 2006-March 2008	
		14. Sponsoring Agency Code	
15. Supplementary Notes Conducted in Cooperation with the U.S. Department of Transportation, Federal Highway Administration			
16. Abstract <p>The research presented herein describes the field verification for the effectiveness of continuity diaphragms for skewed continuous precast, prestressed, concrete girder bridges. The objectives of this research are (1) to perform field load testing on the Burlington Northern Santa Fe (BNSF) overpass and compare measured strains with those determined through the theoretical analyses and (2) to study the effects of continuity diaphragms on stresses and deflections from truck loading on bridge deck slab and bridge girders.</p> <p>The current design concept of continuity diaphragms was examined to determine the effectiveness of the diaphragms in skewed bridges. The bridge parameters that were considered include skew angle, length of the span, beam spacing, the ratio of beam spacing to span (aspect ratio), and the ratio of girder stiffness to that of the slab. A prestressed concrete bridge with continuity diaphragms and a skewed angle of 48° was selected by a team of engineers from the Louisiana Department of Transportation and Development (LADOTD), the Louisiana Transportation Research Center (LTRC), the Federal Highway Agency (FHWA).</p> <p>The BNSF Overpass Bridge is located on US-90 in Jennings, Louisiana. The field verification was performed using a comprehensive instrumentation plan and live load tests as described in this report. The field and theoretical results from this study provided a fundamental understanding of the load transfer mechanism through these diaphragms of skewed, continuous span bridges. The findings in this study on stresses, strains, and deflections in the bridge deck and girders indicated that the effects of the continuity diaphragms on skewed continuous span precast prestressed concrete girder bridges were negligible. The results presented in this report also confirmed the theoretical findings published in LTRC Report 383 titled "Continuity Diaphragm for Skewed Continuous Span Precast Prestressed Concrete Girder Bridges." Continuity diaphragms used in prestressed concrete girder bridges on skewed bents provided additional redundancy in the bridge but caused difficulties in detailing and construction. As the skew angle increases or the girder spacing decreases, the construction becomes more difficult and the effectiveness of the diaphragms becomes questionable. It is also recommended that the use of continuity diaphragms be evaluated based on the need for the enhanced structural redundancy, the reduced expansion joint installation and maintenance costs, and the associated construction difficulties and costs. The outcome of this research will reduce the construction and maintenance costs of bridges throughout Louisiana and the United States.</p>			
17. Key Words Continuity diaphragm, skew angle, continuous span, precast, prestressed, concrete, girders, decks, bridges, flexural stresses, strains, load distribution, axial loads, truck loads, deflection, FEM analysis, LFRD, AASHTO		17. Distribution Statement Unrestricted. This document is available through the National Technical Information Service, Springfield, VA 21161.	
19. Security Classif. (of this report) N/A	20. Security Classif. (of this page) N/A	21. No. of Pages 167	22. Price N/A

Project Review Committee

Each research project will have an advisory committee appointed by the LTRC Director. The Project Review Committee is responsible for assisting the LTRC Administrator or Manager in the development of acceptable research problem statements, requests for proposals, review of research proposals, oversight of approved research projects, and implementation of findings.

LTRC appreciates the dedication of the following Project Review Committee Members in guiding this research study to fruition.

LTRC Manager

Walid R. Alaywan

Senior Structures Research Engineer

Members

Gill Gautreau

Jenan Nakhlé

Casey Allen

Mike Boudreaux

Arturo Aguirre

Directorate Implementation Sponsor

William Temple

Field Verification for the Effectiveness of Continuity Diaphragms for Skewed Continuous P/C P/S Concrete Girder Bridges

by

Aziz Saber, Ph.D., P.E.
Ajay K Mothukuri (Graduate Student)
Prashant Arasangi (Graduate Student)

Civil Engineering Program
Louisiana Tech University
Ruston, LA 71272

LTRC Project No. 06-3ST
State Project No. 736-99-1373

conducted for

Louisiana Department of Transportation and Development
Louisiana Transportation Research Center

The contents of this report reflect the views of the author/principal investigator who is responsible for the facts and the accuracy of the data presented herein. The contents do not necessarily reflect the views or policies of the Louisiana Department of Transportation and Development or the Louisiana Transportation Research Center. This report does not constitute a standard, specification, or regulation.

October 2009

ABSTRACT

The research presented herein describes the field verification for the effectiveness of continuity diaphragms for skewed continuous precast, prestressed, concrete girder bridges. The objectives of this research are (1) to perform field load testing on the Burlington Northern Santa Fe (BNSF) overpass and compare measured strains with those determined through the theoretical analyses and (2) to study the effects of continuity diaphragms on stresses and deflections from truck loading on bridge deck slab and bridge girders.

The current design concept of continuity diaphragms was examined to determine the effectiveness of the diaphragms in skewed bridges. The bridge parameters that were considered include skew angle, length of the span, beam spacing, the ratio of beam spacing to span (aspect ratio), and the ratio of girder stiffness to that of the slab. A prestressed concrete bridge with continuity diaphragms and a skewed angle of 48° was selected by a team of engineers from the Louisiana Department of Transportation and Development (LADOTD), the Louisiana Transportation Research Center (LTRC), the Federal Highway Agency (FHWA).

The BNSF Overpass Bridge is located on US-90 in Jennings, Louisiana. The field verification was performed using a comprehensive instrumentation plan and live load tests as described in this report. The field and theoretical results from this study provided a fundamental understanding of the load transfer mechanism through these diaphragms of skewed, continuous span bridges. The findings in this study on stresses, strains, and deflections in the bridge deck and girders indicated that the effects of the continuity diaphragms on skewed continuous span precast prestressed concrete girder bridges were negligible. The results presented in this report also confirmed the theoretical findings published in LTRC Report 383 titled "Continuity Diaphragm for Skewed Continuous Span Precast Prestressed Concrete Girder Bridges." Continuity diaphragms used in prestressed concrete girder bridges on skewed bents provided additional redundancy in the bridge but caused difficulties in detailing and construction. As the skew angle increases or the girder spacing decreases, the construction becomes more difficult and the effectiveness of the diaphragms becomes questionable. It is also recommended that the use of continuity diaphragms be evaluated based on the need for the enhanced structural redundancy, the reduced expansion joint installation and maintenance costs, and the associated construction difficulties and costs. The outcome of this research will reduce the construction and maintenance costs of bridges throughout Louisiana and the United States.

ACKNOWLEDGMENTS

The research project described herein was sponsored by LTRC and LADOTD under research project number 06-3ST and state project number 736-99-1373.

The researchers want to express their gratitude to the Project Review Committee, many of whom provided direct assistance to the project team as they developed information needed to complete the study. During the course of this research project, the research team at Louisiana Tech University received valuable and much appreciated support and guidance from the LTRC staff and engineers, especially Walid Alaywan.

This study could not have been completed without the assistance of personnel from LADOTD. Personnel from district administration, construction engineering, maintenance, materials, and traffic all contributed to the successful completion of the project. Specifically, Ricky Manuel, Ronnie Belflower, and Wayne Trahan; their efforts are greatly appreciated.

The support provided by the College of Engineering and Science at Louisiana Tech University is much appreciated. Also, the assistance of James Ellingburg and Lance Speer is appreciated.

The assistance and support of the staff and employees at Bridge Diagnosis Inc. is much appreciated.

IMPLEMENTATION STATEMENT

High skew bridges are built every year in the state of Louisiana. The results of this study will be submitted to LADOTD Bridge Design Section for implementation and could be extended to other states.

The use of continuity diaphragms should be evaluated based on the need for the enhanced structural redundancy, the reduced expansion joint installation and maintenance costs and the associated construction difficulties and costs.

While the report was being prepared, the LADOTD constructed a bridge in Natchitoches parish where the continuity diaphragms were eliminated. Instead, girders will have free ends. The deck will be continuous over the girders. A small notch is made at the top and the bottom of the deck at in the region of the girders' ends. An additional stainless steel bar is placed in the top and bottom of the slab at that location.

The detail will be monitored for a couple of years to assess its performance.

TABLE OF CONTENTS

ABSTRACT.....	iii
ACKNOWLEDGMENTS	v
IMPLEMENTATION STATEMENT	vii
TABLE OF CONTENTS.....	ix
LIST OF TABLES	xiii
LIST OF FIGURES	xv
INTRODUCTION	1
Description of Diaphragms	1
OBJECTIVE	5
SCOPE	7
METHODOLOGY	9
Introduction.....	9
Geometry and Location of the Bridge	9
Field Testing and Instrumentation Procedures	10
Field Testing Procedures.....	14
Attaching Strain Transducers.....	15
Assembly of the System.....	16
Performing the Load Test	17
Analysis Overview	18
Method of Approach	19
Girder Element Type IPSL	19
Plate Element Type SBCR.....	20
Prismatic Space Truss Members.....	21
Bridge Properties	21
Aspect Ratio.....	22
Boundary Condition.....	22
AASHTO Loading	22
Influence Line Analysis	23
Locations of the Truck.....	23
DISCUSSION OF RESULTS.....	25
General Discussion	25

Model Verification.....	26
Live Load Tests on the BNSF Overpass.....	26
Live Load Test 1	26
Live Load Test 2.....	28
Live Load Test 3.....	30
Live Load Test 4.....	32
Live Load Test 5.....	34
Live Load Test 6.....	36
Conclusions from the Field Tests	38
Analysis Using HS 20-44 Truck Load.....	38
Stresses in Girders - Positive Moment.....	39
Stresses in Girders - Negative Moment	43
Deflection in Girders - Positive Moment.....	46
Deflection in Girders - Negative Moment	47
Bridge Deck Stresses	48
CONCLUSIONS.....	51
General Summary	51
RECOMMENDATIONS.....	53
ACRONYMS, ABBREVIATIONS, AND SYMBOLS	55
REFERENCES	57
APPENDIX A.....	59
Instrumentation Plans for Maximum Positive Moment in Girders (Case I).....	59
APPENDIX B.....	63
Instrumentation Plans for Maximum Negative Moment in Girders (Case II)	63
APPENDIX C.....	67
Comparison of Strains of Field Measurements vs. FE Predicted Data.....	67
APPENDIX D.....	73
GT STRUDL Input Files for Case I and Case II	73
Case I Truck location for Maximum Positive Moment in the Girder.....	73
Case II Truck Location for Maximum Negative Moment in the Girder.....	84
APPENDIX E.....	95
GT STRUDL Input Files for Case III and Case IV	95

Case III Maximum Positive Moment in Girders without Continuity Diaphragms	95
Case IV Maximum Negative Moment in Girders without Continuity Diaphragms	104
APPENDIX F.....	113
BNSF Overpass Field Testing Pictures.....	113

LIST OF TABLES

Table 1 Description of the structure.....	10
Table 2 List of tests on BNSF overpass.....	11
Table 3 Detail properties of Type-IPSL tridimensional element.....	20
Table 4 Details properties of Type SBCR plate element.....	21
Table 5 AASHTO LRFD bridge design loading condition factors	23
Table 6 Case studies.....	39
Table 7 Comparison of deck stresses of Case I and Case III.....	48
Table 8 Comparison of deck stresses of Case II and Case IV	49
Table 9 Comparisons of strains of field data to the FEM models (GT STRUDL) test 2	67
Table 10 Comparisons of strains of field data to the FEM models (GT STRUDL) test 3	68
Table 11 Comparisons of strains of field data to the FEM models (GT STRUDL) test 4	69
Table 12 Comparisons of strains of field data to the FEM models (GT STRUDL) test 5	70
Table 13 Comparisons of strains of field data to the FEM models (GT STRUDL) test 6	71
Table 14 Maximum stresses in deck top surface of Case I.....	73
Table 15 Maximum stresses in deck bottom surface of Case I.....	73
Table 16 Maximum stresses in deck top surface of Case II	84
Table 17 Maximum stresses in deck bottom surface of Case II	84

LIST OF FIGURES

Figure 1	Girders are simply supported at stage one of construction.....	2
Figure 2	Casting of deck slab and diaphragm for continuity stage two of construction	2
Figure 3	Bridge skew angle	3
Figure 4	Diaphragm skew angle	3
Figure 5	View of BNSF overpass	10
Figure 6	Test truck axle load configuration.....	11
Figure 7	Test truck of GVW 48.66 kips used at site.....	12
Figure 8	Instrumentation on the bridge.....	13
Figure 9	Superstructure accessed by JLG lift	14
Figure 10	JLG lift.....	14
Figure 11	Marking on girder for placing of transducers.....	15
Figure 12	Fixing of transducers	16
Figure 13	Transducers removed from the tabs	16
Figure 14	STS unit connecting transducers	17
Figure 15	Cross section of the bridge with 8-ft. girder spacing.....	18
Figure 16	Typical plate and girder elements.....	19
Figure 17	Truck HS 20-44 axle load configuration	22
Figure 18	Comparison of strains in Girder 1 of test 1	27
Figure 19	Comparison of strains in Girder 2 of test 1	27
Figure 20	Comparison of strains in continuity diaphragm at support Spans 7-8 of test 1.....	28
Figure 21	Comparison of strains in Girder 1 of test 2	29
Figure 22	Comparison of strains of Girder 2 of test 2	29
Figure 23	Comparison of strains in continuity diaphragm of support Spans 7-8 of test 2	30
Figure 24	Comparison of strains of Girder 1 of test 3	31
Figure 25	Comparison of strains of Girder 2 of test 3	31
Figure 26	Comparison of strains in continuity diaphragm of support Spans 7-8 of test 3	32
Figure 27	Comparison of strains in Girder 1 of test 4	33
Figure 28	Comparison of strains in Girder 2 of test 4	33
Figure 29	Comparison of strains in continuity diaphragm in support Spans 7-8 of test 4	34
Figure 30	Comparison of strains in Girder 1 of test 5	35
Figure 31	Comparison of strains in Girder 2 of test 5	35

Figure 32	Comparison of strains in continuity diaphragm in support Spans 7-8 of test 5	36
Figure 33	Comparison of strains in Girder 1 of test 6	37
Figure 34	Comparison of strains in Girder 2 of test 6	37
Figure 35	Comparison of strains in continuity diaphragm in support Spans 7-8 of test 6	38
Figure 36	Comparison of stresses of Case I and Case III for top elements in Girder 1	39
Figure 37	Enlarged view of stresses of top girder elements of Girder 1	40
Figure 38	Comparison of stresses of Case I and Case III for bottom elements in Girder 1 ..	40
Figure 39	Enlarged view of stresses of bottom girder elements of Girder 1	41
Figure 40	Comparison of stresses of Case I and Case III for top elements in Girder 2	41
Figure 41	Enlarged view of stresses of top girder elements of Girder 2	42
Figure 42	Comparison of stresses of Case I and Case III for bottom elements in Girder 2 ..	42
Figure 43	Enlarged view of stresses of bottom girder elements of girder	43
Figure 44	Comparison of stresses of Case II and Case IV for top elements in Girder 1	43
Figure 45	Enlarged view of stresses of top girder elements of Girder 1	44
Figure 46	Comparison of stresses of Case II and Case IV for bottom elements in Girder 1 ..	44
Figure 47	Comparison of stresses of Case II and Case IV for top elements in Girder 2	45
Figure 48	Comparison of stresses of Case II and Case IV for bottom elements in Girder 2 ..	45
Figure 49	Comparison of deflections for Case I and Case III of Girder 1	46
Figure 50	Comparison of deflections of Case I and Case III of Girder 2	46
Figure 51	Comparison of deflections for Case II and Case IV of Girder 1	47
Figure 52	Comparison of deflections for Case II and Case IV of Girder 2	47
Figure 53	Truck location for maximum positive moment in girder	59
Figure 54	Instrumentation plan for Case I	59
Figure 55	Cross section at section A of Case I	60
Figure 56	Cross section at section B of Case I	60
Figure 57	Cross section at section C of Case I	61
Figure 58	Cross section at section D of Case I	61
Figure 59	Truck location for maximum negative moment in girder	63
Figure 60	Instrumentation plan for Case II	63
Figure 61	Cross section at section A of Case II	64
Figure 62	Cross section at section B of Case II	64
Figure 63	Cross section at section C of Case II	65
Figure 64	Cross section at section D of Case II	65

Figure 65	Bending stress distribution of top elements in Girder 1 of Case I.....	74
Figure 66	Bending stress distribution of bottom elements in Girder 1 of Case I	74
Figure 67	Bending stress distribution of top elements in Girder 2 of Case I.....	75
Figure 68	Bending stress distribution of bottom elements in Girder 2 of Case I	75
Figure 69	Bending stress distribution of top elements in Girder 3 of Case I.....	76
Figure 70	Bending stress distribution of bottom elements in Girder 3 of Case I	76
Figure 71	Bending stress distribution of top elements in Girder 4 of Case I.....	77
Figure 72	Bending stress distribution of bottom elements in Girder 4 of Case I	77
Figure 73	Bending stress distribution of top elements in Girder 5 of Case I.....	78
Figure 74	Bending stress distribution of bottom elements in Girder 5 of Case I	78
Figure 75	Bending stress distribution of top elements in Girder 6 of Case I.....	79
Figure 76	Bending stress distribution of bottom elements in Girder 6 of Case I	79
Figure 77	Bending stress distribution of bottom elements in Girder 6 of Case I	80
Figure 78	Axial force distribution in continuity diaphragm at support Span8-9 for Case I..	80
Figure 79	Maximum deflection in Girder 1 of Case I	81
Figure 80	Maximum deflection in Girder 2 of Case I	81
Figure 81	Maximum deflection in Girder 3 of Case I	82
Figure 82	Maximum deflection in Girder 4 of Case I	82
Figure 83	Maximum deflection in Girder 5 of Case I	83
Figure 84	Maximum deflection in Girder 6 of Case I	83
Figure 85	Bending stress distribution of top elements in Girder 1 of Case II.....	85
Figure 86	Bending stress distribution of bottom elements in Girder 1 of Case II.....	85
Figure 87	Bending stress distribution of top elements in Girder 2 of Case II.....	86
Figure 88	Bending stress distribution of bottom elements in Girder 2 of Case II.....	86
Figure 89	Bending stress distribution of top elements in Girder 3 of Case II.....	87
Figure 90	Bending stress distribution of bottom elements in Girder 3 of Case II.....	87
Figure 91	Bending stress distribution of top elements in Girder 4 of Case II.....	88
Figure 92	Bending stress distribution of bottom elements in Girder 4 of Case II.....	88
Figure 93	Bending stress distribution of top elements in Girder 5 of Case II.....	89
Figure 94	Bending stress distribution of bottom elements in Girder 5 of Case II.....	89
Figure 95	Bending stress distribution of top elements in Girder 6 of Case II.....	90
Figure 96	Bending stress distribution of bottom elements in Girder 6 of Case II.....	90
Figure 97	Axial force distribution in continuity diaphragm at support Span7-8 for Case II.	91

Figure 98 Axial force distribution in continuity diaphragm at support Span8-9 for Case II.	91
Figure 99 Maximum deflection in Girder 1 of Case II	92
Figure 100 Maximum deflection in Girder 2 of Case II	92
Figure 101 Maximum deflection in Girder 3 of Case II	93
Figure 102 Maximum deflection in Girder 4 of Case II	93
Figure 103 Maximum deflection in Girder 5 of Case II	94
Figure 104 Maximum deflection in Girder 6 of Case II	94
Figure 105 Bending stress distribution of top elements in Girder 1 of Case III.....	95
Figure 106 Bending stress distribution of bottom elements in Girder 1 of Case III.....	95
Figure 107 Bending stress distribution of top elements in Girder 2 of Case III.....	96
Figure 108 Bending stress distribution of bottom elements in Girder 2 of Case III.....	96
Figure 109 Bending stress distribution of top elements in Girder 3 of Case III.....	97
Figure 110 Bending stress distribution of bottom elements in Girder 3 of Case III.....	97
Figure 111 Bending stress distribution of top elements in Girder 4 of Case III.....	98
Figure 112 Bending stress distribution of bottom elements in Girder 4 of Case III.....	98
Figure 113 Bending stress distribution of top elements in Girder 5 of Case III.....	99
Figure 114 Bending stress distribution of bottom elements in Girder 5 of Case III.....	99
Figure 115 Bending stress distribution of top elements in Girder 6 of Case III.....	100
Figure 116 Bending stress distribution of bottom elements in Girder 6 of Case III.....	100
Figure 117 Maximum deflection in Girder 1 of Case III.....	101
Figure 118 Maximum deflection in Girder 2 of Case III.....	101
Figure 119 Maximum deflection in Girder 3 of Case III.....	102
Figure 120 Maximum deflection in Girder 4 of Case III.....	102
Figure 121 Maximum deflection in Girder 5 of Case III.....	103
Figure 122 Maximum deflection in Girder 6 of Case III.....	103
Figure 123 Bending stress distribution of top elements in Girder 1 of Case IV.....	104
Figure 124 Bending stress distribution of bottom elements in Girder 1 of Case IV	104
Figure 125 Bending stress distribution of top elements in Girder 2 of Case IV.....	105
Figure 126 Bending stress distribution of bottom elements in Girder 2 of Case IV	105
Figure 127 Bending stress distribution of top elements in Girder 3 of Case IV.....	106
Figure 128 Bending stress distribution of bottom elements in Girder 3 of Case IV	106
Figure 129 Bending stress distribution of top elements in Girder 4 of Case IV.....	107
Figure 130 Bending stress distribution of bottom elements in Girder 4 of Case IV	107

Figure 131	Bending stress distribution of top elements in Girder 5 of Case IV	108
Figure 132	Bending stress distribution of bottom elements in Girder 5 of Case IV	108
Figure 133	Bending stress distribution of top elements in Girder 6 of Case IV	109
Figure 134	Bending stress distribution of bottom elements in Girder 6 of Case IV	109
Figure 135	Maximum deflection in Girder 1 of Case IV.....	110
Figure 136	Maximum deflection in Girder 2 of Case IV.....	110
Figure 137	Maximum deflection in Girder 3 of Case IV.....	111
Figure 138	Maximum deflection in Girder 4 of Case IV.....	111
Figure 139	Maximum deflection in Girder 5 of Case IV.....	112
Figure 140	Maximum deflection in Girder 6 of Case IV.....	112
Figure 141	Gauge located at the bottom of the Girder 1	113
Figure 142	Tabs on the Girder 1 after removing the transducer.....	113
Figure 143	Initial marking on the girder for placing transducer.....	114
Figure 144	Gauge located at the top flange of the girder	114
Figure 145	Tabs on the Girder 1 after removing the transducer.....	115
Figure 146	Initial marking on the girder for placing transducer.....	115
Figure 147	Gauge located at the bottom of the Girder 1	116
Figure 148	Tabs on the Girder 1 after removing the transducer.....	116
Figure 149	Initial marking on the girder for placing transducer.....	117
Figure 150	Gauge located at the top flange of the Girder 1.....	117
Figure 151	Tabs on the Girder 1 after removing the transducer.....	118
Figure 152	Gauge located at the bottom of the Girder 1	118
Figure 153	Tabs on the Girder 1 after removing the transducer.....	119
Figure 154	Initial marking on the girder for placing transducer.....	119
Figure 155	Gauge located at the bottom of the Girder 2	120
Figure 156	Gauge located at the top flange of the Girder 2.....	120
Figure 157	Tabs on the Girder 2 after removing the transducer.....	121
Figure 158	Gauge located at the bottom of the Girder 2	121
Figure 159	Tabs on the Girder 2 after removing the transducer.....	122
Figure 160	Initial marking on the girder for placing transducer.....	122
Figure 161	Tabs on the Girder 2 after removing the transducer.....	123
Figure 162	Gauge located at the top flange of the Girder 2.....	123
Figure 163	Gauge located at the bottom of the Girder 2	124

Figure 164	Tabs on the Girder 2 after removing the transducer.....	124
Figure 165	Initial marking on the girder for placing transducer.....	125
Figure 166	Gauge located at the top flange of the Girder 3.....	125
Figure 167	Tabs on the Girder 3 after removing the transducer.....	126
Figure 168	Initial marking on the girder for placing transducer.....	126
Figure 169	Gauge located at the bottom of the Girder 3	127
Figure 170	Tabs on the Girder 3 after removing the transducer.....	127
Figure 171	Initial marking on the girder for placing transducer.....	128
Figure 172	Gauge located at the top flange of the Girder 4.....	128
Figure 173	Tabs on the Girder 4 after removing the transducer.....	129
Figure 174	Initial marking on the girder for placing transducer.....	129
Figure 175	Gauge located at the bottom of the Girder 4	130
Figure 176	Tabs on the Girder 4 after removing the transducer.....	130
Figure 177	Initial marking on the girder for placing transducer.....	131
Figure 178	Gauge located at the top flange of the Girder 1.....	131
Figure 179	Tabs on the Girder 4 after removing the transducer.....	132
Figure 180	Initial marking on the girder for placing transducer.....	132
Figure 181	Gauge located at the bottom of the Girder 5	133
Figure 182	Tabs on the Girder 5 after removing the transducer.....	133
Figure 183	Gauge located at the top flange of the Girder 6.....	134
Figure 184	Tabs on the Girder 6 after removing the transducer.....	134
Figure 185	Gauge located at the bottom of the Girder 6	135
Figure 186	Tabs on the Girder 6 after removing the transducer.....	135
Figure 187	Initial marking on the continuity diaphragm for placing transducer.....	136
Figure 188	Gauge located on the continuity diaphragm of support Span 7-8	136
Figure 189	Initial marking on the continuity diaphragm for placing transducer.....	137
Figure 190	Gauge located on the continuity diaphragm of support Span 7-8	137
Figure 191	Gauge located on the continuity diaphragm of support Span 7-8	138
Figure 192	Tabs on the continuity diaphragm after removing the transducer.....	138
Figure 193	Gauge located on the continuity diaphragm of support Span 7-8	139
Figure 194	Tabs on the continuity diaphragm after removing the transducer.....	139
Figure 195	Initial marking on the continuity diaphragm for placing transducer.....	140
Figure 196	Gauge located on the continuity diaphragm of support Span 7-8	140

Figure 197 Gauge located on the continuity diaphragm of support Span 7-8 141
Figure 198 Gauge located on the continuity diaphragm of support Span 7-8 141

INTRODUCTION

The majority of highway bridges are built as cast-in-place reinforced concrete slabs and prestressed concrete girders. The simple-span precast, prestressed, concrete girders made continuous through cast-in-place decks and diaphragms have been widely used in the United States since the 1960's. Composite action between the slabs and girders is assured by the shear connectors on the top of the girders. The design guidelines for bridges in the American Association of State Highway and Transportation Officials (AASHTO) Standard Design Specifications Section 8.12 indicate that diaphragms should be installed for T-girder spans and may be omitted where structural analysis shows adequate strength [1]. Similar discussions are presented in the Load Resistance Factor Design (LRFD) Bridge Design Code (AASHTO 2004). The advantages of continuity diaphragms are the reduced expansion joint installation and maintenance costs, the improved riding quality, and the enhanced structural redundancy. Furthermore, the effects of diaphragms are not accounted for in the proportioning of girders. Therefore, the use of diaphragms should be investigated.

In 2004, LTRC sponsored the theoretical investigation on the effects of continuity diaphragms for skewed continuous span precast, prestressed, concrete girder bridges. The results of the research were published in LTRC Final Report 383. The research team, Saber et al., reported that continuity diaphragms used in the prestressed girder bridges on skewed bents cause difficulties in detailing and construction. Details for small skewed bridges ($> 30^\circ$ from perpendicular) have not been a problem for LADOTD, but as the skew angle increases or the girder spacing decreases, the connection and the construction becomes more difficult. Also, results of the research indicated that the continuity diaphragms could be eliminated without any significant effects on the stresses or deflections in the bridge girders.

Description of Diaphragms

AASHTO Standard Specifications for Highway Bridges 2002, defines a diaphragm as a transverse stiffener that is placed between girders in order to maintain section geometry. A similar description of a diaphragm can be found in the LRFD. For many years, diaphragms have been thought to contribute to the overall distribution of the live loads in bridges. Depending on the type of bridge, the diaphragms may take different forms. Cast-in-place concrete diaphragms are the most common in prestressed, concrete I-girder bridge construction. Full depth diaphragms are terminated at the end of the sloping portion of the bottom flange. Generally, the diaphragm is integrated with the deck through continuous reinforcement and is tied to the I-girder through anchor bars [2].

Continuity diaphragms are used to achieve continuity over the supports. The continuity is achieved at the time of the construction phase. In stage one, the girders are placed as simply-supported as shown in Figure 1. In stage two, the bridge deck slab and diaphragms are cast in place to form the continuous girder as shown in Figure 2.

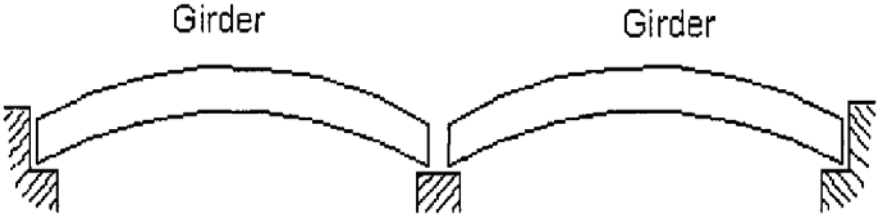


Figure 1
Girders are simply supported at stage one of construction

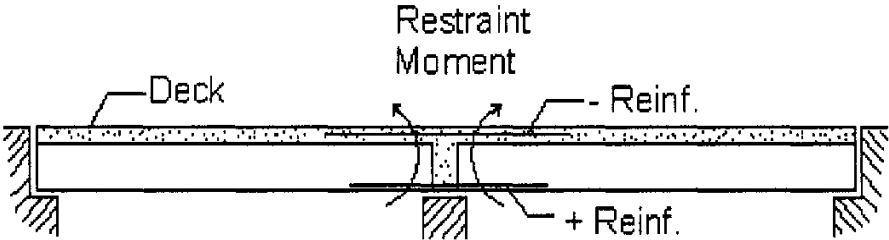


Figure 2
Casting of deck slab and diaphragm for continuity stage two of construction

The skew angle of the bridge is the angle between the centerline of a support and a line normal to the roadway centerline, shown as β in Figure 3. The skew angle of the diaphragm is the angle between the centerline of the diaphragm and the roadway centerline, shown as α in Figure 4.

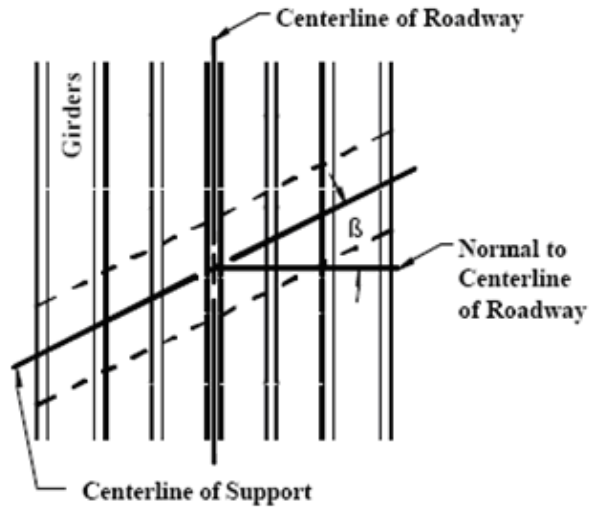


Figure 3
Bridge skew angle

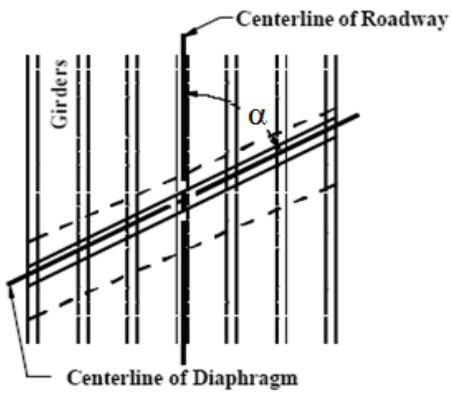


Figure 4
Diaphragm skew angle

OBJECTIVE

The objectives of this research were to:

- Perform field load testing on the BNSF overpass and compare measured strains with those determined through theoretical analyses.
- Determine the effects of continuity diaphragms in the load transfer mechanism in prestressed concrete skewed bridges.

SCOPE

The scope of the study was to:

- Perform a live load test that will verify the strains in the continuity diaphragms and bridge girders on the BNSF Overpass Bridge (structure number 07270030708821).
- Study the effects of continuity diaphragms on the stresses and deflections from truck loading on continuous slab and girder bridges.
- Make recommendations on the use of continuous diaphragms on highway bridges based on results of the analyses.

METHODOLOGY

Introduction

The purpose of this investigation is to conduct field verification for the findings of the analytical studies performed in LTRC Report 383. The methodology and details of the BNSF overpass, instrumentation plans, field testing procedures, and the analytical models in Georgia Tech Structural Design Language (GT STRUDL) are presented in this section.

Geometry and Location of the Bridge

The bridge used for the field testing is located on US 90 in Jefferson Davis Parish the BNSF overpass structure number is 07270030708821. The bridge consists of 15 spans; 12 spans have 5 prestressed concrete girders that are AASHTO Type II. The length of each girder is 50 ft. (15.4 m). The remaining three spans on the bridge (Span 7, 8, and 9) have six AASHTO Type III girders with two continuity diaphragms at the supports located at Span 7-8 and Span 8-9. Along the centerline of Spans 7 and 9, there is a span length of 56 ft. (17.2 m); Span 8 has a length of 79 ft. (24.3 m). The spacing between the girders is 8 ft. (2.5 m) center to center. Spans 7, 8, and 9 have four half-depth intermediate diaphragms. There is one half-depth intermediate diaphragm in Spans 7 and 9 and two in Span 8. A half- depth intermediate diaphragm indicates that the diaphragm starts at the bottom edge of the top flange and ends at the top edge of the bottom flange. The three spans also have end diaphragms located at the ends of the support at Span 6-7 and Span 8-9. The end diaphragms start at the top edge of the top flange and end at the sloping portion of the bottom flange. Spans 7, 8, and 9 were considered for this study because they include the continuity diaphragms. The details of the bridge are summarized and presented in Table 1. The bottom view of the bridge is shown in Figure 5.

Table 1
Description of the structure

Structure Identification	Structure 07270030708821
Location	US 90, Jennings, LA
Structure Type	PS/C T-beam bridge
Number of Spans	15
Span Lengths	Varying
Skew	48° at the center line of the bridge
Beams	6 – prestress AASHTO Type III beams at 8’ on center
Continuity Diaphragms	2 (one at support span 7-8 and another at support span 8-9)
Deck	RC Deck 8” Possibly additional 2” of concrete overlay but none specified in plans.
Curbs and Parapets	Cast in place R/C Parapets on outside of exterior beams.
Spans included in study	Spans 7, 8, and 9



Figure 5
View of BNSF overpass

Field Testing and Instrumentation Procedures

Field tests were done on the BNSF overpass to verify the finite element models in GT STRUDL. Six live load tests were performed using a test truck with a gross vehicle weight (GVW) of 48.66 kips. The purpose of each test is given in Table 2. Strains from all of the field tests are collected and compared to the finite element models developed using GT STRUDL. Axle weights and spacing of the test truck are shown in Figure 6. A picture of the test truck is shown in Figure 7.

Table 2
List of tests on BNSF overpass

Test	Description	Reference Point	Critical location Distance from south end of bridge	Direction
1	Strains collected for positive moment in the girders	X=0, Y=0, at south corner, exterior edge of the curb	X=5 ft 9 in, Y=97 ft.	West to East
2	Strains collected for positive moment in the girders	X=0, Y=0, at south corner, exterior edge of the curb	X=5 ft 9 in, Y=83 ft.	West to East
3	Strains collected for positive moment in the girders	X=0, Y=0, at south corner, exterior edge of the curb	X=5 ft 9 in, Y=85.5 ft.	West to East
4	Strains collected for negative moment in the girders	X=0, Y=0, at south corner, exterior edge of the curb	X=8 ft 9 in, Y=63 ft.	East to West
5	Strains collected for negative moment in the girders	X=0, Y=0, at south corner, exterior edge of the curb	X=8 ft 9 in, Y=77 ft.	East to West
6	Strains collected for negative moment in the girders	X=0, Y=0, at south corner, exterior edge of the curb	X=8 ft 9 in, Y=74.5 ft.	East to West

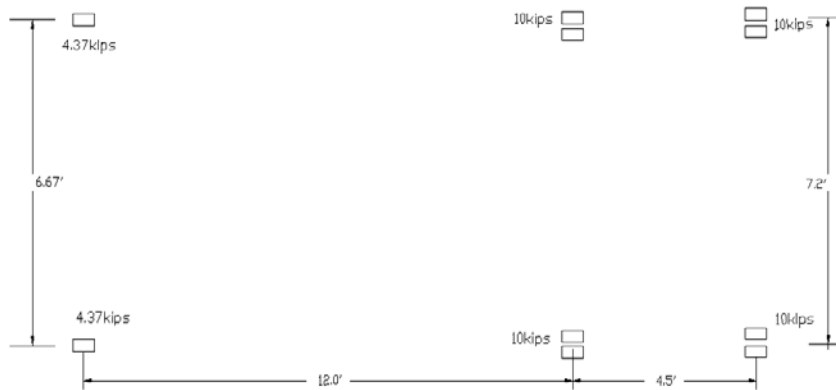


Figure 6
Test truck axle load configuration



Figure 7
Test truck of GVW 48.66 kips used at site

The superstructure of the bridge was instrumented with 25 reusable transducers. The location of the transducers can be seen in Figure 8. The transducers were placed at the critical locations in Spans 7 and Span 8. Several transducers were placed on Span 8 since it was the longest span in the bridge and would give the largest response to the applied loads. Girders 1 and 2 were instrumented with five gauges each. Girders 3, 4, 5, and 6 were instrumented with two gauges each. Continuity diaphragms were instrumented with seven gauges. For each beam, two gauges were placed at the same location; one at the top of the flange and one at the bottom of the girder. Gauges on the top flange were placed 3 inches below the deck, gauges on the bottom side of the girders were placed 4 inches from one end. For the continuity diaphragms five gauges were placed 6 inches below the deck, and two gauges were placed 6 inches above the bottom of the continuity diaphragm.

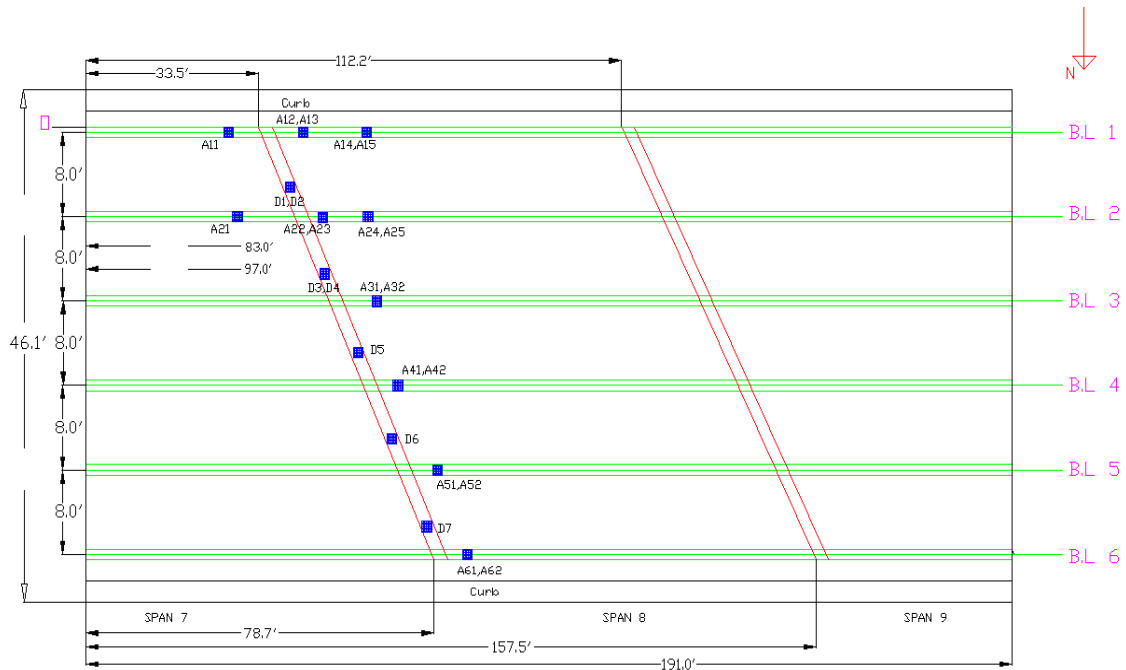


Figure 8
Instrumentation on the bridge

LADOTD provided the JLG lift shown in Figures 9 and 10. The load tests were performed by driving a 48.66-kip test truck across the bridge at a crawling speed of approximately 3 to 5 mph along two different lateral paths. The first path, passenger side wheels were 5 ft. 9 in. off from the south curb/railing, and the second path driver side wheels were 8 ft. 9 in. from the south curb/railing. For each lateral path, there are three different longitudinal positions on which the truck traveled. The lateral and the longitudinal paths of the test truck are explained in Table 2. The distance X and Y, shown in the table, are measured from the back tire of the test truck.



Figure 9
Superstructure accessed by JLG lift



Figure 10
JLG lift

Field Testing Procedures

The following list of procedures has been followed during the field test on the BNSF overpass. The instrumentation plan was developed for the structure, the strain transducers were attached, and the testing equipment was prepared for test [4].

Attaching Strain Transducers

The tab attachment method is used for attaching strain transducers to structural members.

1. Place two tabs in the mounting piece. Place the transducer over the mounts and then tighten the nuts until they are snug. This procedure allows the tabs to mount without putting stress on the transducer.
2. Mark the centerline of the transducer location on the structure. Place marks 1.5 inches on either side of the centerline. Using a hand grinder, remove paint or scale from these areas as shown in Figure 11. If attaching to concrete, lightly grind the surface to remove any scale. If the paint is thick, use a chisel to remove most of it before grinding.
3. Very lightly grind the bottom of the transducer tabs to remove any oxidation or other contaminants.
4. Apply a thin line of adhesive to the bottom of each transducer tab.
5. Spray each tab and the contact area on the structural member with the adhesive accelerator.
6. Mount the transducer in its proper location and apply a light force to the tabs (not the center of the transducer) for approximately 10 seconds as shown in Figure 12.

After the test was completed, the nuts were carefully loosened from the tabs and the transducers were removed as shown in Figure 13.



Figure 11
Marking on girder for placing of transducers



Figure 12
Fixing of transducers

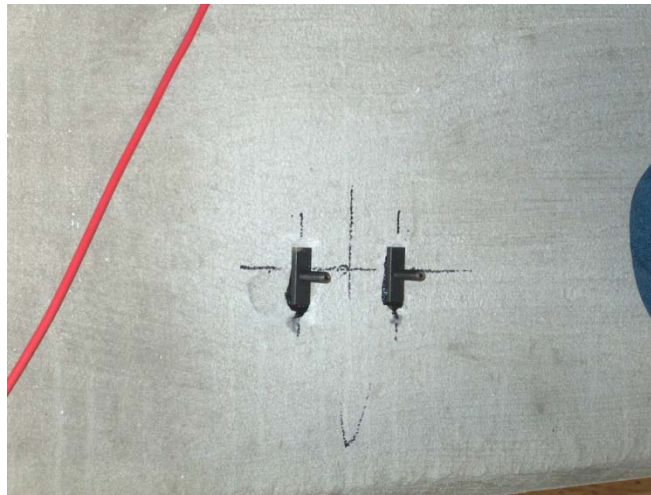


Figure 13
Transducers removed from the tabs

Assembly of the System

Once the transducers were mounted, they were connected to a structural testing system (STS) unit. These units are placed near the transducer locations in such a manner to allow four transducers to be plugged in as shown in Figure 14. Each STS unit could be clamped to the bridge girders. Since the transducers identified themselves to the system, there was no need to follow a special order. The only information that was recorded was the transducer serial number and its location on the structure. Once all STS units were connected in a series, one cable was connected to the power supply located near the computer. The 9-pin serial cable was connected between the computer and the power supply. The system was then ready to acquire data.



Figure 14
STS unit connecting transducers

Performing the Load Test

The general testing sequence is as follows:

1. Transducers are mounted and the system is connected and turned on.
2. The deck is marked out for each truck pass. Locations of the truck to travel on these three spans are predetermined. A total of six tests are carried out on these given paths. The paths of the truck were determined in such a way that when the truck travels it gives the maximum possible strains in the gauges that are fixed on the bridge. Next, a chalk mark is made on the deck locating the longitudinal path and transverse location of the driver's side front wheel. The truck is aligned on this mark for all subsequent tests in this lane.
3. The driver is instructed that the test vehicle must be kept in the proper location on the bridge. Another important item is that the vehicles maintain a relatively constant rate of speed during the entire test.
4. Wheelbase and axle width dimensions are measured with a tape and recorded.
5. The program is started and the number of channels indicated is verified. If the number of channels indicated does not match the actual number of channels, a malfunction has occurred and must be corrected before testing commences.
6. The transducers are initialized (zeroed out) with the balance option. If a transducer cannot be initialized, it should be inspected to ensure that it has not been damaged.
7. The desired test length, sample rate, and output file name are selected. A test length of 4 minutes and a sample rate of 50 Hz were selected when testing.

8. When all parties are ready to commence the test, the run test option is selected which places the system in an activated state. An effort should be made to get the truck across with no other traffic on the bridge.
9. When the test has been completed and the system is still recording data, hit “S” to stop collecting data and finish writing the recorded data to disk.
10. A total of six live load tests were done to have proper understanding of the behavior of the continuity diaphragms and its interaction with the girders.

Analysis Overview

The finite element models used in this investigation simulate the behavior of the BNSF overpass. This section describes the various finite element models and analysis done in GT STRUDL [9]. Six finite element models of the BNSF overpass were simulated and analyzed for a live load of a 48.66-kip test truck. The strains from the finite element models were compared to the strain results from the field. Two more finite element models were simulated and analyzed for the HS 20-44 truck. One model was the standard BNSF (with continuity diaphragms) overpass and the other model was the BNSF overpass without continuity diaphragms. The results such as stresses, strains, deflections in girders, and stresses in the deck are compared to see the effects of continuity diaphragms. The finite element models in GT STRUDL have a cross section shown in Figure 15 and the typical plate and girder arrangement is shown in Figure 16.

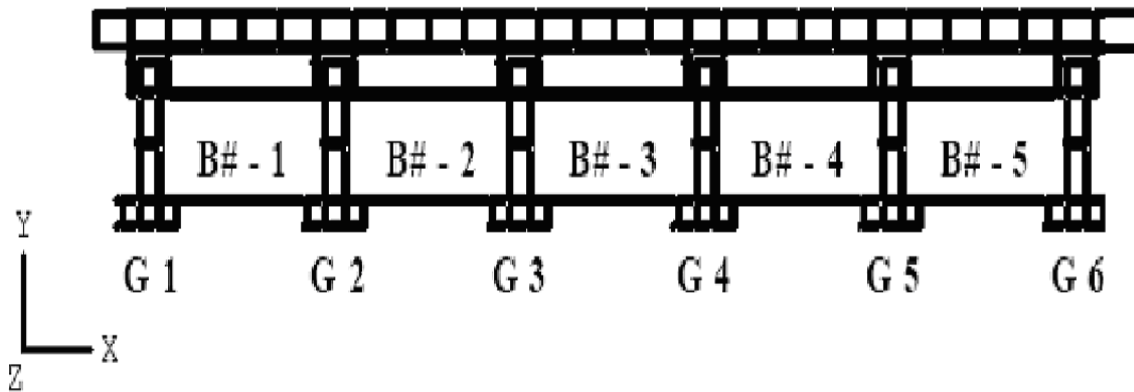


Figure 15
Cross section of the bridge with 8-ft. girder spacing

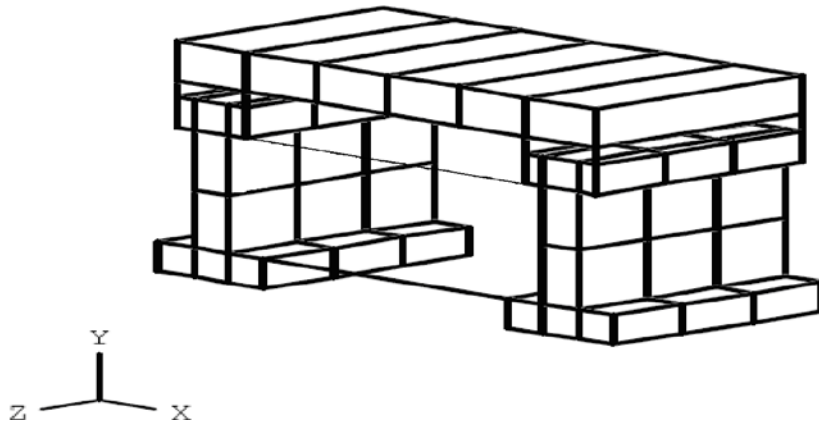


Figure 16
Typical plate and girder elements

Method of Approach

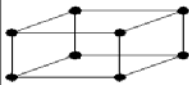
Finite element modeling is one of the most popular and common methods used in analyzing complicated structures. The advancement of software technology in construction made the analysis of difficult models much easier. Finite element models of the bridge are developed in GT STRUDL, which simulates the nature of the skewed continuous span bridge. Girders are modeled using Type Iso Parametric Solid Linear (IPSL) Tridimensional element. Type SBCR plate elements are used for bridge decks. Prismatic Space Truss members are used to model the continuity diaphragms, the connection between the deck plate elements, and the girder elements.

Girder Element Type IPSL

GT STRUDL explains the properties of Type Tridimensional Finite elements in the user guide. These types of finite elements are used to model the behavior of the three dimensional solid bodies. It is a solid 8 node element with three translational degrees of freedom in the global X, Y, and Z directions at each node. Only force type loads may be applied to these tridimensional elements.

The Type IPSL is capable of carrying both joint loads and element loads. Joint loads may define concentration loads, while element loads may define edge loads, surface loads, or body loads. GT STRUDL is capable of listing the output for stress, strain, and element forces for Type IPSL Tridimensional elements at each node. Average stress, average strain, average principal stress, average principal strain, and average von misses at each node can also be calculated. The details of the Type IPSL element are shown in Table 3.

Table 3
Detail properties of Type-IPSL tridimensional element

Element		Output									
Name	Shape	List					Calculate Average				
	Resultants	Stress	Strain	Principal Stresses	Principal Strain	Element Forces	Stresses	Strain	Principal Stresses	Principal Strain	von Mises
IPSL		N	N			N	X	X	X	X	X

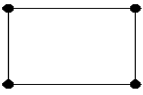
N - Output Element Nodes

Plate Element Type SBCR

GT STRUDL explains the properties of Type plate elements in the user guide. Type plate finite elements are generally used in models that involve both stretching and bending behavior. It is a two dimensional flat plate element most commonly used in modeling of the thin walled and curved structures. The Type Plate finite elements are considered as a superposition of Type Plane stress and Type plate bending finite elements. For flat plate structures, the stretching and bending behavior is uncoupled, but for the structures where the elements do not lie in the same plane, the stretching and bending behavior is coupled.

Type SBCR plate finite element is a four node element capable of carrying both joint loads and element loads. The joint loads may define concentrated loads, while the element loads may define surface loads or body loads. GT STRUDL is capable of listing the output for in plane stresses at the centroid and moment resultants, the shear resultant, and element forces at each node for Type SBCR plate elements. The average stresses, average principal stresses, average resultants, average principal membrane, principal bending, and average Von misses at each node may also be calculated. The details of the Type SBCR plate element are shown in Table 4.

Table 4
Details properties of Type SBCR plate element

Element		Output									
Name	Shape	List				Calculate Average					
		Stress/Moment	Shear Resultants	Strain/Curvature	Element Forces	Stresses	Principal Stresses	Resultants	Principal Membrane Resultants	Principal Bending Resultants	von Mises
SBCR		*	N		N	X	X	X	X	X	X

N - Output Element Nodes

* - In Plane-Stress at Centroid, Moments Resultants at Nodes

Prismatic Space Truss Members

GT STRUDL explains the properties of space truss members in the user guide. Generally space truss members are used when a member experiences only axial force. Space truss members cannot take force loads or moment loads; only axial loads and the self weight of members are generated as joint loads.

Prismatic member properties are defined directly; the section properties are constant over the entire length of the member. GT STRUDL also assumes the section properties' values according to the material specified.

Bridge Properties

To simulate the field conditions of the bridge in finite element models of GT STRUDL, some assumptions were made to minimize analyzing errors. The following assumptions are made in finite element models of GT STRUDL:

- The slab has uniform thickness over the entire width and length of the bridge.
- All girders are identical and parallel to each other.
- Full composite action is assumed between the girder and slab.

Aspect Ratio

It is the ratio of the longest dimension in the element to the shortest dimension of the same element. Aspect ratios close to 1 indicate that the mesh size is small or fine, and aspect ratios close to 4 indicate that the mesh size is large or coarse. Aspect ratios closer to 1 give more fine results than aspect ratios that are closer to 4.

$$\text{Aspect Ratio} = \frac{\text{Longest Dimension in the element}}{\text{Shortest Dimension in the element}} \leq 4$$

In the finite element models of the BNSF overpass, the minimum aspect ratio for the elements was 1.09 and the maximum was 2.14.

Boundary Condition

The restraints for the model is considered as four joints across the width at the base of the girder, at the end and intermediate supports, and two joints at the connection between the plate element to the rigid member at the end supports as pins.

AASHTO Loading

A uniform dead load of 150 pcf (24 kN/m³) was applied to all elements and members to account for the self-weight of the concrete. The truck loading on the bridge was according to Chapter 3 of the AASHTO Bridge Design Specifications; an HS20-44 truck was used with the bridge model. The truck loading includes two 32-kip (142-kN) axles spaced 14 ft. (4 m) and one 8-kip (35-kN) axle spaced 14 ft. (4 m) from the first 32-kip (142-kN) axle as shown in Figure 17. A uniform surface load of 0.58 psi (4 kPa) was also placed on the deck to account for future overlays. In addition to these loads, a wind load of 0.35 psi (2.4 kPa) was placed according to the AASHTO Bridge Design Specifications. Wind load was applied perpendicular to the windward exterior girder. The loading condition used in the analyzing of the model is given by the *AASHTO LFRD Bridge Design Specifications* as shown in Table 5.

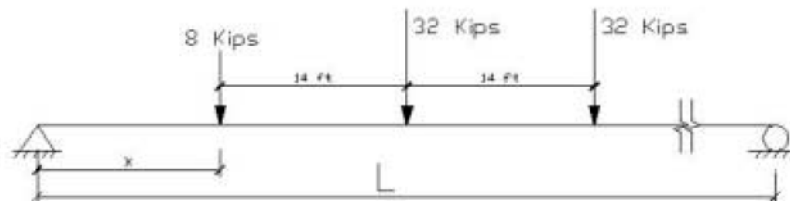


Figure 17
Truck HS 20-44 axle load configuration

Table 5
AASHTO LRFD bridge design loading condition factors

Sl. No	Loading	Dead Load	Vehicular Load (LL)	Live Load Surcharge (LS)	Wind Load (WS)
1	Strength I Min.	0.90	1.75	1.75	0.0
2	Strength I Max.	1.25	1.75	1.75	0.0
3	Strength II Min.	0.90	1.35	1.35	0.0
4	Strength II Max.	1.25	1.35	1.35	0.0
5	Strength III Min.	0.90	0.0	0.0	1.40
6	Strength III Max.	1.25	0.0	0.0	1.40
7	Strength V Min.	0.90	1.35	1.35	0.40
8	Strength V Max.	1.25	1.35	1.35	0.40
9	Service I	1.0	1.0	1.0	0.30
10	Service II	1.0	1.30	1.30	0.0
11	Fatigue	0.0	0.75	0.75	0.0

Influence Line Analysis

Axle loads provided in LRFD AASHTO chapter 3 are applied in the model. To get the maximum moment location, GT STRUDL is used to generate the influence lines to determine the position of the axle loads. Influence lines were computed along the length of the bridge and across the width of the bridge to determine the critical location of the truck on the bridge [14]. In this analysis, a unit load is placed at 1-ft. intervals over the length and width of the bridge; the obtained deflections are superpositioned to get the critical location of the truck. Hand calculations and computer generated models in GT STRUDL are used to determine the critical load locations. The truck loads were applied in both directions, from left to right and from right to left. In this way of analyzing, there are two critical locations where the truck can be placed; one location is for maximum positive moment and the other is for maximum negative moment. In this study, an HS20-44 truck and a GVW 48.6-kip test truck are used in the analysis [13].

Locations of the Truck

From the influence line analysis, the truck location is determined and placed on the finite element model to get maximum moments. Case I deals with truck location for the maximum positive moment in the girder, and Case II deals with truck location for the maximum negative moment in the girder. Case III is similar to Case I, except continuity diaphragms were not used. The same could be said about Case IV, which is similar to Case II, except for the use of the continuity diaphragms. The details for these cases are shown in Appendix A and B.

DISCUSSION OF RESULTS

General Discussion

The BNSF overpass was investigated through finite element models from GT STRUDL. Theoretical results and field data were compared to calibrate finite element models of the bridge and to determine the effects of the continuity diaphragms on skewed continuous bridges. Stresses, strains, deflections in girders and stresses in decks for the HS20-44 truck for FE models of the BNSF overpass with continuity diaphragms were compared to FE models of the BNSF overpass without continuity diaphragms.

Instrumentation plans were prepared for field tests. Details of truck locations and strain gauge positions for the maximum positive moment in the girder are shown in Appendix A. Also, details of the maximum negative moment in the girder are shown in Appendix B.

Six live load tests were completed on the bridge with a GVW 48.66-kip test truck. The strains obtained from the field were compared to those obtained from the finite element analysis using GT STRUDL. The comparisons of strains for all the six tests are shown in Appendix C.

The theoretical studies were based on HS20-44 truck loads. Case I deals with the maximum positive moment in the girders with continuity diaphragms, and Case II deals with the maximum negative moment in the girders with continuity diaphragms. The input files, output from GT STRUDL, the stress plots for the girders, and the deflection plots of the girders for both cases are presented in Appendix D. The same HS 20-44 truck is used in the analysis for Case III and Case IV. Case III deals with the maximum positive moment in the girders without continuity diaphragms, and Case IV deals with the maximum negative moment in the girders without continuity diaphragms. The input files, stress plots for the girders, and deflection plots for both cases are presented in Appendix E.

The same load and boundary conditions were used in the analysis for Cases I and III. Also, the results at the same locations were used in the comparison to get a better idea of the behavior of girders, decks, and diaphragms. The same procedures were used for Cases II and IV. Based on these comparisons, the effects of continuity diaphragms in continuous skewed bridges were determined.

Model Verification

Live Load Tests on the BNSF Overpass

A total of six live load tests were conducted on the bridge with a GVW 48.66-kip test truck. The first three field tests come under Case I, and the next three tests come under Case II. Each case dealt with different truck positions, and strain data was collected for each case. The data from the field was compared to the GT STRUDL FE models of the bridge. The gauge numbers and locations are shown in the bridge instrumentation plans presented in Appendix A. A complete comparison for all data is presented in Appendix C. The critical strain values obtained in Girder 1, Girder 2, and the continuity diaphragm at the support between Spans 7 and 8 are summarized in the following section.

The critical strains in girders and continuity diaphragms in the bridge from FEM models were compared with field data. The theoretical results are conservative because they are less than 10 percent higher than the collected ones. These differences can be caused by the approximation in the boundary conditions of the bridge and the changes in the material characteristics of concrete. Therefore, it is concluded that the FEM provides a good basis for further theoretical analyses using HS20-44 truck loads to determine the effectiveness of the continuity diaphragms.

Live Load Test 1

The test truck traveled west to east at 3 to 5 mph. When the test truck's back tire crossed the 97-ft. mark, the truck was stopped. Data was collected on the bridge from the point where the truck started moving to the point where the truck stopped. The 97 ft. were marked from a reference point, which is the south corner of the exterior curb. In the transverse direction, the distance of the truck from the south exterior curb was 5 ft. 9 in. Predicted and actual strains are within 10 percent as shown in Figures 18, 19, and 20. The gauge number and location are shown in the bridge instrumentation plans in Appendix A.

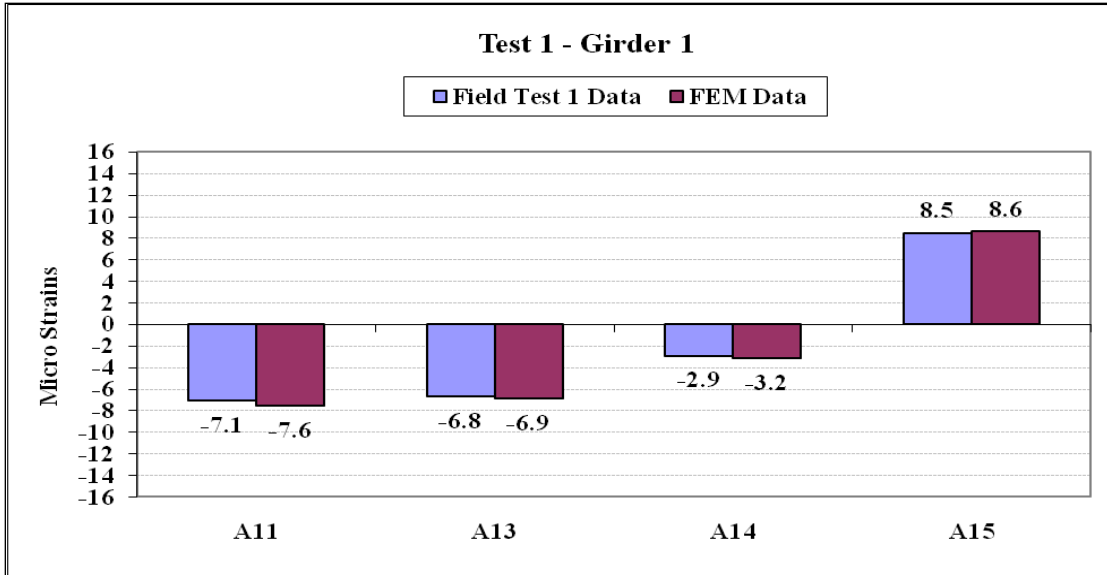


Figure 18
Comparison of strains in Girder 1 of test 1

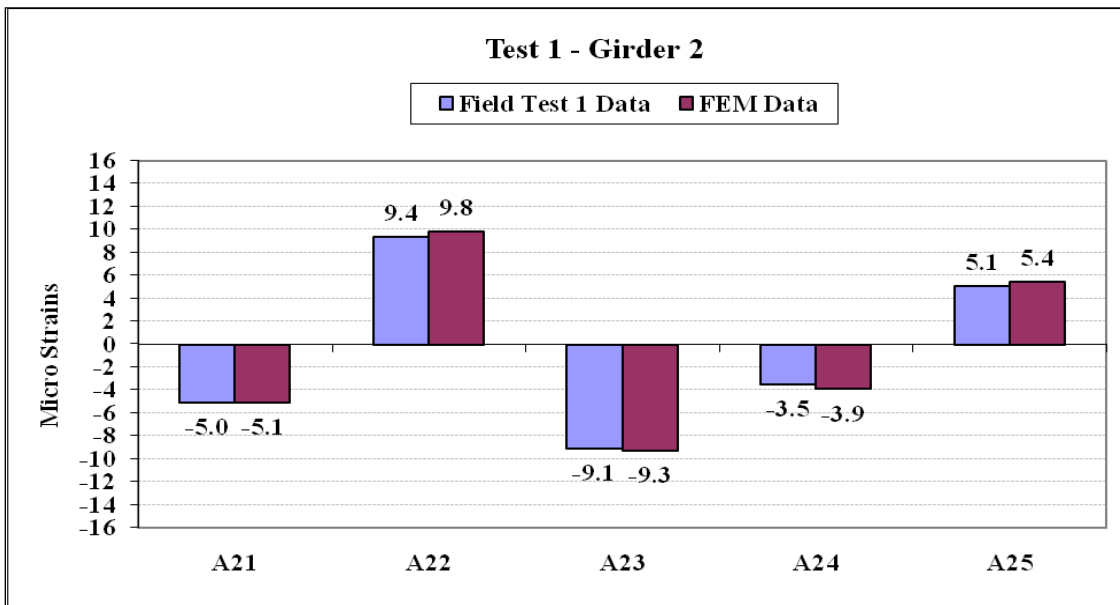


Figure 19
Comparison of strains in Girder 2 of test 1

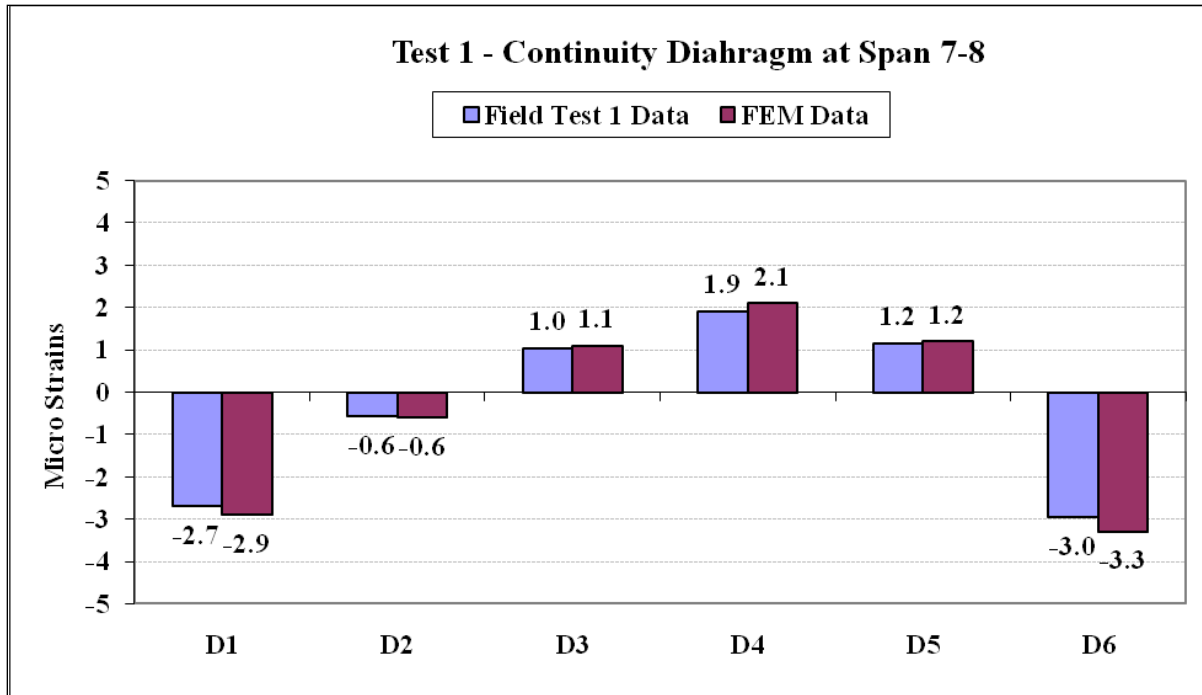


Figure 20
Comparison of strains in continuity diaphragm at support Spans 7-8 of test 1

Live Load Test 2

The test truck traveled west to east at 3 to 5 mph. When the test truck’s back tire crossed the 83-ft. mark, the truck was stopped and data was collected. The 83 ft. were marked from a reference point which is the south corner of the exterior curb. In the transverse direction, the truck was traveling 5 ft. 9 in. from the south exterior curb. Predicted and actual strains are within 10 percent as shown in Figures 21, 22, and 23. The gauge number and location are shown in the bridge instrumentation plans in Appendix A.

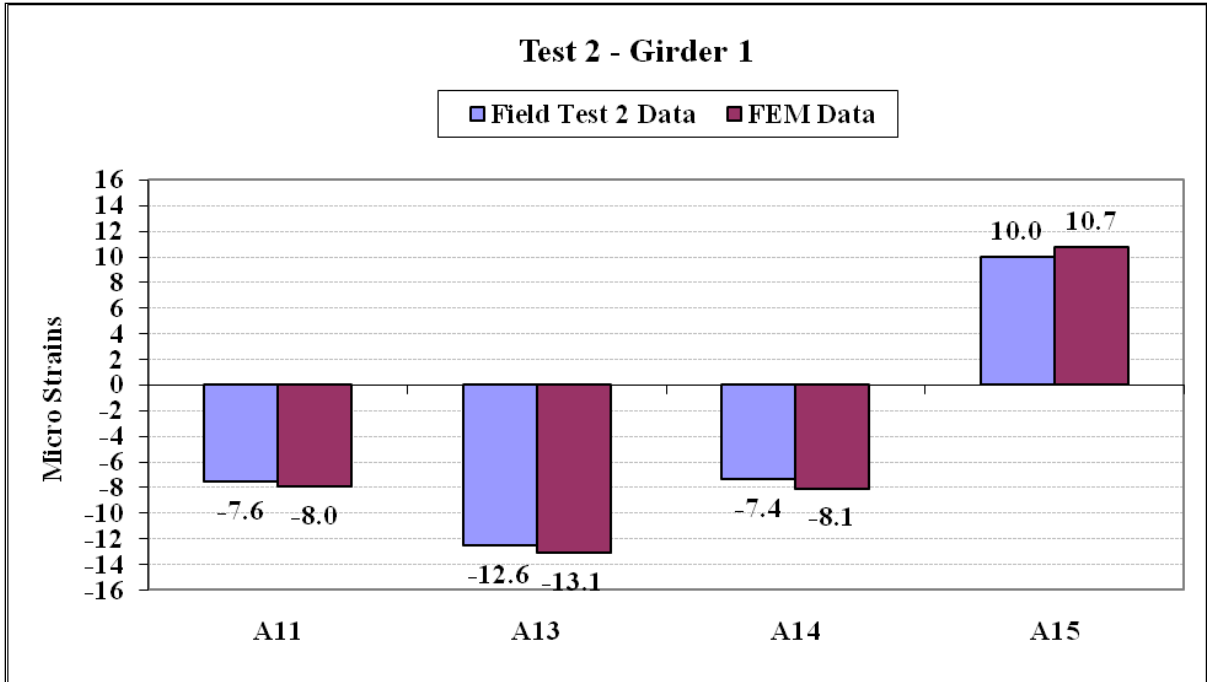


Figure 21
Comparison of strains in Girder 1 of test 2

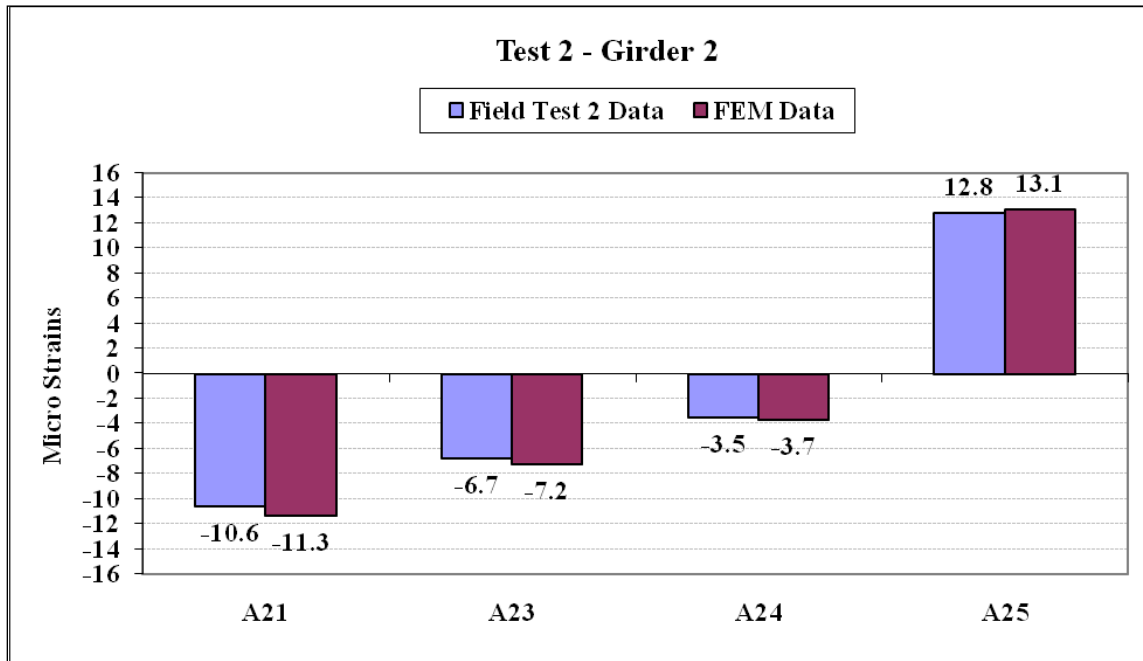


Figure 22
Comparison of strains of Girder 2 of test 2

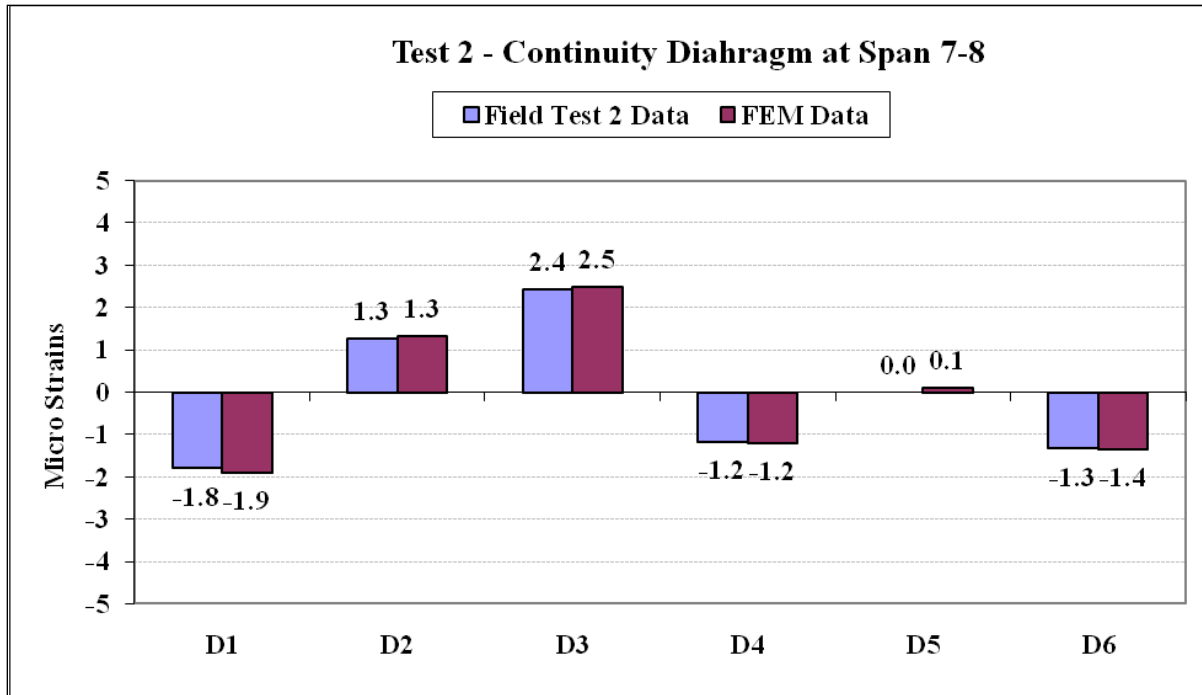


Figure 23
Comparison of strains in continuity diaphragm of support Spans 7-8 of test 2

Live Load Test 3

The test truck traveled west to east at 3 to 5mph. When the test truck’s front tire crossed the 69-ft. mark, the truck was stopped. Data was collected on the bridge from the point where the truck started moving to the point where the truck stopped. The 69 ft. were marked from a reference point which is the south corner of the exterior curb. In the transverse direction, the test truck was traveling at 5 ft. 9 in. from the south exterior curb. Predicted and actual strains are within 10 percent as shown in Figures 24, 25, and 26. The gauge number and location are shown in the bridge instrumentation plans in Appendix A.

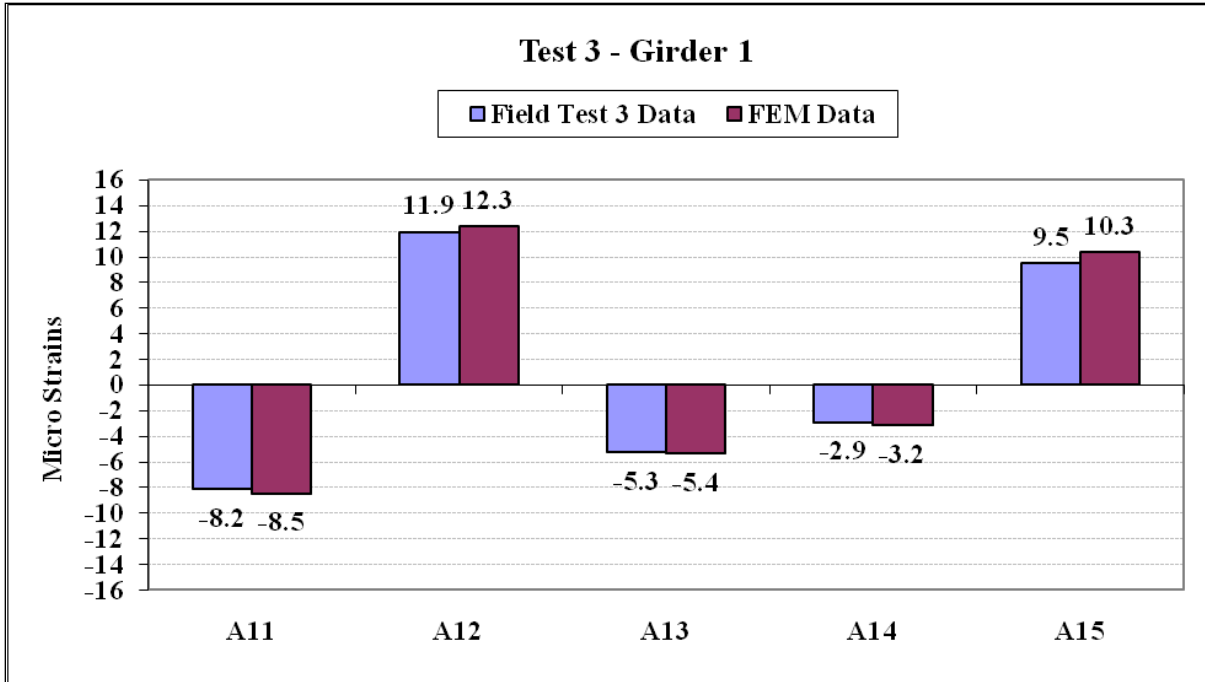


Figure 24
Comparison of strains of Girder 1 of test 3

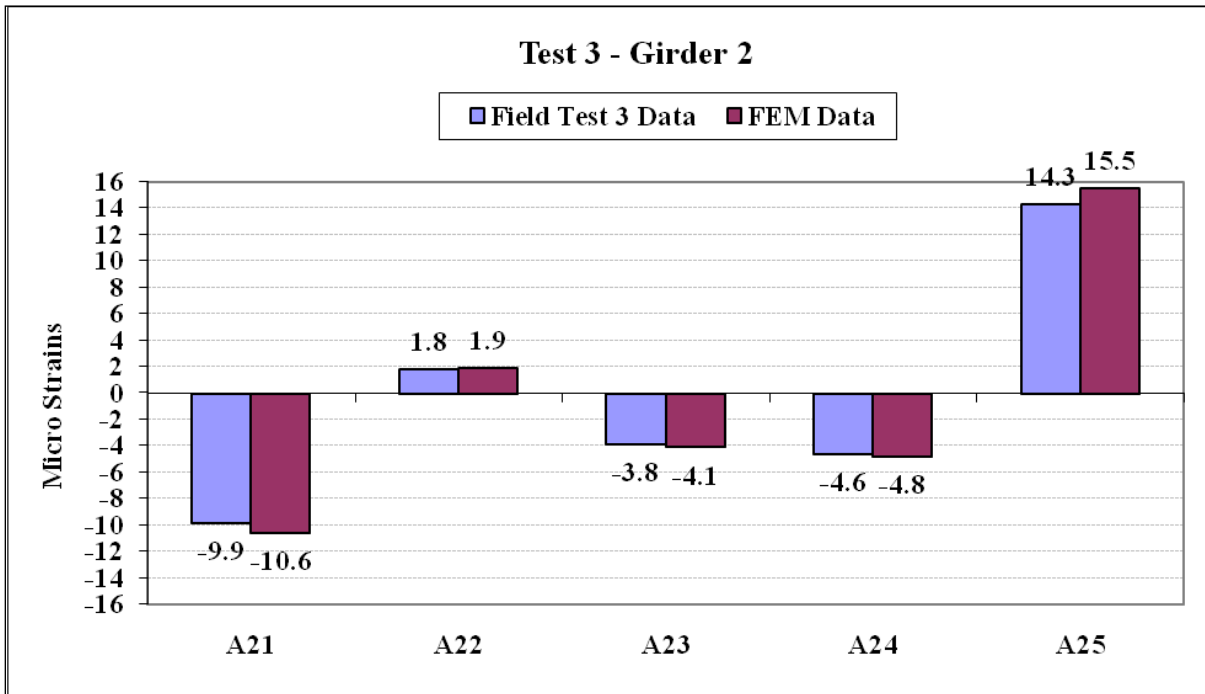


Figure 25
Comparison of strains of Girder 2 of test 3

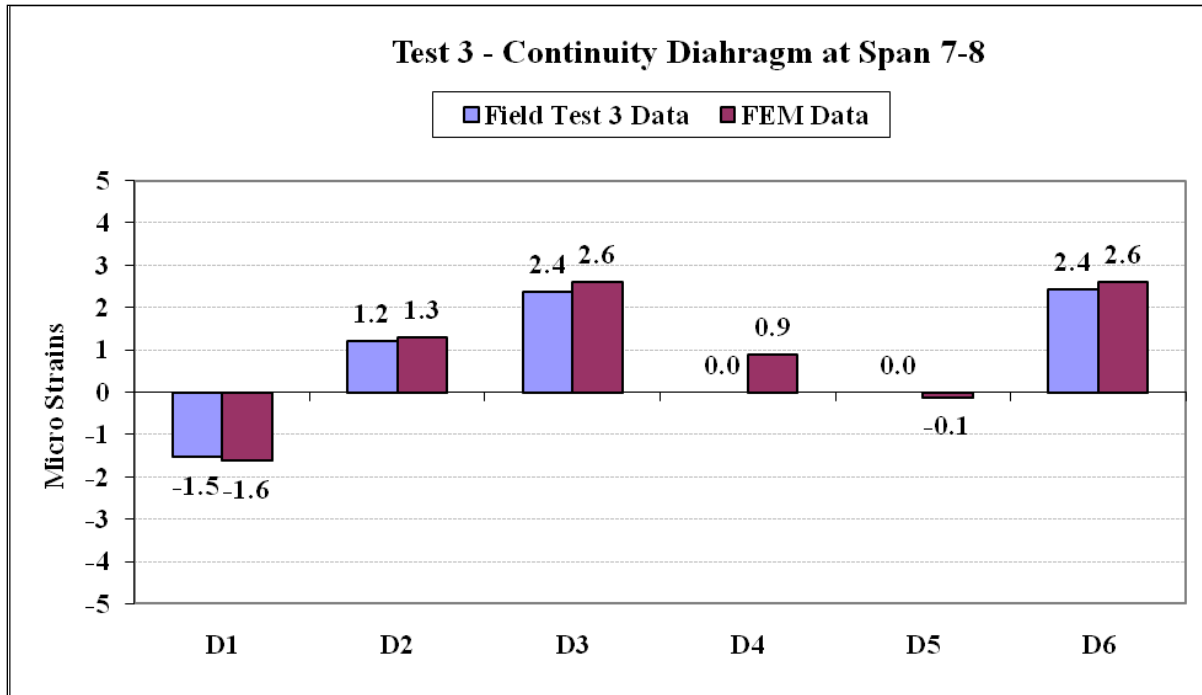


Figure 26
Comparison of strains in continuity diahragm of support Spans 7-8 of test 3

Live Load Test 4

The test truck traveled from east to west at 3 to 5 mph. When the test truck's back tire crossed the 63-ft. mark, the truck was stopped and data was collected. The 63 ft. were marked from a reference point which is the south corner of the exterior curb. In the transverse direction, the truck was traveling 8 ft. 9 in. from the south exterior curb. Predicted and actual strains are within 10 percent as shown in Figures 27, 28, and 29. The gauge number and location are shown in the bridge instrumentation plans in Appendix A.

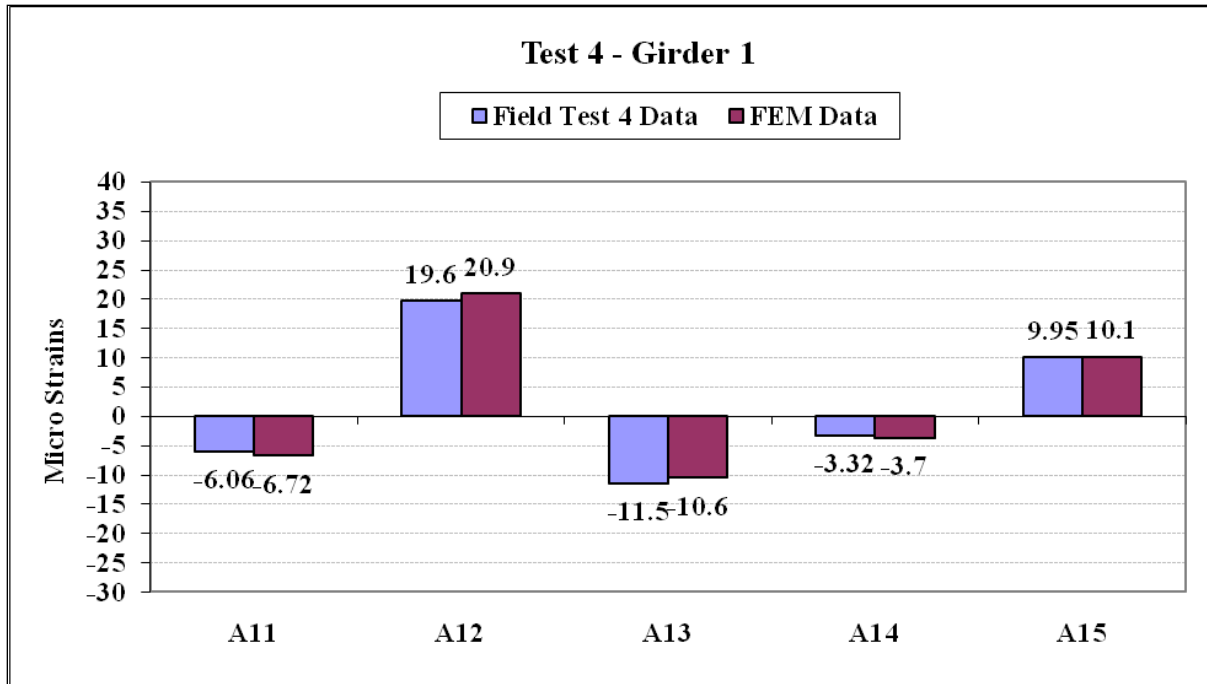


Figure 27
Comparison of strains in Girder 1 of test 4

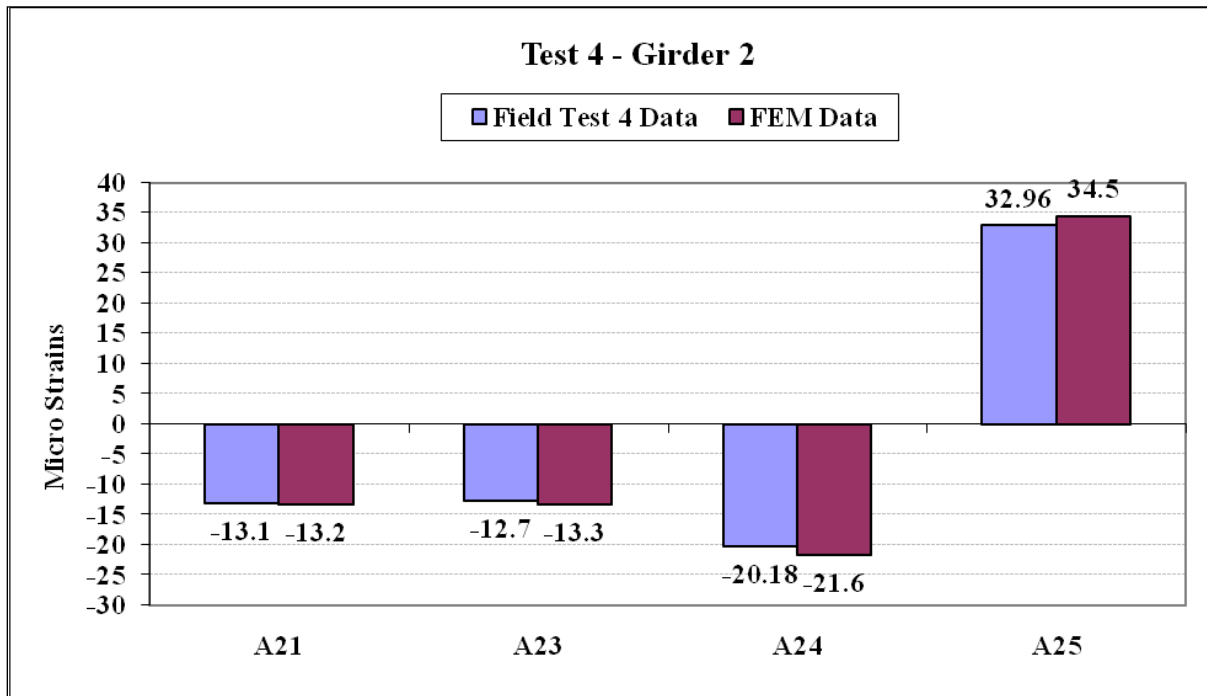


Figure 28
Comparison of strains in Girder 2 of test 4

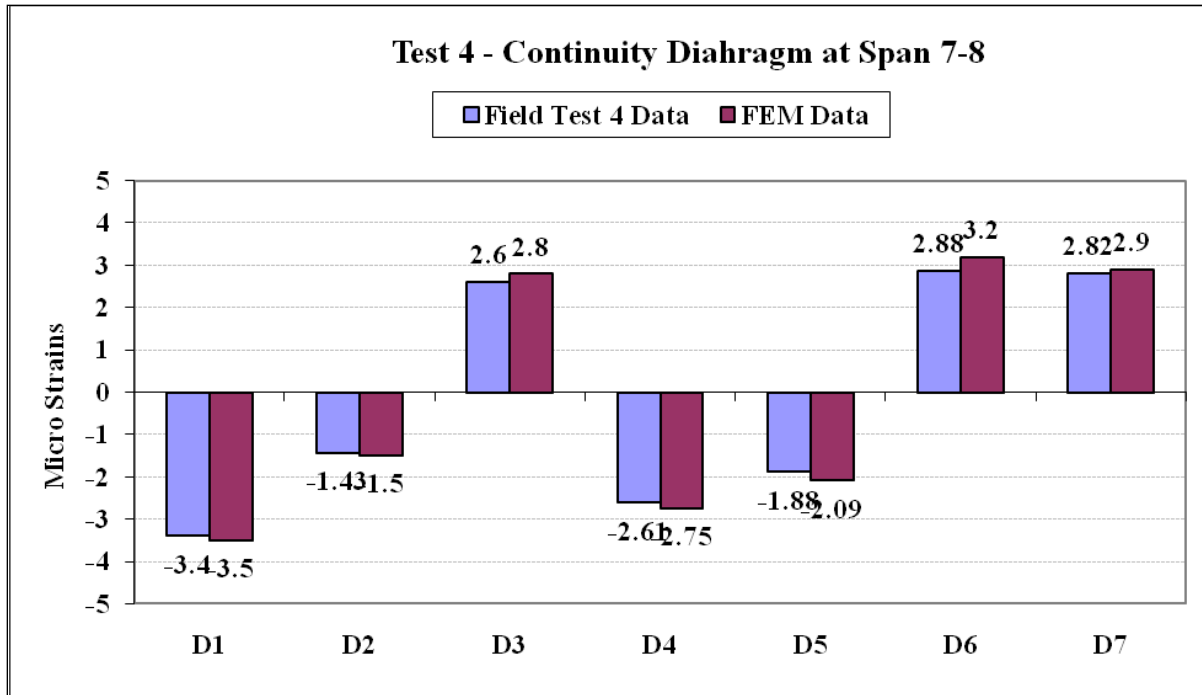


Figure 29
Comparison of strains in continuity diaphragm in support Spans 7-8 of test 4

Live Load Test 5

The test truck traveled east to west at 3 to 5 mph. When the test truck’s back tire crossed the 77-ft. mark, the truck was stopped. Data was collected on the bridge from the point where the truck started moving to the point where the truck stopped. The 77 ft. were marked from a reference point which is the south corner of the exterior curb. In the transverse direction, the truck was traveling 8 ft. 9 in. from the south end exterior curb. Predicted and actual strains are within 10 percent as shown in Figures 30, 31, and 32. The gauge number and location are shown in the bridge instrumentation plans in Appendix A.

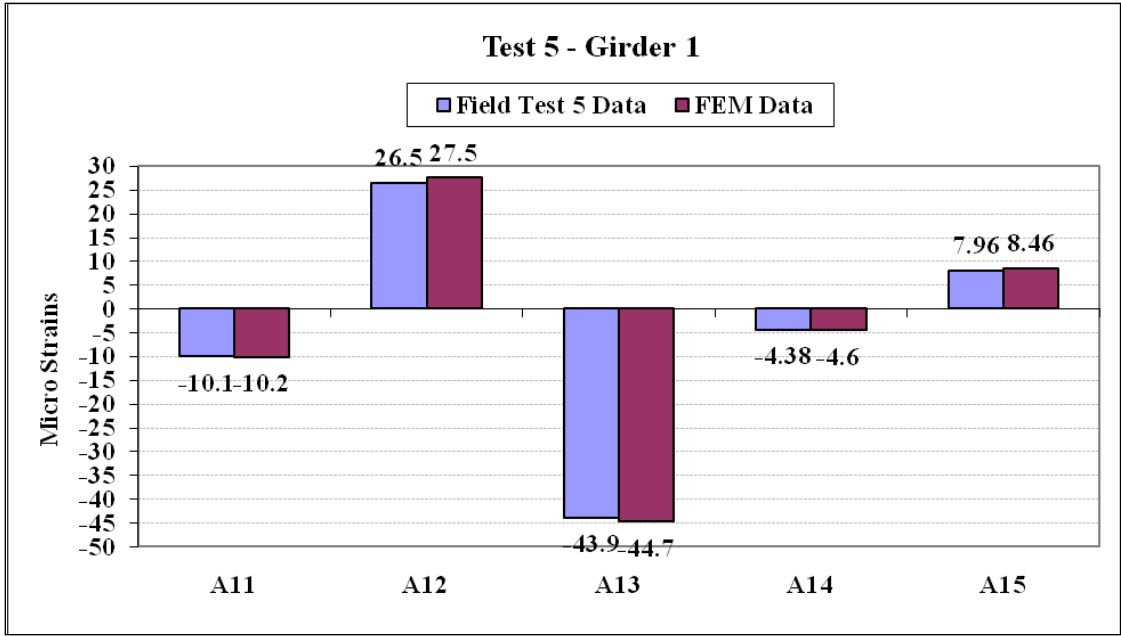


Figure 30
Comparison of strains in Girder 1 of test 5

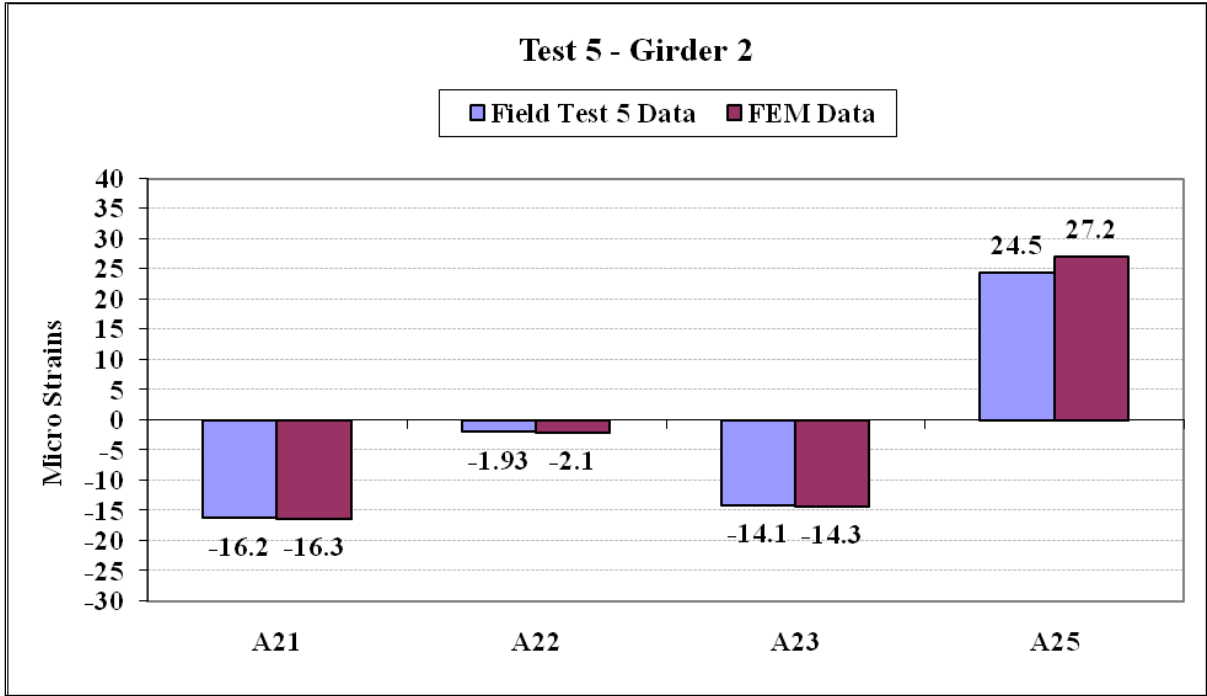


Figure 31
Comparison of strains in Girder 2 of test 5

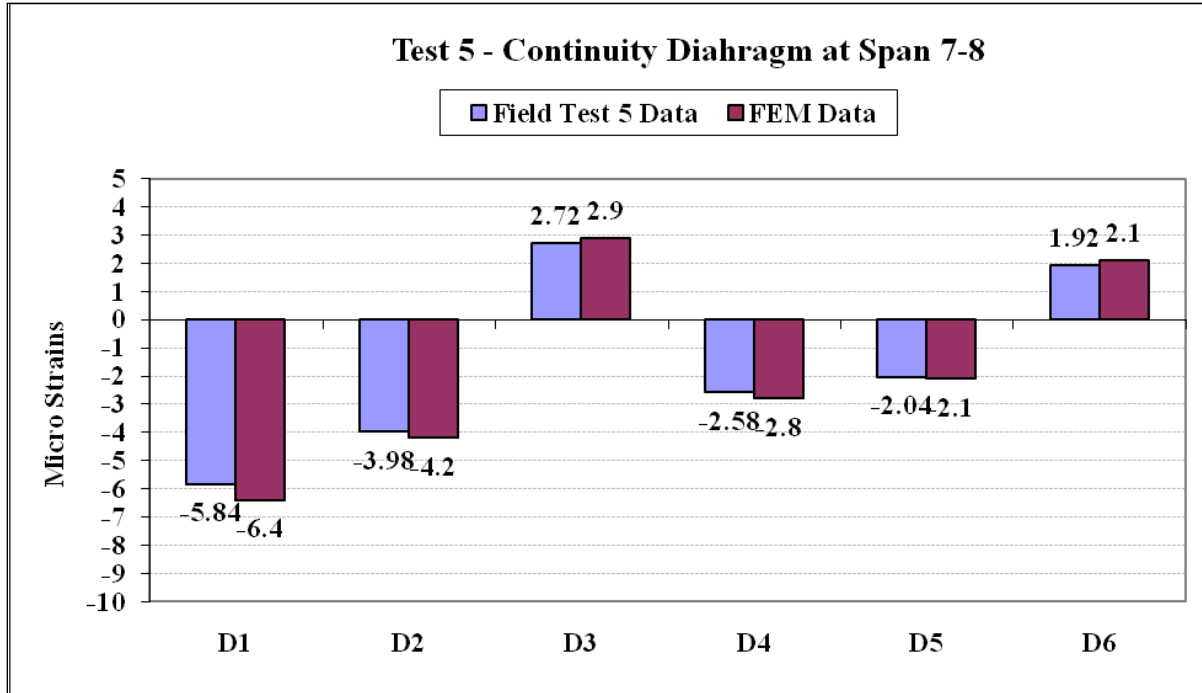


Figure 32
Comparison of strains in continuity diaphragm in support Spans 7-8 of test 5

Live Load Test 6

The test truck traveled east to west at 3 to 5 mph. When the test truck’s front tire crossed the 91-ft. mark, the truck was stopped and data was collected. The 91 ft. were marked from a reference point which is the south corner of the exterior curb. In the transverse direction, the truck was traveling at 8 ft. 9 in. from the south end exterior curb. Predicted and actual strains are within 10 percent as shown in Figures 33, 34, and 35. The gauge number and location are shown in the bridge instrumentation plans in Appendix A.

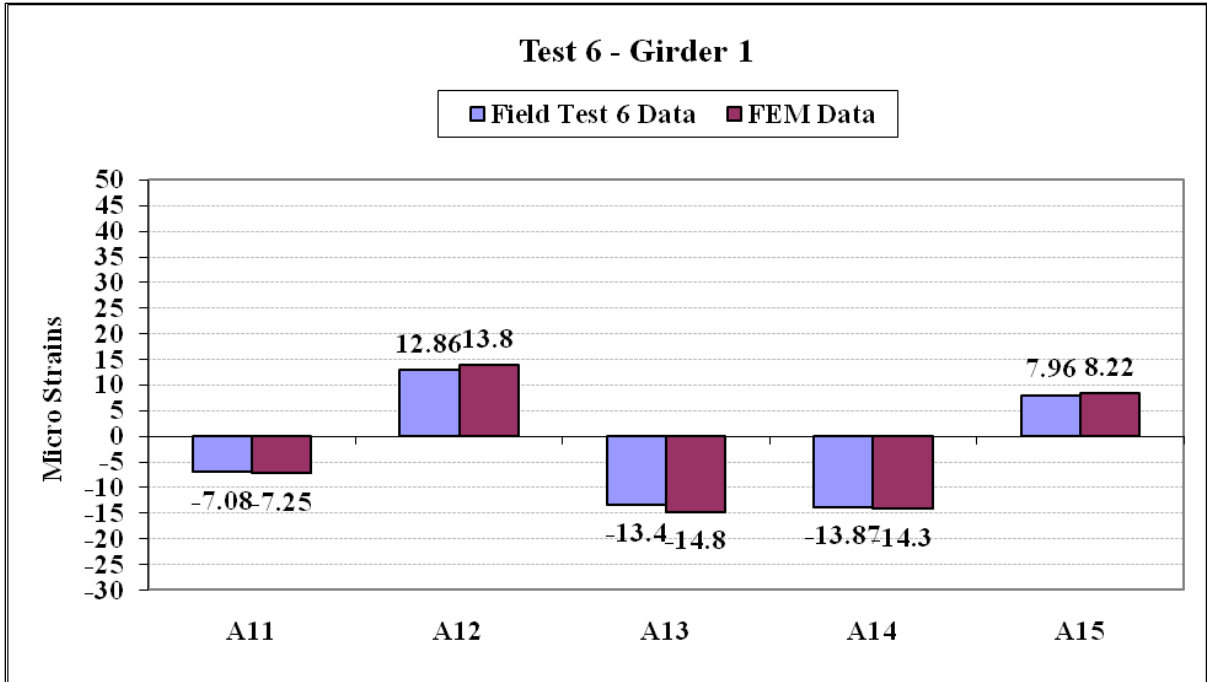


Figure 33
Comparison of strains in Girder 1 of test 6

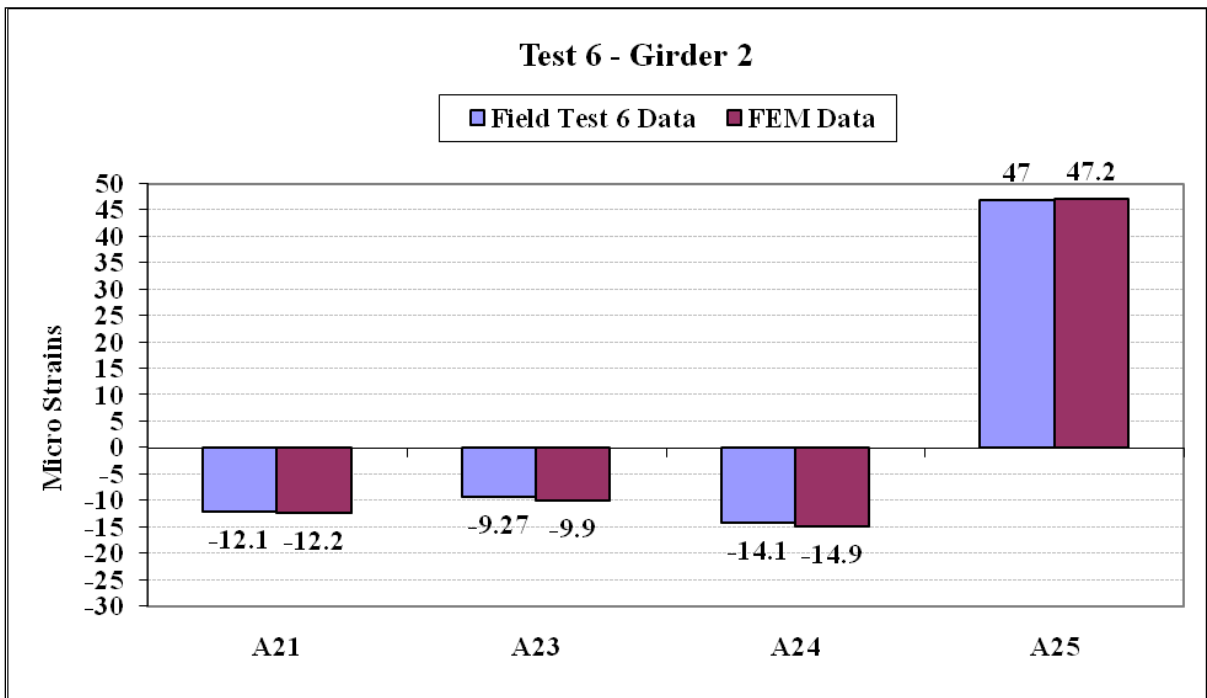


Figure 34
Comparison of strains in Girder 2 of test 6

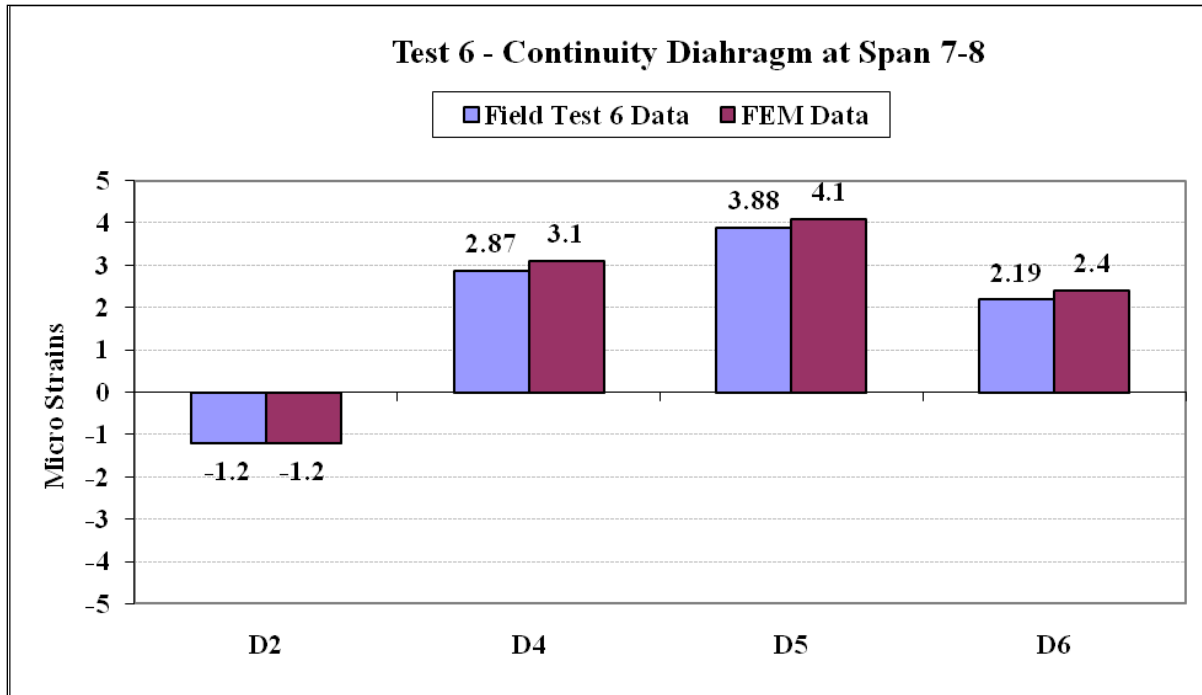


Figure 35
Comparison of strains in continuity diahgram in support Spans 7-8 of test 6

Conclusions from the Field Tests

The finite element models of the BNSF overpass in the GT STRUDL, when compared to the field tests, showed a good correlation in the strain data. Furthermore, analyses using the HS20-44 truck were performed to determine the effects of continuity diaphragms in the skewed continuous prestressed concrete bridges.

Analysis Using HS 20-44 Truck Load

The finite element model of the BNSF overpass was used with HS20-44 truck loads. A total of four different cases were considered, two cases for the maximum positive and negative moment in the bridge, and two bridge models, one with continuity diaphragms and one without. The stresses, deflections, and strains were compared to determine the effects of continuity diaphragms on the bridge girders and bridge deck. The results are presented in Appendices D and E.

Table 6
Case studies

Bridge Girders	With Continuity Diaphragms	Without Continuity Diaphragms
Max. Positive Moment	Case I	Case III
Max. Negative Moment	Case II	Case IV

The results for bridge girders 1 and 2 and the stresses in the bridge deck are compared for the four different cases and presented in Figures 36 to 52 and Tables 7 and 8.

Stresses in Girders- Positive Moment

The stresses were compared for the top elements and bottom elements of Girder 1 and Girder 2 of Case I and Case III. The results are shown in Figure 36 to Figure 43. Case I refers to the maximum positive moment in the girders with continuity diaphragms, and Case III refers to the maximum positive moment in the girders without continuity diaphragms. The effects of continuity diaphragms on maximum stresses in bridge girders are negligible.

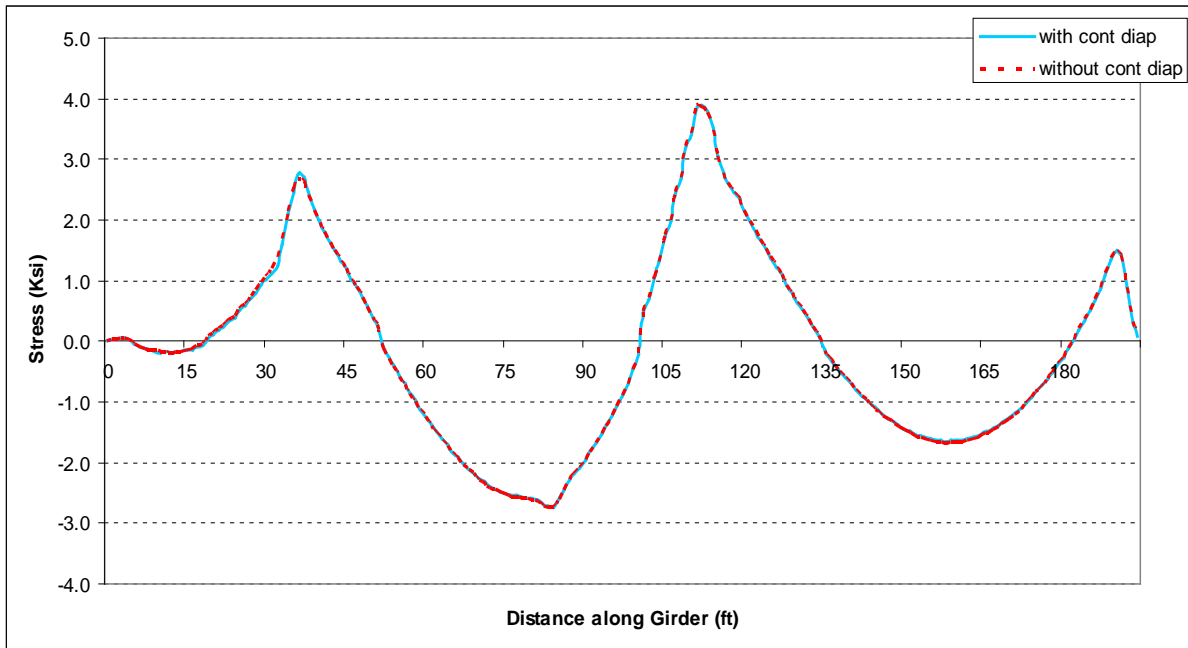


Figure 36
Comparison of stresses of Case I and Case III for top elements in Girder 1

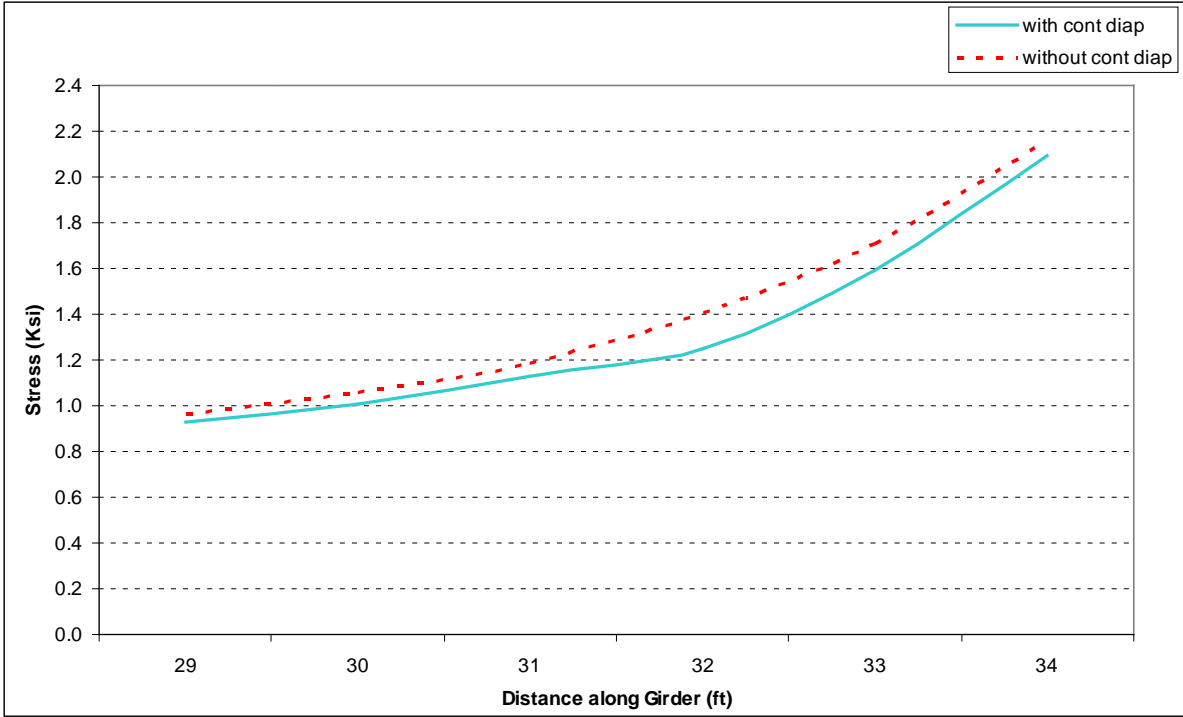


Figure 37
Enlarged view of stresses of top girder elements of Girder 1



Figure 38
Comparison of stresses of Case I and Case III for bottom elements in Girder 1

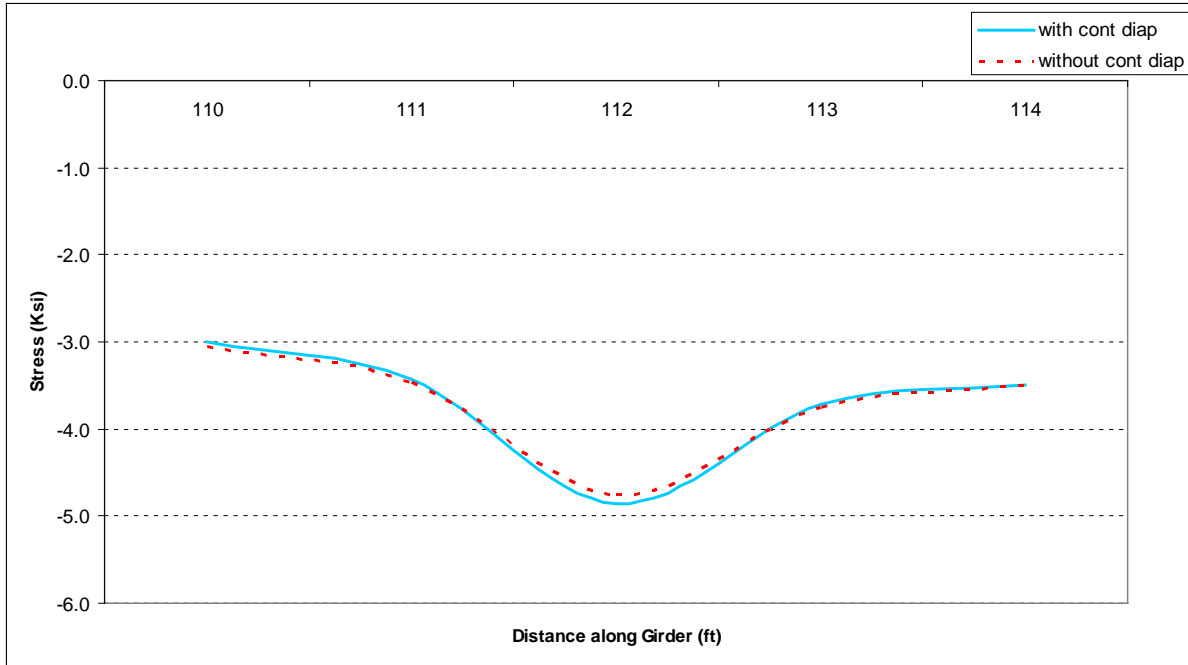


Figure 39
Enlarged view of stresses of bottom girder elements of Girder 1

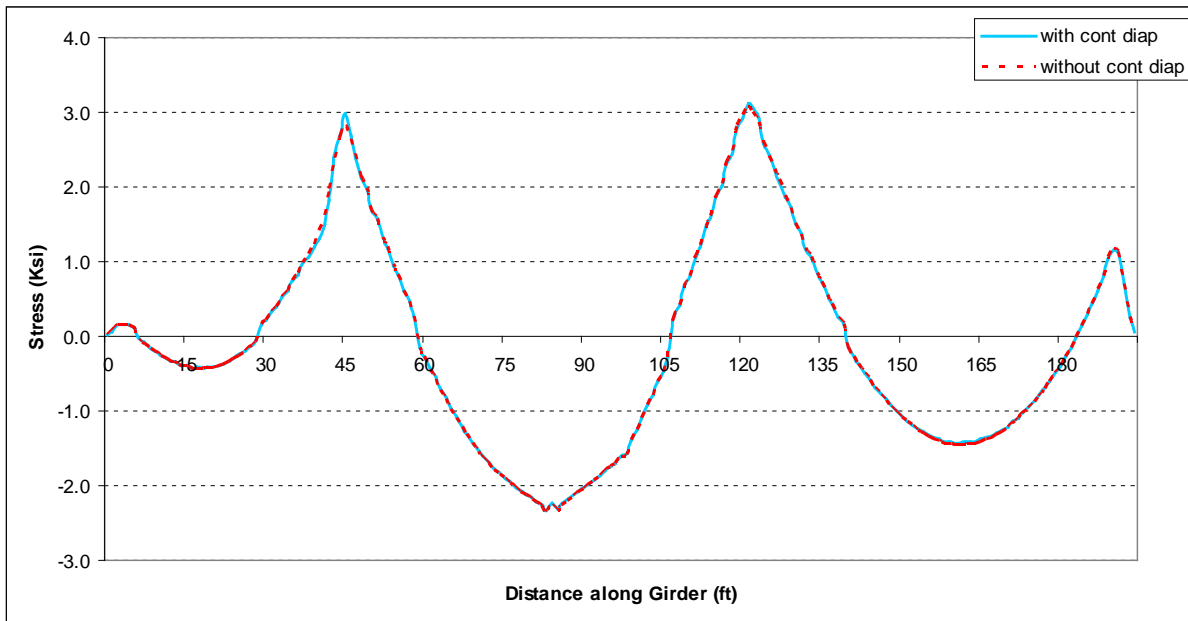


Figure 40
Comparison of stresses of Case I and Case III for top elements in Girder 2

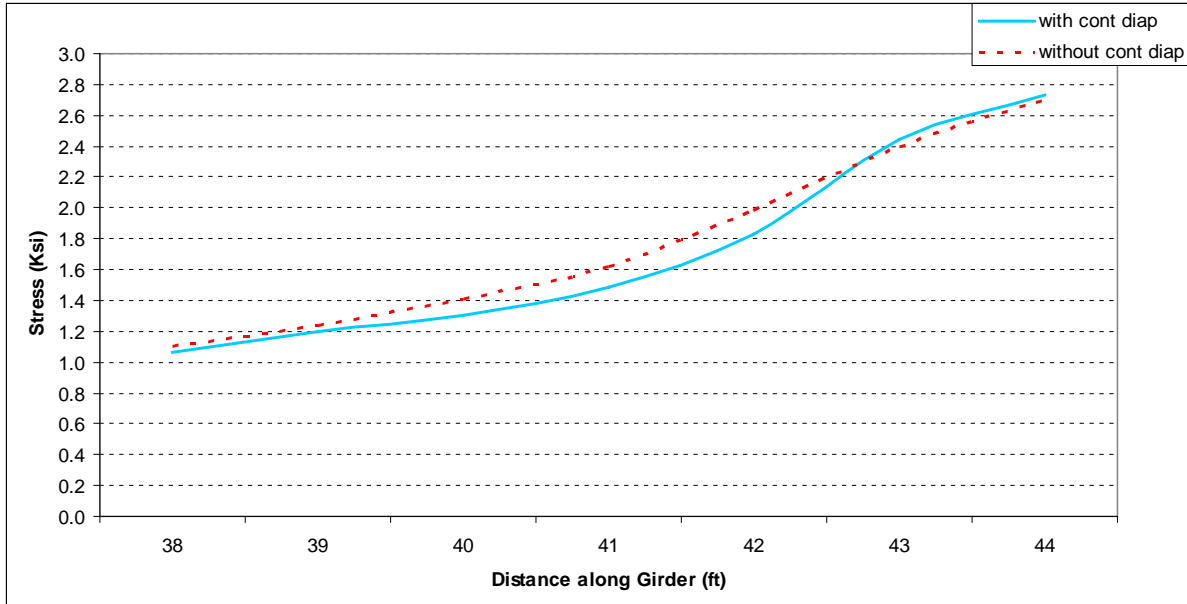


Figure 41
Enlarged view of stresses of top girder elements of Girder 2

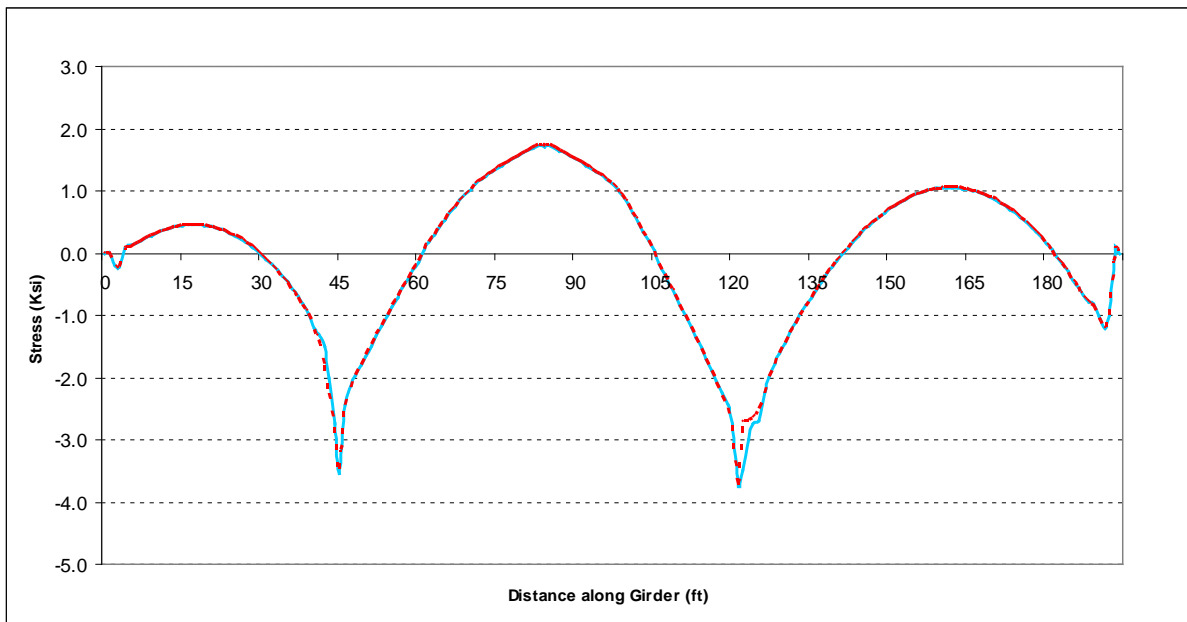


Figure 42
Comparison of stresses of Case I and Case III for bottom elements in Girder 2

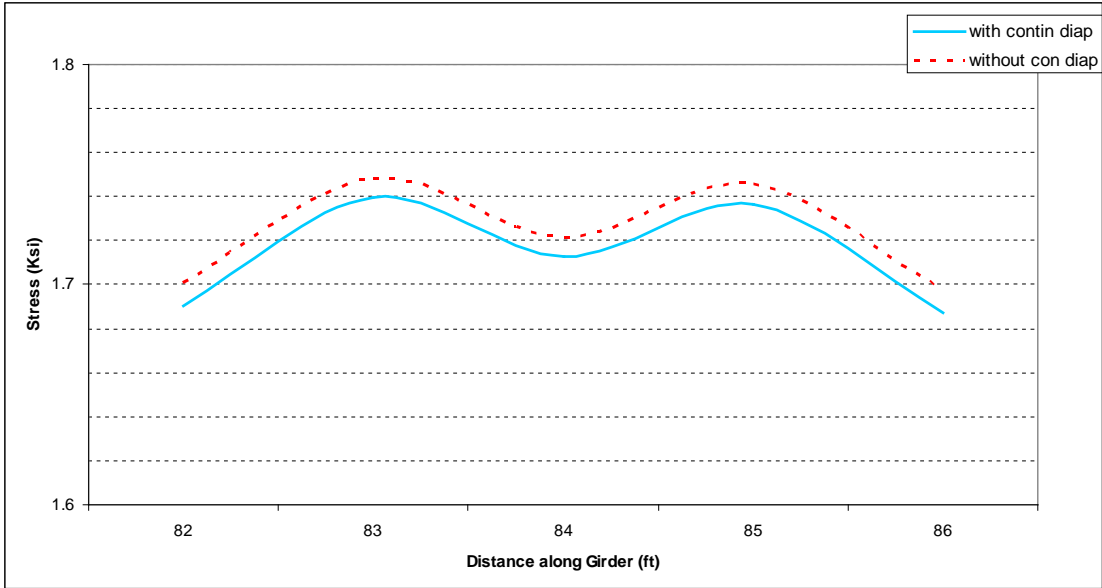


Figure 43
Enlarged view of stresses of bottom girder elements of girder

Stresses in Girders - Negative Moment

Figures 44 to 48 show the comparison of stresses for the top and bottom elements of Girder 1 and 2 from Cases II and IV. Case II refers to the maximum negative moment in the girders with continuity diaphragms, and Case IV refers to the maximum negative moment in the girders without continuity diaphragms. The effects of continuity diaphragms on maximum stresses in bridge girders are negligible.

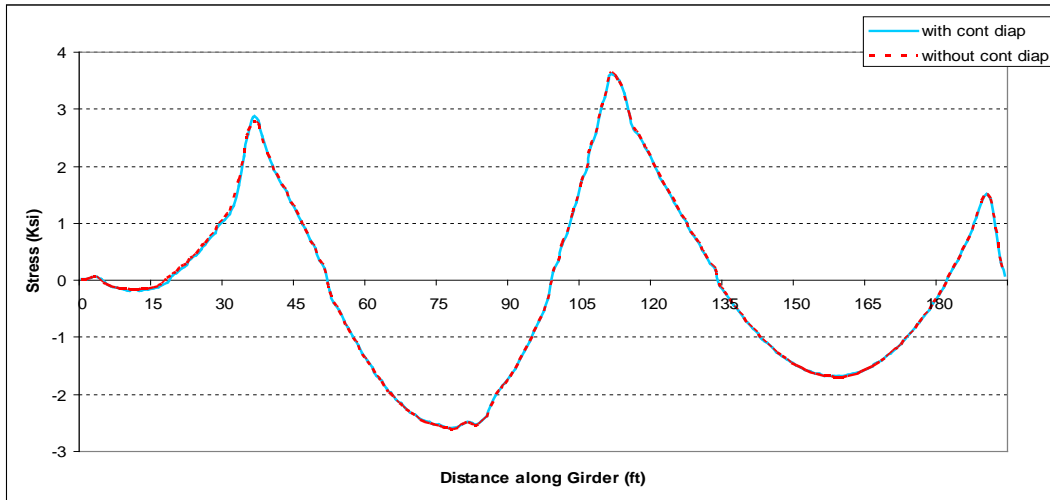


Figure 44
Comparison of stresses of Case II and Case IV for top elements in Girder 1



Figure 45
Enlarged view of stresses of top girder elements of Girder 1

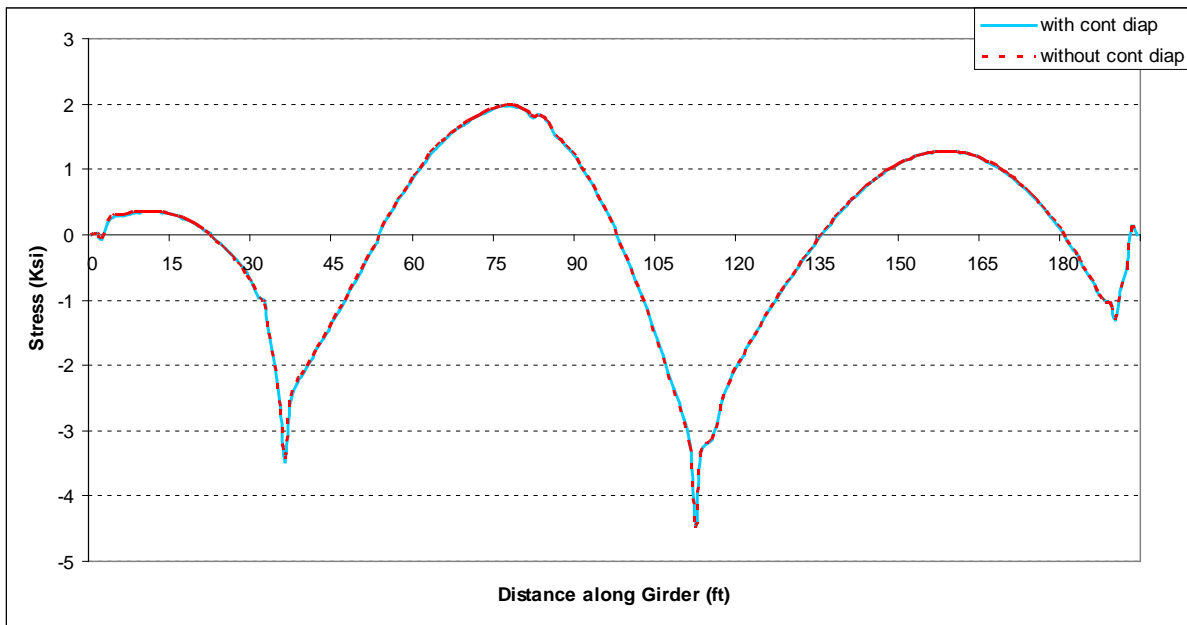


Figure 46
Comparison of stresses of Case II and Case IV for bottom elements in Girder 1

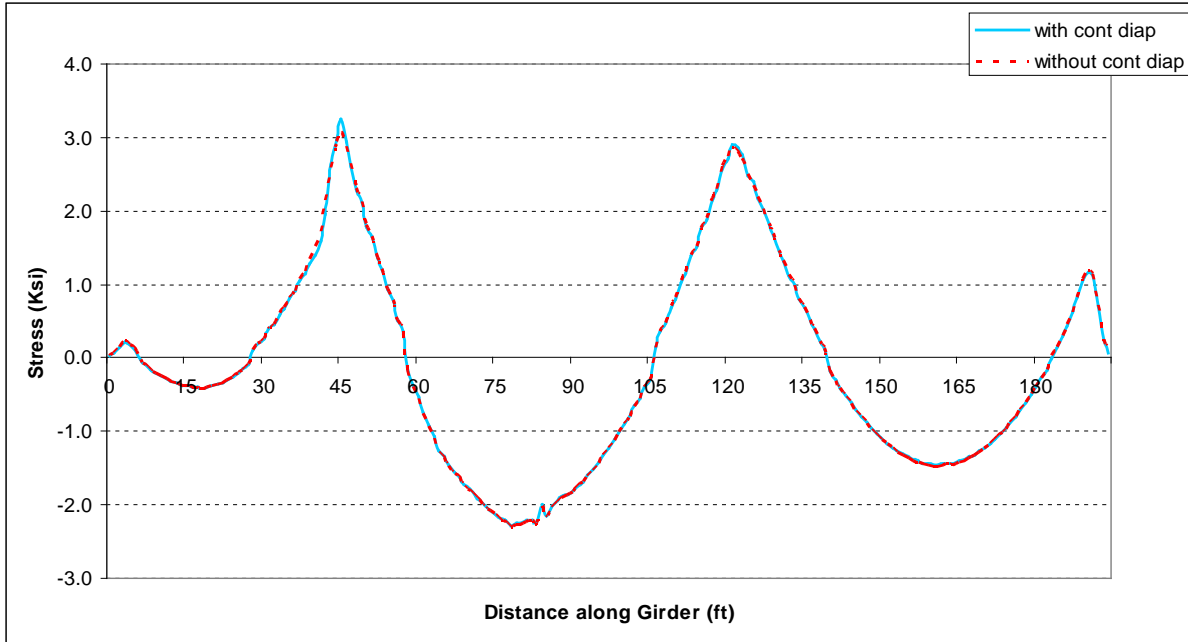


Figure 47
Comparison of stresses of Case II and Case IV for top elements in Girder 2

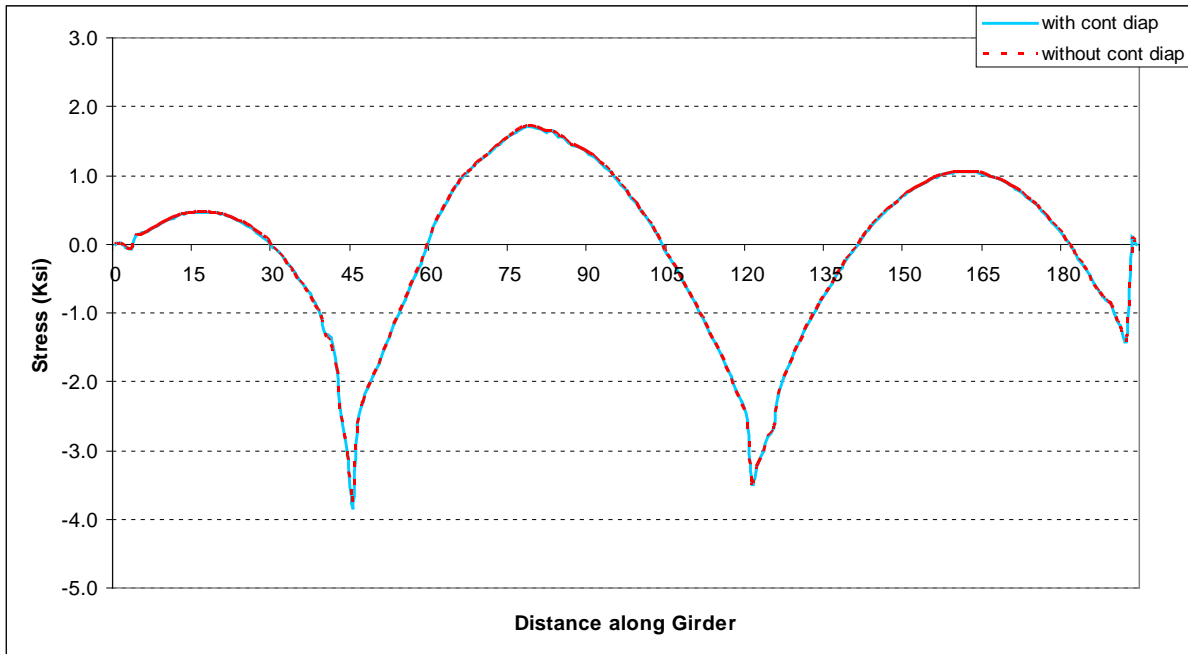


Figure 48
Comparison of stresses of Case II and Case IV for bottom elements in Girder 2

Deflection in Girders - Positive Moment

The comparisons of the deflections for the Girder 1 and Girder 2 of Case I and Case III are shown in Figures 49 and 50. Case I refers to the maximum positive moment in the girders with continuity diaphragms, and Case III refers to the maximum positive moment in the girders without continuity diaphragms. The effects of continuity diaphragms on maximum deflection in bridge girders are negligible.

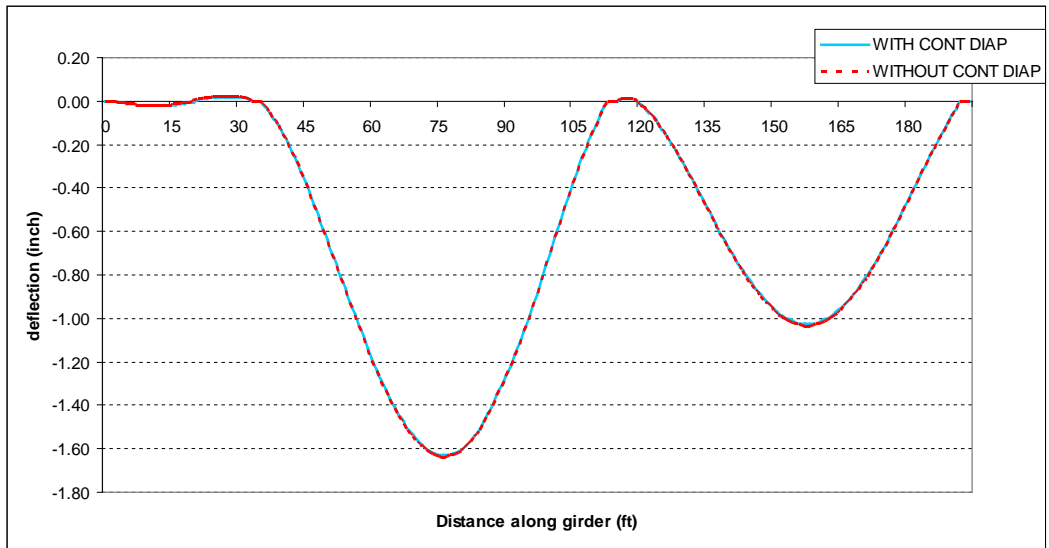


Figure 49
Comparison of deflections for Case I and Case III of Girder 1

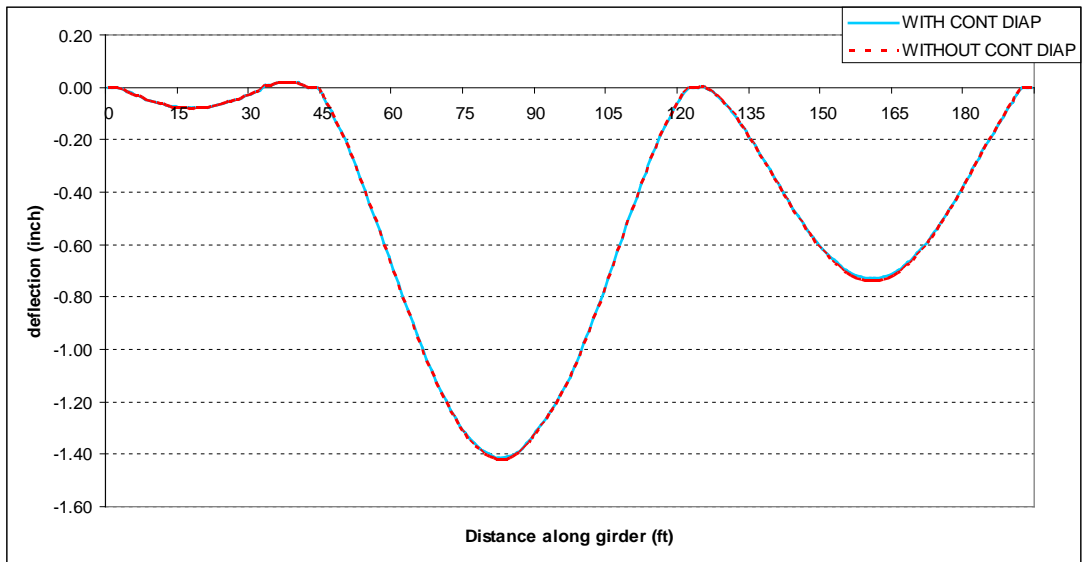


Figure 50
Comparison of deflections of Case I and Case III of Girder 2

Deflection in Girders - Negative Moment

The comparison of deflections for Girder 1 and Girder 2 of Case II and Case IV are shown in Figures 51 and 52. Case II refers to the maximum negative moment in the girders with continuity diaphragms, and Case IV refers to the maximum negative moment in the girders without continuity diaphragms. The effects of continuity diaphragms on maximum deflection in bridge girders are negligible.

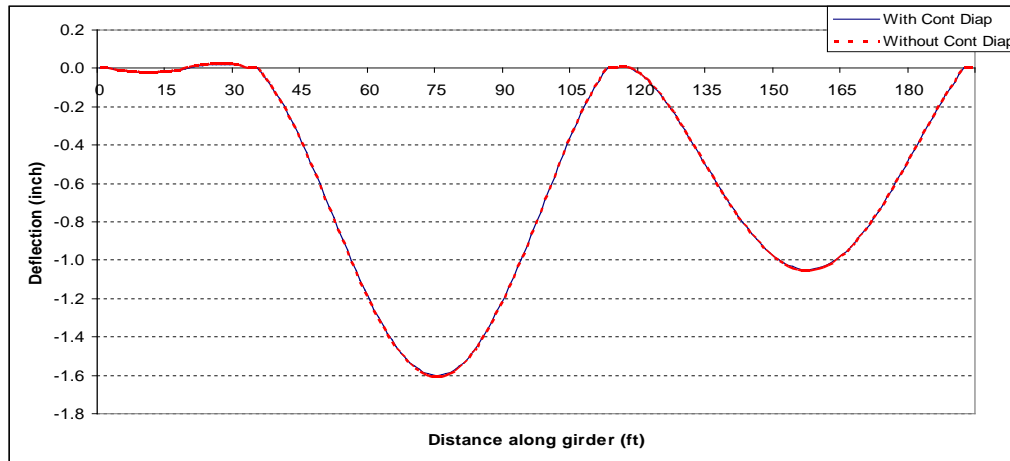


Figure 51
Comparison of deflections for Case II and Case IV of Girder 1

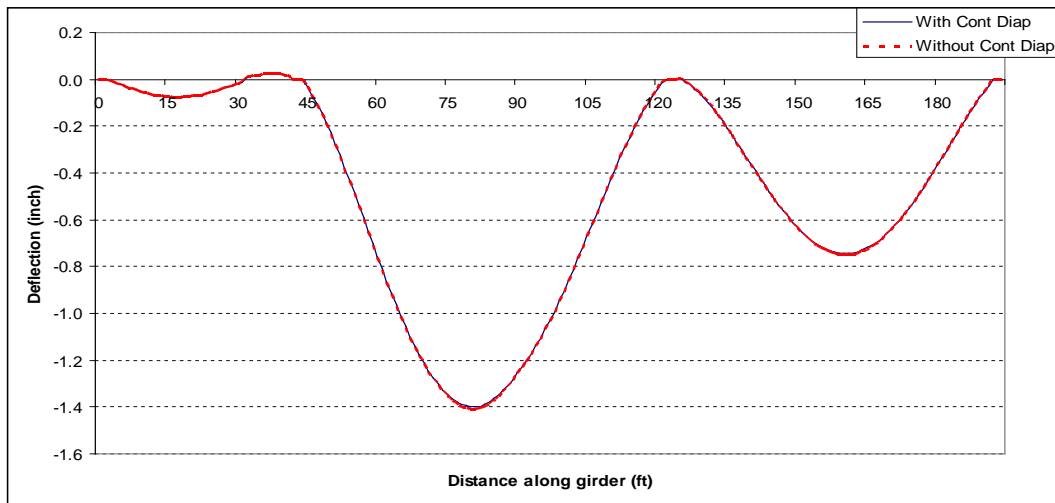


Figure 52
Comparison of deflections for Case II and Case IV of Girder 2

Bridge Deck Stresses

The stresses in the bridge deck were first compared for Case I and Case III, then for Case II and Case IV. A summary of the results are shown in Tables 7 and 8. The results due to the different load conditions were compared at the same locations in the bridge deck in order to get a better idea of the bridge deck behavior and the effects of the continuity diaphragms. In all cases, the effects of continuity diaphragms on maximum stresses in bridge deck are negligible.

Table 7
Comparison of deck stresses of Case I and Case III

Result	Location	Stress Case I (ksi)	Stress case III (ksi)	Joint
Sxx	top	Max. 1.17	1.11	308119
		Min. -0.68	-0.687	112621
Syy	top	Max. 0.956	0.949	116820
		Min. -0.887	-0.889	112621
Sxy	top	Max. 0.35	0.351	112922
		Min. -0.45	-0.457	117722
Sxx	bottom	Max. 0.68	0.687	112621
		Min. -1.17	-1.11	308119
Syy	bottom	Max. 0.882	0.884	112621
		Min. -0.957	-0.948	116820
Sxy	bottom	Max. 0.455	0.457	117722
		Min. -0.349	-0.351	112922

Table 8
Comparison of deck stresses of Case II and Case IV

Result	Location	Stress Case II (ksi)	Stress case IV (ksi)	Joint
Sxx	top	Max. 1.31	1.25	308119
		Min. -1.0	-1	111722
Syy	top	Max. 0.871	0.86	116820
		Min. -0.987	-0.989	111722
Sxy	top	Max. 0.352	0.354	112023
		Min. -0.49	-0.492	207522
Sxx	bottom	Max. 1.0	1	111722
		Min. -1.31	-1.25	308119
Syy	bottom	Max. 0.983	0.985	111722
		Min. -0.870	-0.86	116820
Sxy	bottom	Max. 0.489	0.492	207522
		Min. -0.352	-0.354	112023

CONCLUSIONS

General Summary

The presented research describes the field verification for the effectiveness of continuity diaphragms for skewed, continuous, precast, prestressed, concrete girder bridges. LTRC Final Report 383 presented the results of the investigation on the effects of continuity diaphragms for skewed continuous span, precast, prestressed, concrete, girder bridges. The theoretical results from finite element models suggested a need to eliminate the continuity diaphragms and have a field verification of the bridges. The work reported here provides the field verification on the effectiveness of continuity diaphragms in continuous precast prestressed skewed bridges.

A prestressed, concrete bridge with continuity diaphragms and a skewed angle of 48° was selected by a team of engineers from LADOTD, LTRC, and FHWA. Field tests were done on the BNSF overpass using a test truck of GVW 48.66 kips and a comprehensive instrumentation plan. Six live load tests were conducted and data from each was stored. The finite element models of the BNSF overpass in the GT STRUDL, when compared to the field tests showed a good correlation in the strain data. Hence the modeling using the finite element approach in GT STRUDL simulated the BNSF overpass.

The HS 20-44 truck is used for further finite element analysis on the bridge. Two models were modeled for better study of the effects of the continuity diaphragms. One model was the BNSF overpass analyzed for the HS 20-44 truck. The other model was the same BNSF overpass without the continuity diaphragms. Comparison of the stresses, strains, deflections in the bridge girders and stresses in the bridge deck were made. The results indicated that there was a negligible variation between these two models, and that the continuity diaphragms may be omitted.

RECOMMENDATIONS

The field and theoretical results from this study provided a fundamental understanding of the load transfer mechanism through these diaphragms of skewed, continuous span bridges. The findings in this study indicated that the effects of the continuity diaphragms on skewed, continuous span, precast, prestressed concrete girder bridges were negligible. Continuity diaphragms used in prestressed concrete girder bridges on skewed bents provided additional redundancy in the bridge but caused difficulties in detailing and construction. As the skew angle increases or the girder spacing decreases, the construction becomes more difficult and the effectiveness of the diaphragms becomes questionable.

Therefore, it is recommended that the use of continuity diaphragms be evaluated based on the need for the enhanced structural redundancy, the reduced expansion joint installation and maintenance costs, and the associated construction difficulties and costs. Where the continuity diaphragms are not used, girders will have free ends. The deck will be continuous over the girders. A small notch is made at the top and the bottom of the deck in the region of the girders' ends. An additional stainless steel bar is placed in the top and bottom of the slab at that location. The detail needs to be monitored for performance.

The outcome of this research will reduce the construction and maintenance costs of bridges throughout the state of Louisiana and United States.

ACRONYMS, ABBREVIATIONS, AND SYMBOLS

AASHTO	American Association of State Highway and Transportation Officials
BNSF	Burlington North Santa Fe
DOTD	Department of Transportation and Development
FHWA	Federal Highway Administration
GT STRUDL	Georgia Tech Structural Design Language
GVW	Gross Vehicular Weight
ft.	foot
kip	1,000 lb.
LADOTD	Louisiana Department of Transportation and Development
lb.	pound
IPSL Element	Iso Parametric Solid Linear Element used in FE Analysis
LRFD	Load Resistance Factor Design
LTRC	Louisiana Transportation Research Center
PRC	Project Review Committee
SBCR	Finite Element Module used in FE analysis
STS	Structural Testing System

REFERENCES

1. *AASHTO Load Resistance Factor Design Bridge Design Specifications. Third Edition.* American Association of State Highway and Transportation Officials, Washington, D.C. 2004.
2. *AASHTO Standard Specifications for Highway Bridges. Seventeenth Edition.* American Association of State Highway and Transportation Officials, Washington, D.C. 2002.
3. Aziz, T.S.; Cheung M.S.; and Bakht B. (1978) "Development of a Simplified Method of Lateral Load Distribution for Bridge Superstructure." Transportation Research Record No. 665, pp. 37-44.
4. Bridge Diagnostics, Inc., "Integrated Approach to Load Rating Instruction Manual," 2001.
5. "Bridge Design Manual," LADOTD Fourth Edition.
6. Cheung, M.S.; Jategaonkar, R.; and Jaeger, L.G. (1986). "Effects of Intermediate Diaphragms in Distributing Live loads in Beam-and-Slab Bridges." Canadian Journal of Civil Engineering. Vol. 13, pp. 278-292.
7. Griffin, J.J. (1997). "Influence of Diaphragms on Load Distribution in P/C I-Girder Bridges." Ph.D. Dissertation, University of Kentucky.
8. GT STRUDL Version 28. Georgia Institute of Technology, Atlanta, GA.
9. Libin, Yin. (2004). "Continuity of Bridges Composed of Simple-Span Precast Prestressed Concrete Girders Made Continuous," Ph.D. Dissertation, New Jersey Institute of Technology.
10. National Cooperative Highway Research Program Report 519, Washington, D.C. 2004.
11. Saber, A.; Roberts, F.; Toups, J.; and Alaywan, W. (2007). "Effects of Continuity Diaphragm for Skewed Continuous Span Precast Prestressed Concrete Girder Bridges," the Precast/Prestressed Concrete Institute (PCI) Journal.
12. Saber, A.; Toups, J.; Guice, L.; and Tayebi, A. "Continuity Diaphragm for Skewed Continuous Span Precast Prestressed Concrete Girder Bridges," LADOTD-LTRC report FHWA/LA 04/383, July 2003.
13. Saber, A.; Toups J., and Alaywan, W.; (2005). "Effects of Continuity on Load Transfer in Prestressed Concrete Skewed Bridges," Proceedings of the Third International Structural Engineering and Construction Conference, Japan.
14. Saber, A.; Toups, J.; and Tayebi, A. 2003. "Continuity Diaphragms for AASHTO Type II Girders," Proceedings of the Second International Structural Engineering and Construction Conference, August, Rome-Italy.
15. Toups, J. D.2003. "Continuity diaphragms for skewed continuous span precast prestressed concrete girder bridges," Thesis, Louisiana Tech University.

APPENDIX A

Instrumentation Plans for Maximum Positive Moment in Girders (Case I)

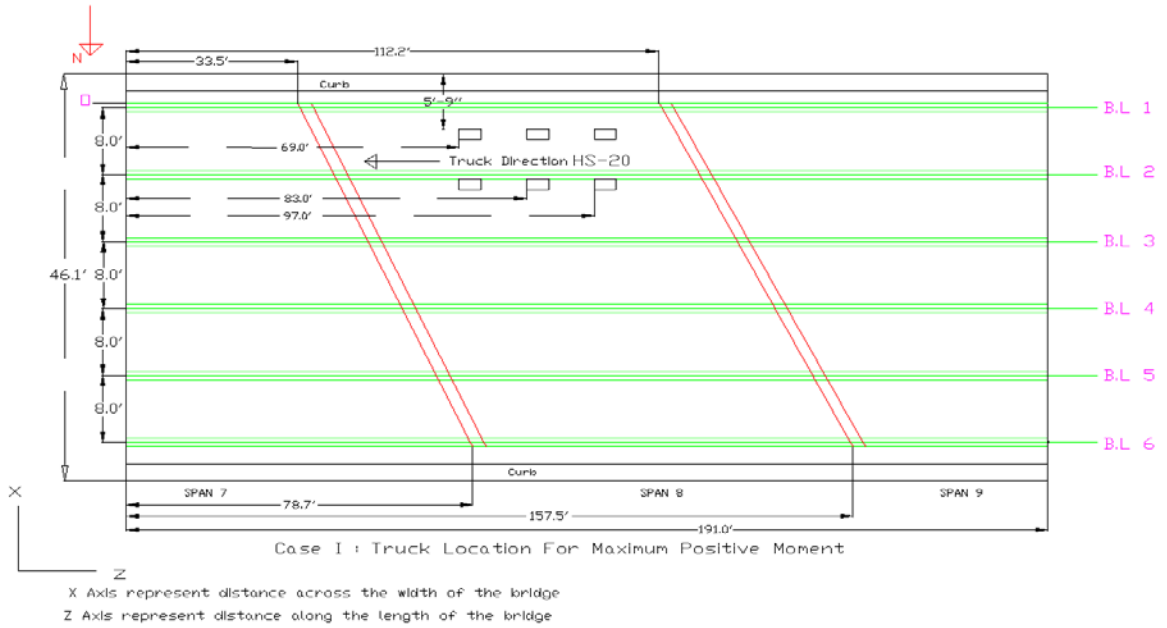


Figure 53
Truck location for maximum positive moment in girder

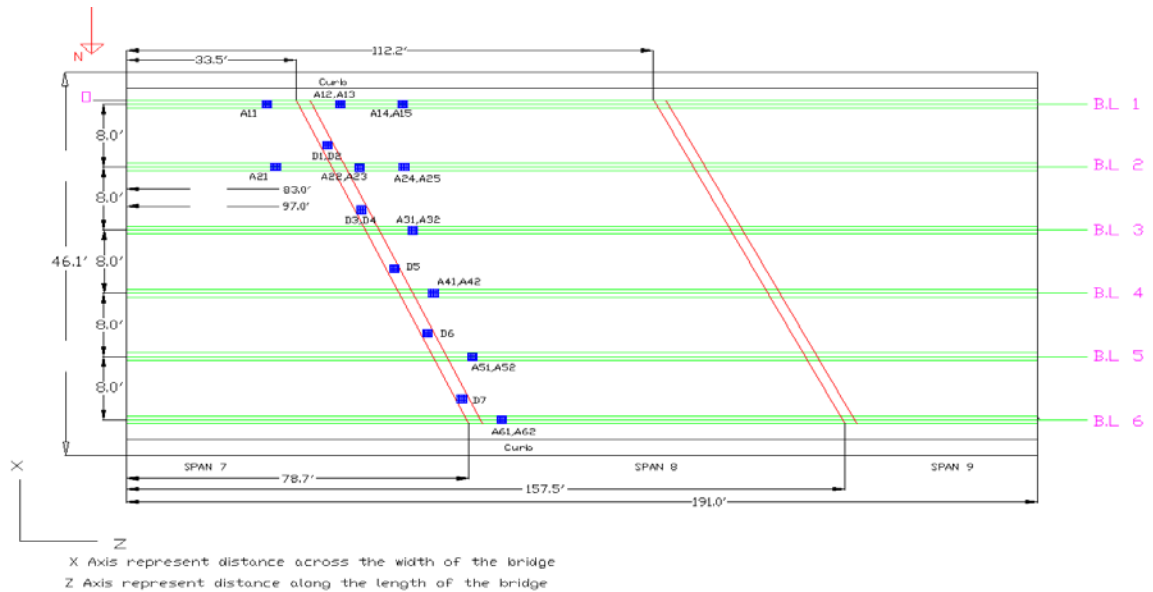


Figure 54
Instrumentation plan for Case I

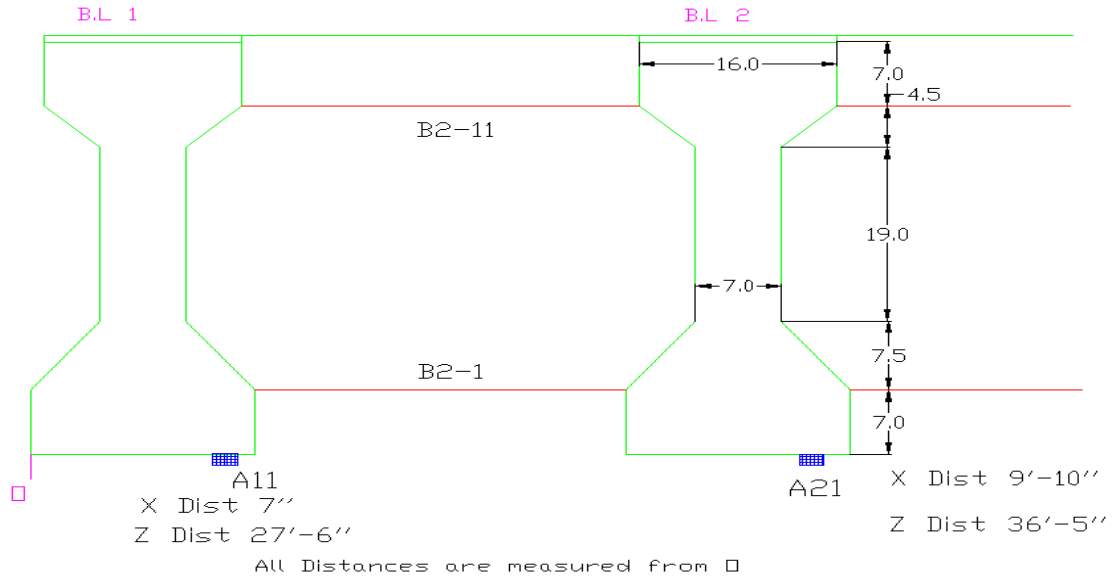


Figure 55
Cross section at section A of Case I

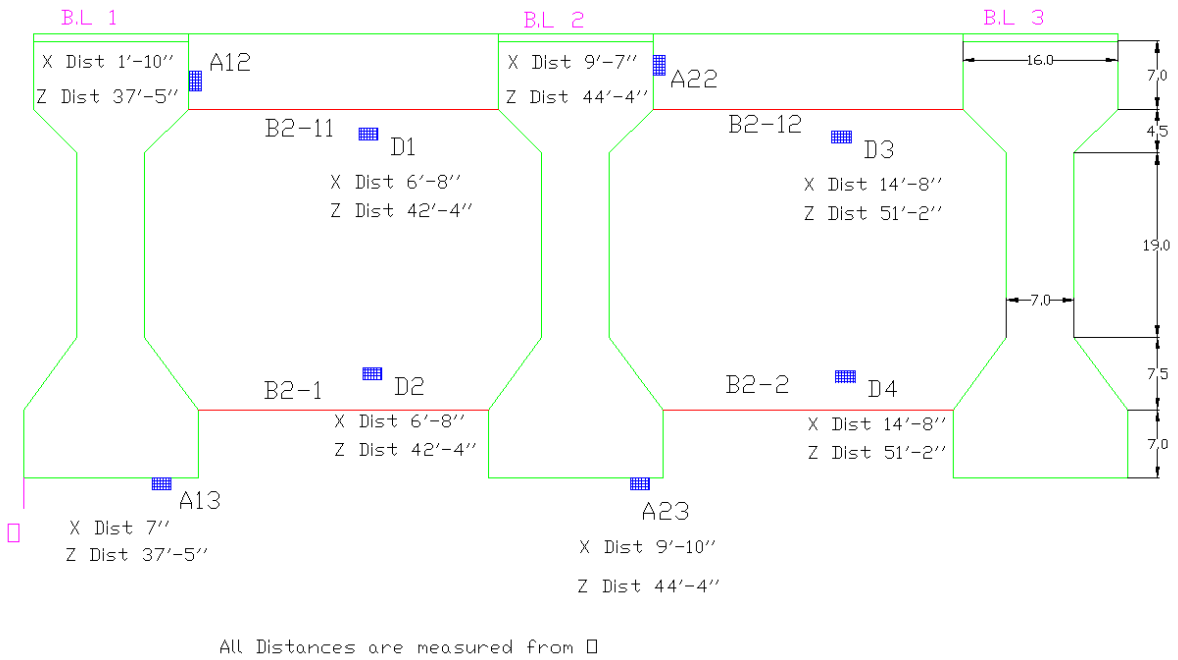


Figure 56
Cross section at section B of Case I

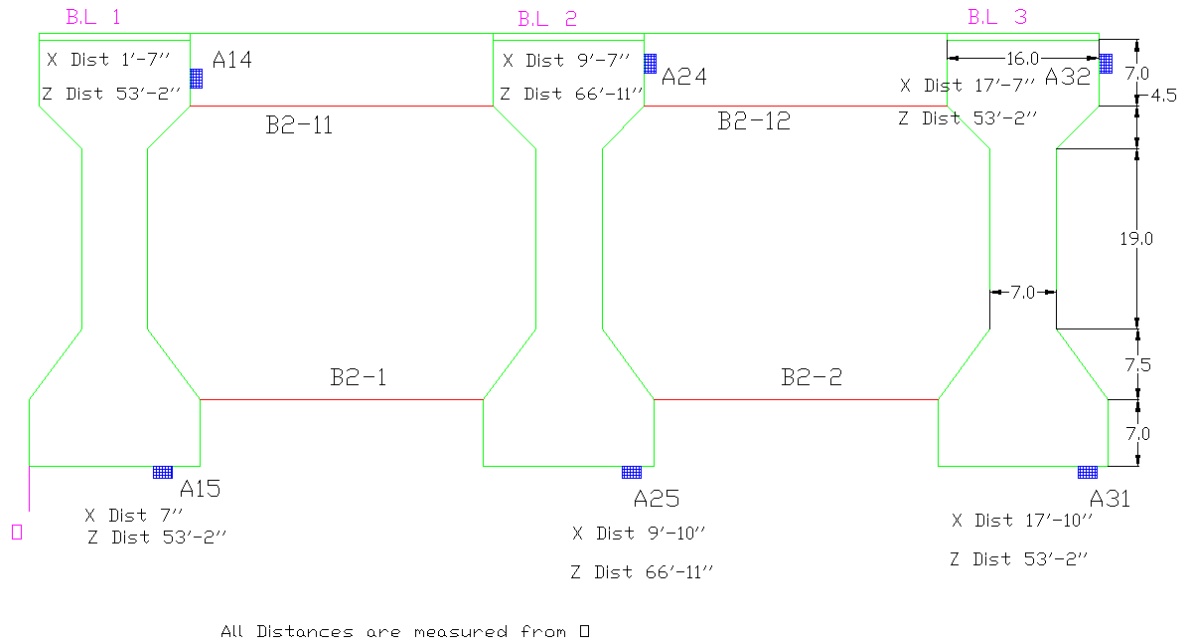


Figure 57
Cross section at section C of Case I

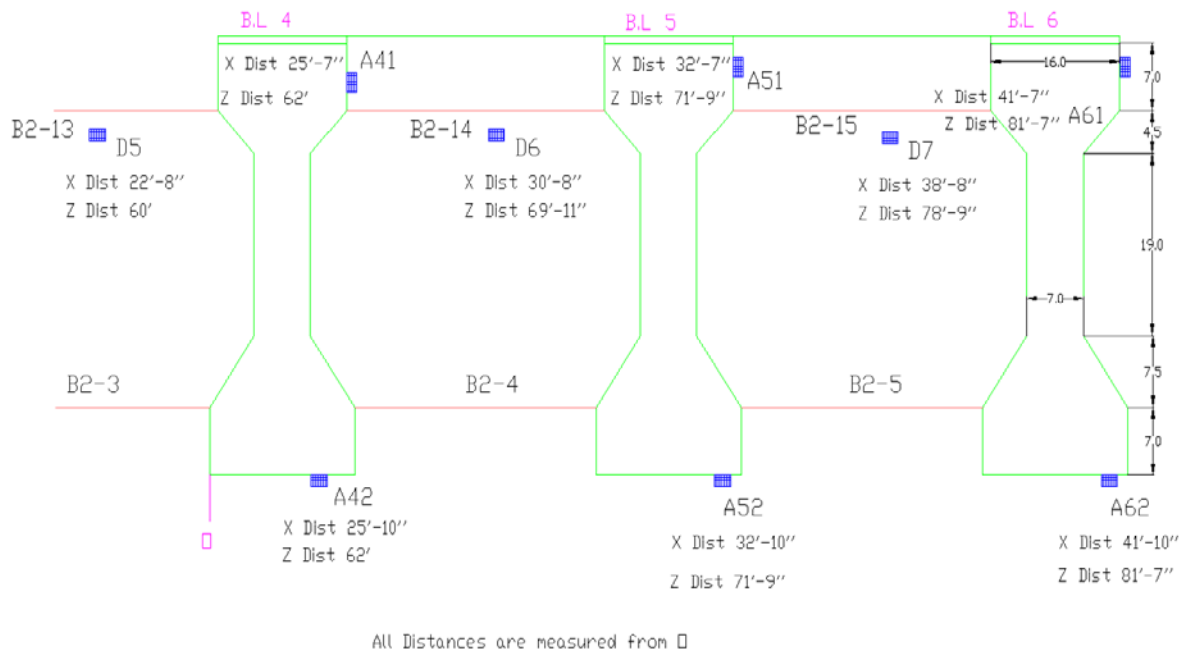


Figure 58
Cross section at section D of Case I

APPENDIX B

Instrumentation Plans for Maximum Negative Moment in Girders (Case II)

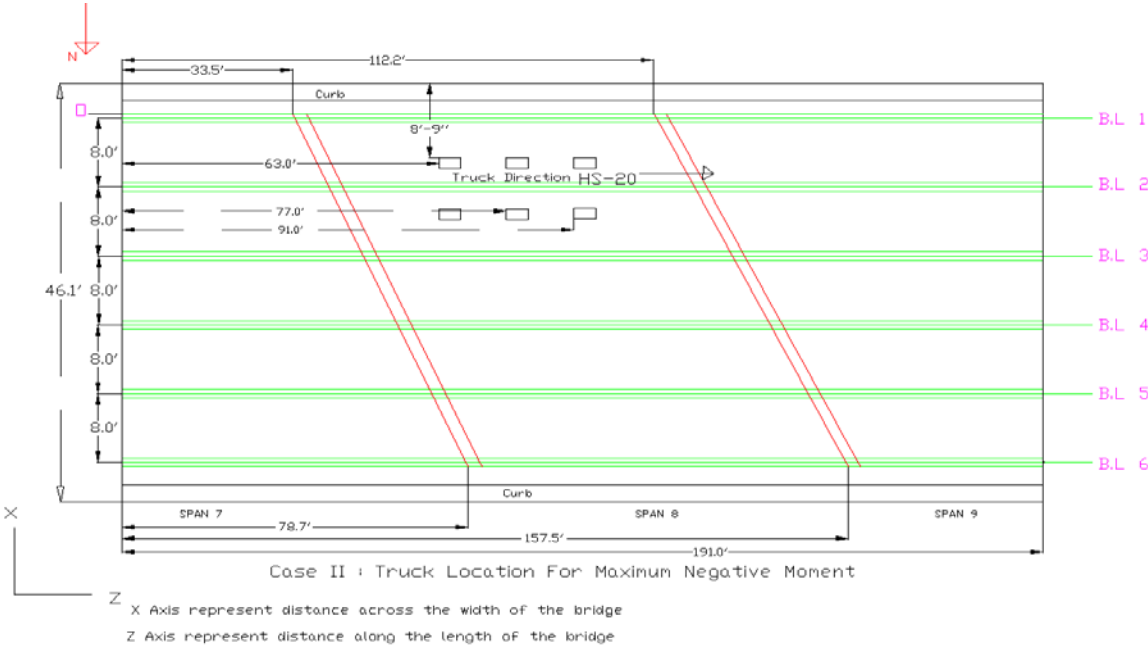


Figure 59
Truck location for maximum negative moment in girder

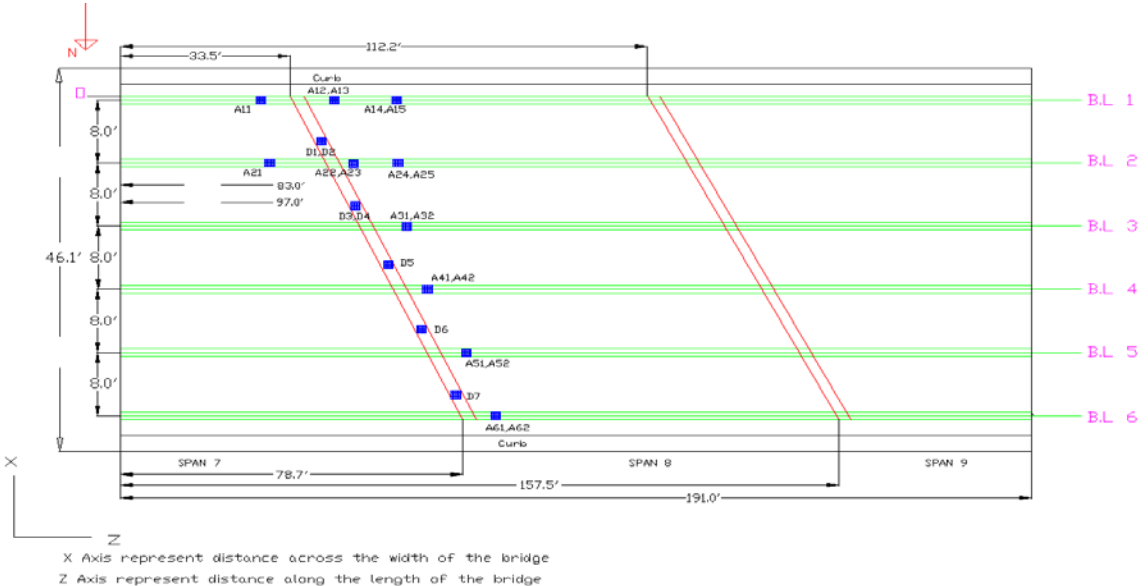


Figure 60
Instrumentation plan for Case II

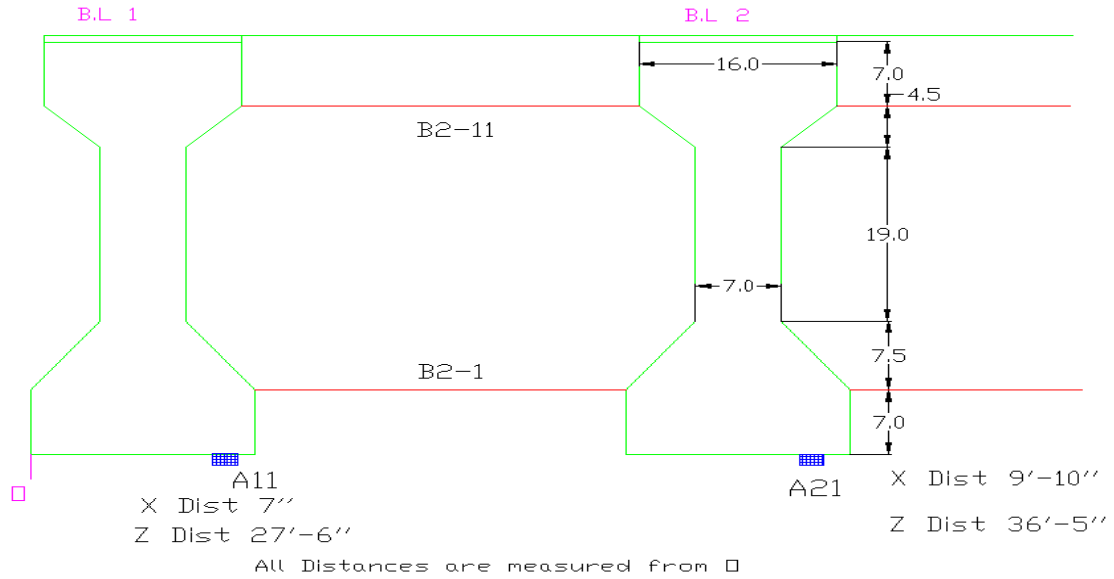


Figure 61
Cross section at section A of Case II

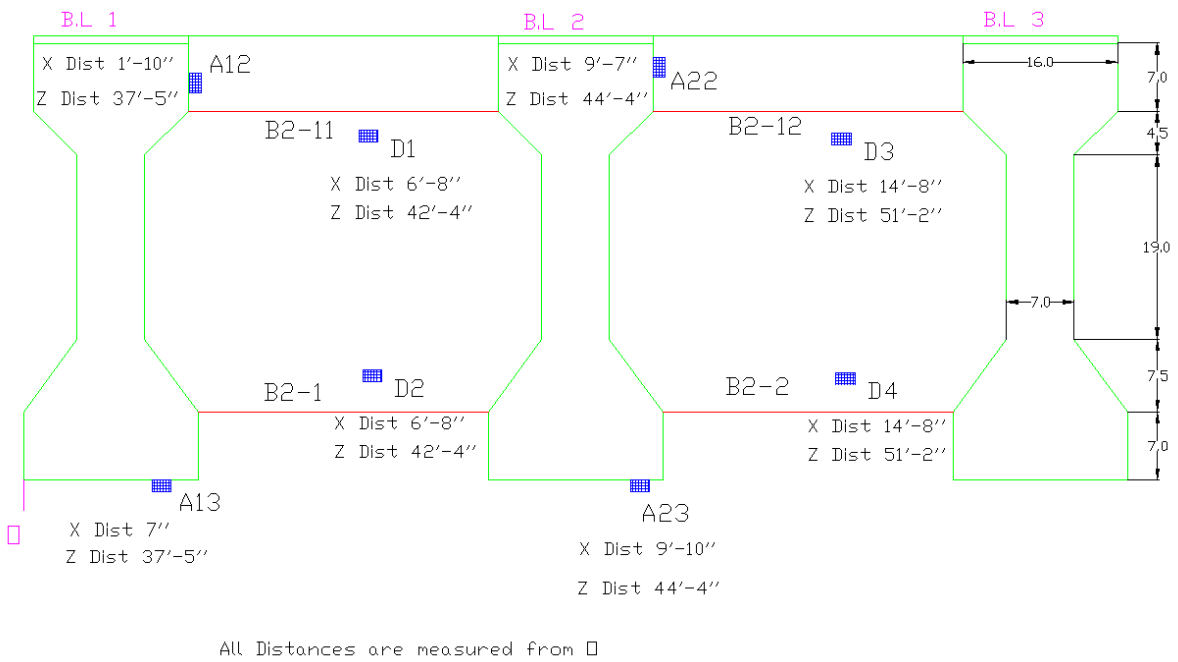


Figure 62
Cross section at section B of Case II

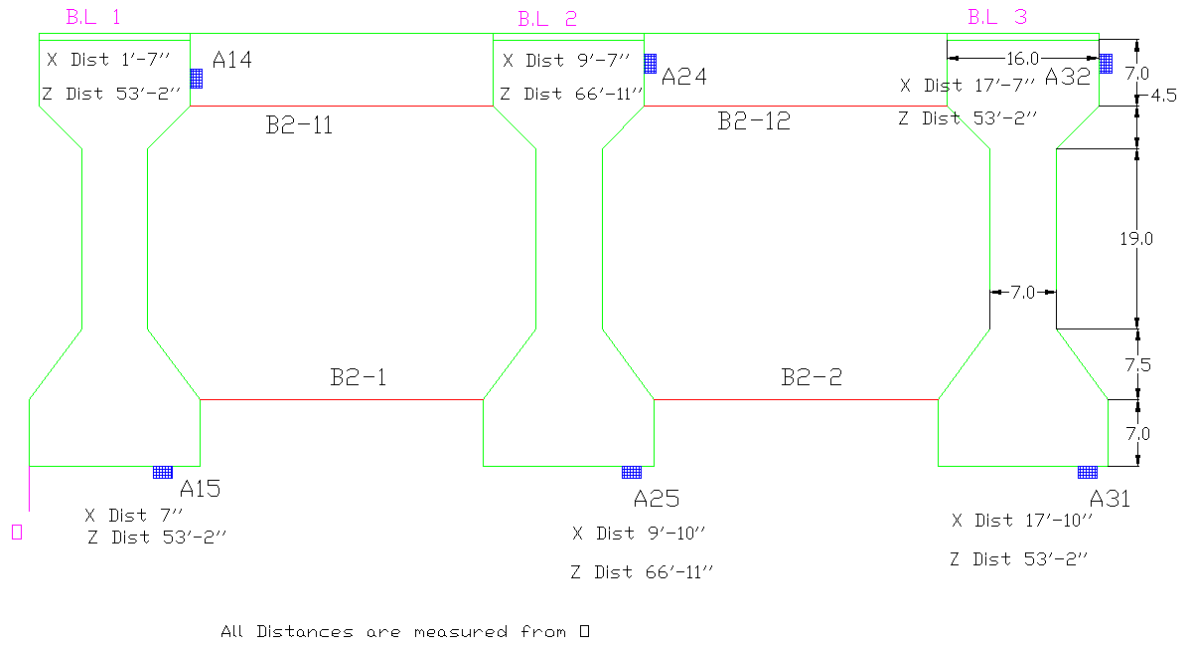


Figure 63
Cross section at section C of Case II

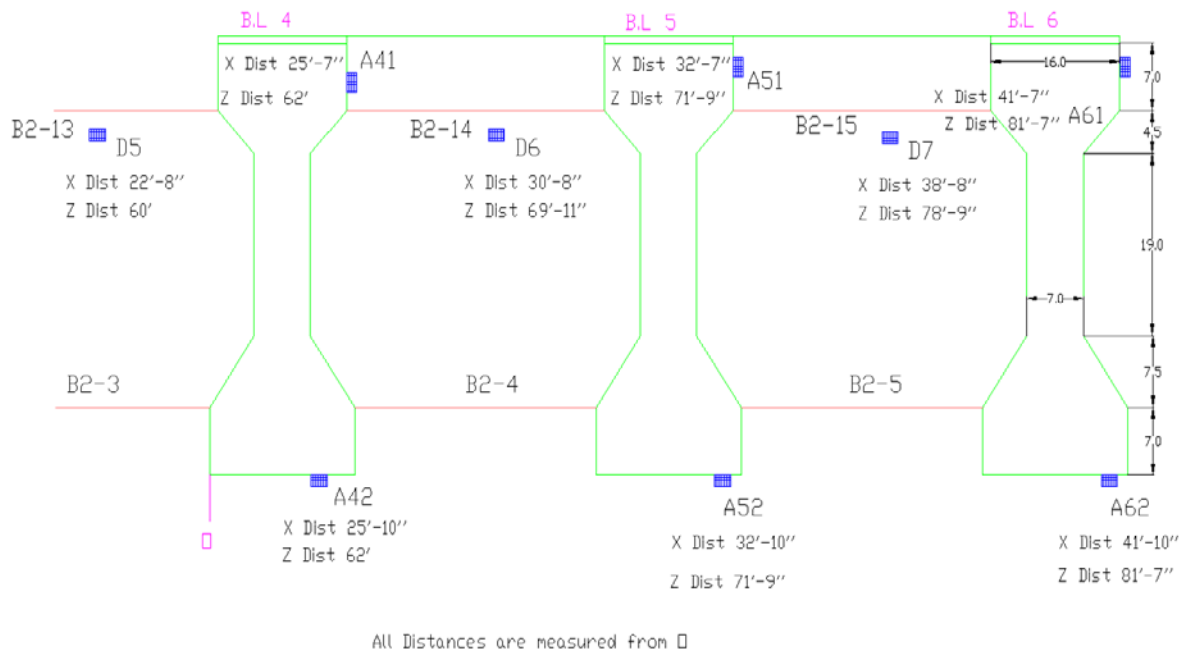


Figure 64
Cross section at section D of Case II

APPENDIX C

Comparison of Strains of Field Measurements vs. FE Predicted Data

Table 9
Comparisons of strains of field data to the FEM models (GT STRUDL) test 2

Location		Gauge Number		Strain Data From Field	Strain Data From FEM	FEM Data Higher by
		Field Gauge	FEM Node	E-06	E-06	
Girder 1	Top	A12	B1137	gauge failed		
	Bottom	A11	B1407	-7.6	-8.0	5%
	Bottom	A13	B1138	-12.6	-13.1	4%
	Top	A14	B1182	-7.4	-8.1	9%
	Bottom	A15	B1092	10.0	10.7	7%
Girder 2	Top	A22	B1145	gauge failed		
	Bottom	A21	B1406	-10.6	-11.3	6%
	Bottom	A23	B1146	-6.7	-7.2	7%
	Top	A24	B1392	-3.5	-3.7	5%
	Bottom	A25	B1148	12.8	13.1	3%
Girder 3	Top	A31	B1170	8.0	8.7	8%
	Bottom	A32	B1171	-3.0	-3.3	8%
Girder 4	Top	A41	B1174	2.4	2.5	2%
	Bottom	A42	B1175	-3.6	-3.8	6%
Girder 5	Top	A51	B1176	1.4	1.5	4%
	Bottom	A52	B1178	-0.3	-0.3	10%
Girder 6	Top	A61	B1179	-1.1	-1.2	7%
	Bottom	A62	B1180	0.9	1.0	5%
Continuity Diaphragm	Top	D1	B1192	-1.8	-1.9	5%
	Bottom	D2	B1136	1.3	1.3	5%
	Top	D3	B1193	2.4	2.5	2%
	Bottom	D4	B1169	-1.2	-1.2	2%
	Top	D5	B1194	0.0	0.1	
	Top	D6	B1365	-1.3	-1.4	1%
	Top	D7	B1373	gauge failed		

Table 10
Comparisons of strains of field data to the FEM models (GT STRUDL) test 3

Location		Gauge Number		Strain Data From Field	Strain Data From FEM	FEM Data Higher by
		Field Gauge	FEM Node	E-06	E-06	
Girder 1	Bottom	A11	B1407	-8.2	-8.5	4%
	Top	A12	B1137	11.9	12.3	3%
	Bottom	A13	B1138	-5.3	-5.4	2%
	Top	A14	B1182	-2.9	-3.2	8%
	Bottom	A15	B1092	9.5	10.3	8%
Girder 2	Bottom	A21	B1406	-9.9	-10.6	7%
	Top	A22	B1145	1.8	1.9	5%
	Bottom	A23	B1146	-3.8	-4.1	6%
	Top	A24	B1392	-4.6	-4.8	4%
	Bottom	A25	B1148	14.3	15.5	8%
Girder 3	Top	A31	B1170	9.0	9.6	7%
	Bottom	A32	B1171	-2.2	-2.3	6%
Girder 4	Top	A41	B1174	3.0	3.1	5%
	Bottom	A42	B1175	3.3	3.5	5%
Girder 5	Top	A51	B1176	1.5	1.5	2%
	Bottom	A52	B1178	-0.4	-0.4	3%
Girder 6	Top	A61	B1179	-1.0	-1.1	10%
	Bottom	A62	B1180	3.4	3.5	4%
Continuity Diaphragm	Top	D1	B1192	-1.5	-1.6	6%
	Bottom	D2	B1136	1.2	1.3	7%
	Top	D3	B1193	2.4	2.6	8%
	Bottom	D4	B1169	0.0	0.9	Very small
	Top	D5	B1194	0.0	-0.1	Very small
	Top	D6	B1365	2.4	2.6	6%
	Top	D7	B1373	gauge failed		

Table 11
Comparisons of strains of field data to the FEM models (GT STRUDL) test 4

Location		Gauge Number		Strain Data From Field	Strain Data From FEM	FEM Data Higher by
		Field Gauge	FEM Node	E-06	E-06	
Girder 1	Bottom	A11	B1407	-6.06	-6.72	10%
	Top	A12	B1137	19.6	20.9	6%
	Bottom	A13	B1138	-11.5	-10.6	-8%
	Top	A14	B1182	-3.32	-3.7	10%
	Bottom	A15	B1092	9.95	10.1	1%
Girder 2	Top	A22	B1145	gauge failed		
	Bottom	A21	B1406	-13.1	-13.2	1%
	Bottom	A23	B1146	-12.7	-13.3	5%
	Top	A24	B1392	-20.18	-21.6	7%
	Bottom	A25	B1148	32.96	34.5	4%
Girder 3	Top	A31	B1170	7.91	8.8	10%
	Bottom	A32	B1171	-3.29	-3.6	9%
Girder 4	Top	A41	B1174	1.1	1.22	10%
	Bottom	A42	B1175	-5.95	-6.3	6%
Girder 5	Top	A51	B1176	1.61	1.74	7%
	Bottom	A52	B1178	gauge failed		
Girder 6	Top	A61	B1179	gauge failed		
	Bottom	A62	B1180	2.73	2.87	5%
Continuity Diaphragm	Top	D1	B1192	-3.4	-3.5	3%
	Bottom	D2	B1136	-1.43	-1.5	5%
	Top	D3	B1193	2.6	2.8	7%
	Bottom	D4	B1169	-2.61	-2.75	5%
	Top	D5	B1194	-1.88	-2.09	10%
	Top	D6	B1365	2.88	3.2	10%
	Top	D7	B1373	2.82	2.9	3%

Table 12
Comparisons of strains of field data to the FEM models (GT STRUDL) test 5

Location		Gauge Number		Strain Data From Field	Strain Data From FEM	FEM Data Higher by
		Field Gauge	FEM Node	E-06	E-06	
Girder 1	Bottom	A11	B1407	-10.1	-10.2	1%
	Top	A12	B1137	26.5	27.5	4%
	Bottom	A13	B1138	-43.9	-44.7	2%
	Top	A14	B1182	-4.38	-4.6	5%
	Bottom	A15	B1092	7.96	8.46	6%
Girder 2	Bottom	A21	B1406	-16.2	-16.3	1%
	Top	A22	B1145	-1.93	-2.1	8%
	Bottom	A23	B1146	-14.1	-14.3	1%
	Bottom	A25	B1148	24.5	27.2	10%
	Top	A24	B1392	gauge failed		
Girder 3	Top	A31	B1170	15.95	16	0%
	Bottom	A32	B1171	-6.77	-6.8	0%
Girder 4	Top	A41	B1174	-5.84	-6.4	9%
	Bottom	A42	B1175	4.93	4.9	-1%
Girder 5	Top	A51	B1176	1.74	1.75	1%
	Bottom	A52	B1178	0.87	0.9	3%
Girder 6	Top	A61	B1179	1.9	1.82	-4%
	Bottom	A62	B1180	2.88	2.96	3%
Continuity Diaphragm	Top	D1	B1192	-5.84	-6.4	9%
	Bottom	D2	B1136	-3.98	-4.2	5%
	Top	D3	B1193	2.72	2.9	6%
	Bottom	D4	B1169	-2.58	-2.8	8%
	Top	D5	B1194	-2.04	-2.1	3%
	Top	D6	B1365	1.92	2.1	9%
	Top	D7	B1373	gauge failed		

Table 13
Comparisons of strains of field data to the FEM models (GT STRUDL) test 6

Location		Gauge Number		Strain Data From Field	Strain Data From FEM	FEM Data Higher by
		Field Gauge	FEM Node	E-06	E-06	
Girder 1	Bottom	A11	B1407	-7.08	-7.25	2%
	Top	A12	B1137	12.86	13.8	7%
	Bottom	A13	B1138	-13.4	-14.8	9%
	Top	A14	B1182	-13.87	-14.3	3%
	Bottom	A15	B1092	7.96	8.22	3%
Girder 2	Bottom	A21	B1406	-12.1	-12.2	1%
	Bottom	A23	B1146	-9.27	-9.9	6%
	Top	A24	B1392	-14.1	-14.9	5%
	Bottom	A25	B1148	47	47.2	0%
	Top	A22	B1145	gauge failed		
Girder 3	Top	A31	B1170	17.97	18.7	4%
	Bottom	A32	B1171	-6.8	-7.04	3%
Girder 4	Top	A41	B1174	-7.8	-8.2	5%
	Bottom	A42	B1175	3.97	3.76	-6%
Girder 5	Top	A51	B1176	5.81	5.7	-2%
	Bottom	A52	B1178	-0.59	-0.62	4%
Girder 6	Top	A61	B1179	-3.88	-4.14	6%
	Bottom	A62	B1180	1.92	1.97	3%
Continuity Diaphragm	Bottom	D2	B1136	-1.2	-1.2	0%
	Bottom	D4	B1169	2.87	3.1	7%
	Top	D5	B1194	3.88	4.1	5%
	Top	D6	B1365	2.192	2.4	9%
	Top	D7	B1373	gauge failed		
	Top	D1	B1192	gauge failed		
	Top	D3	B1193	gauge failed		

APPENDIX D

GT STRUDL Input Files for Case I and Case II

Case I Truck location for Maximum Positive Moment in the Girder

Table 14
Maximum stresses in deck top surface of Case I

Distance X , Z (ft)	Joint	Result	Result	Location		Stress (Mpa)	Stress (ksi)
16.25 , 53.15	308119	Sxx	Longitudinal	Top	Max	8.06	1.17
3.4 , 82.68	112621				Min	-4.74	-0.688
1.6 , 110.24	116820	Syy	Transverse	Top	Max	6.59	0.956
3.4 , 82.68	112621				Min	-6.11	-0.887
5.21 , 84.65	112922	Sxy	Shear	Top	Max	2.41	0.35
5.21 , 116.14	117722				Min	-3.1	-0.45

Table 15
Maximum stresses in deck bottom surface of Case I

Distance X , Z (ft)	Joint	Result	Result	Location		Stress (Mpa)	Stress (ksi)
3.4 , 82.68	112621	Sxx	Longitudinal	Bottom	Max	4.74	0.688
16.25, 53.15	308119				Min	-8.06	-1.17
3.4 , 82.68	112621	Syy	Transverse	Bottom	Max	6.08	0.882
1.6 , 110.24	116820				Min	-6.6	-0.957
5.21 , 116.14	117722	Sxy	Shear	Bottom	Max	3.13	0.455
5.21 , 84.65	112922				Min	-2.41	-0.349

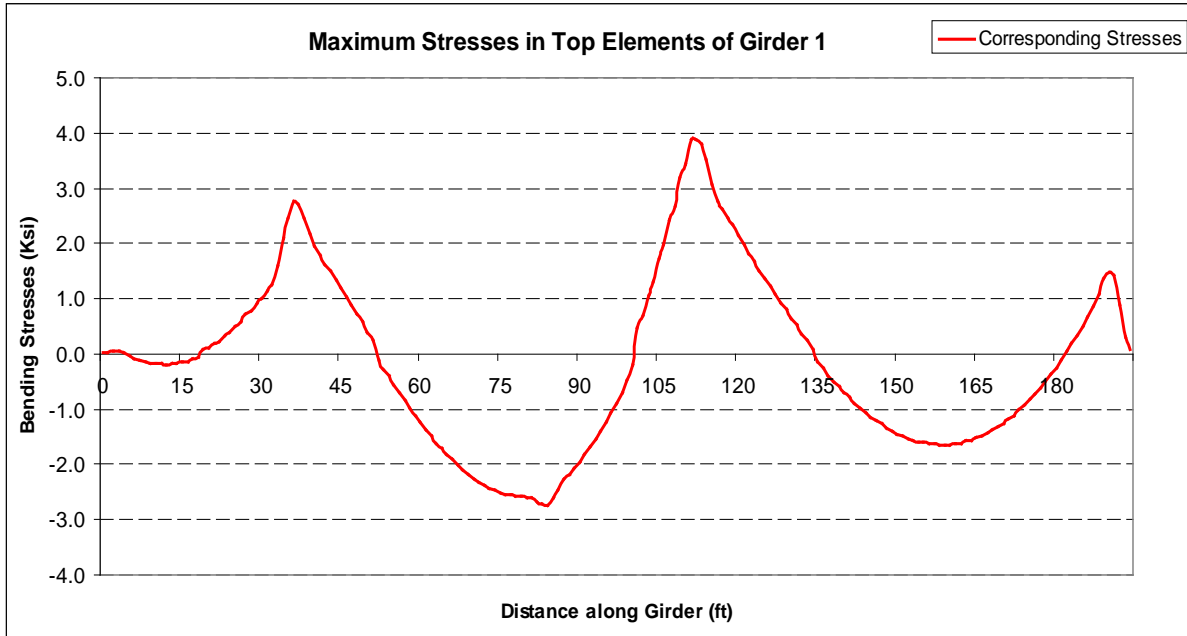


Figure 65
Bending stress distribution of top elements in Girder 1 of Case I

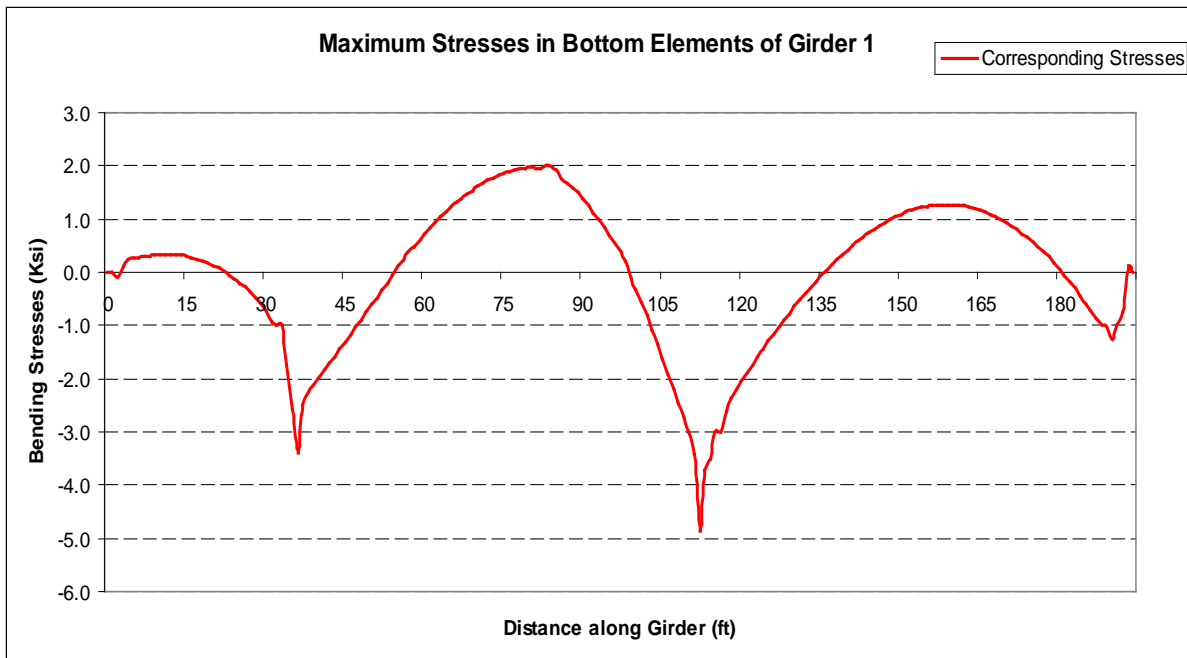


Figure 66
Bending stress distribution of bottom elements in Girder 1 of Case I

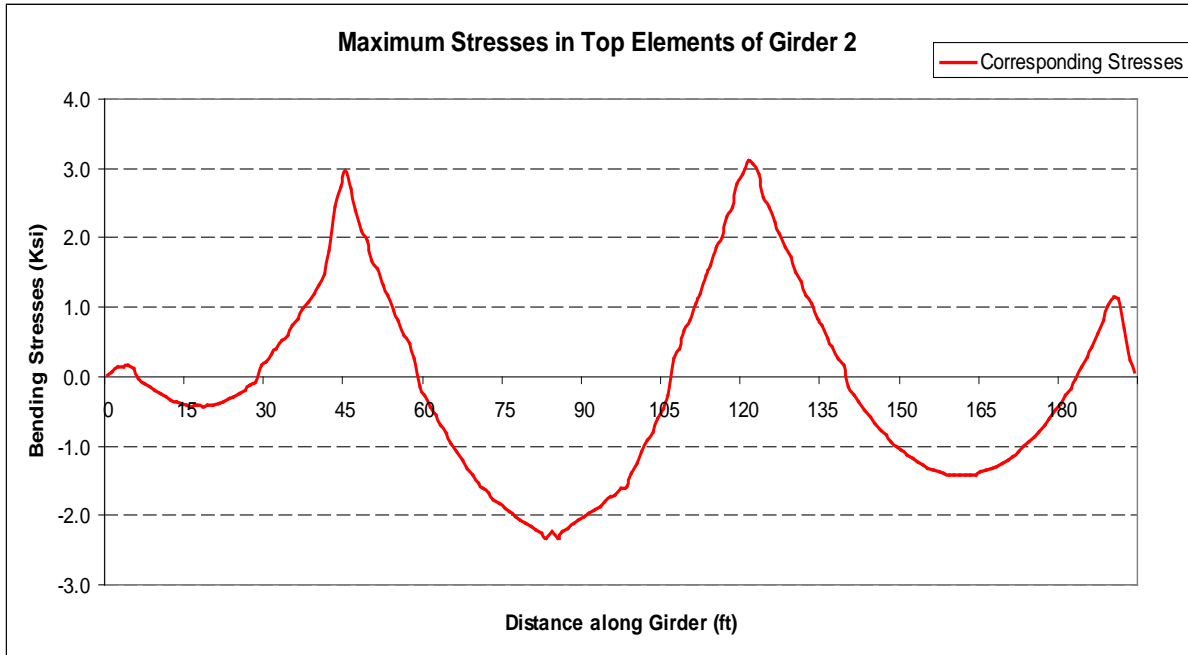


Figure 67
Bending stress distribution of top elements in Girder 2 of Case I

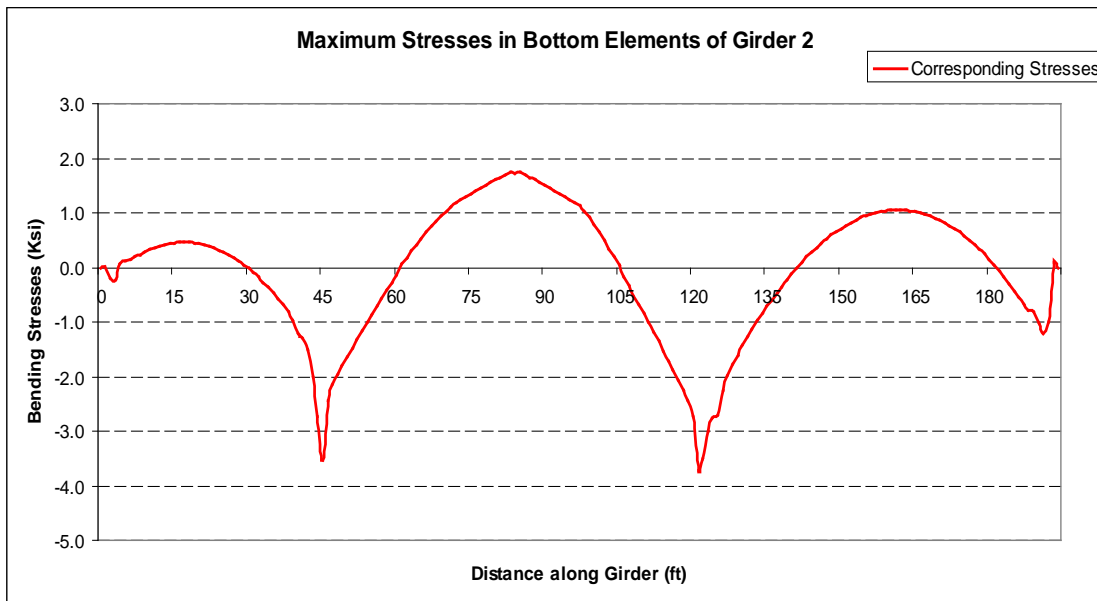


Figure 68
Bending stress distribution of bottom elements in Girder 2 of Case I

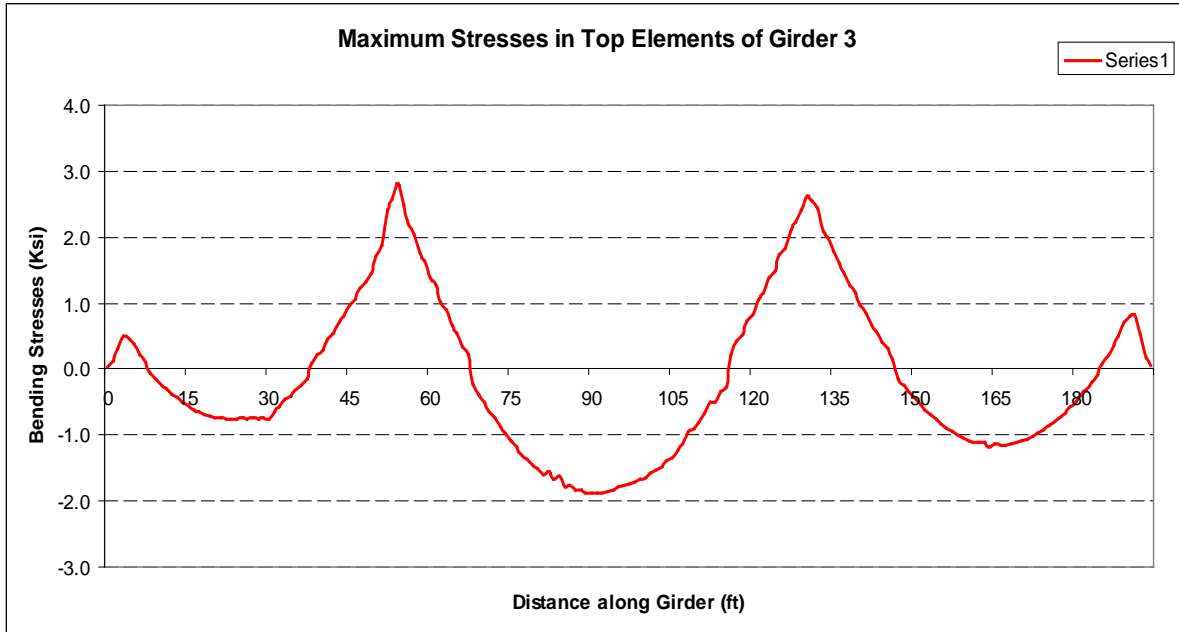


Figure 69
Bending stress distribution of top elements in Girder 3 of Case I

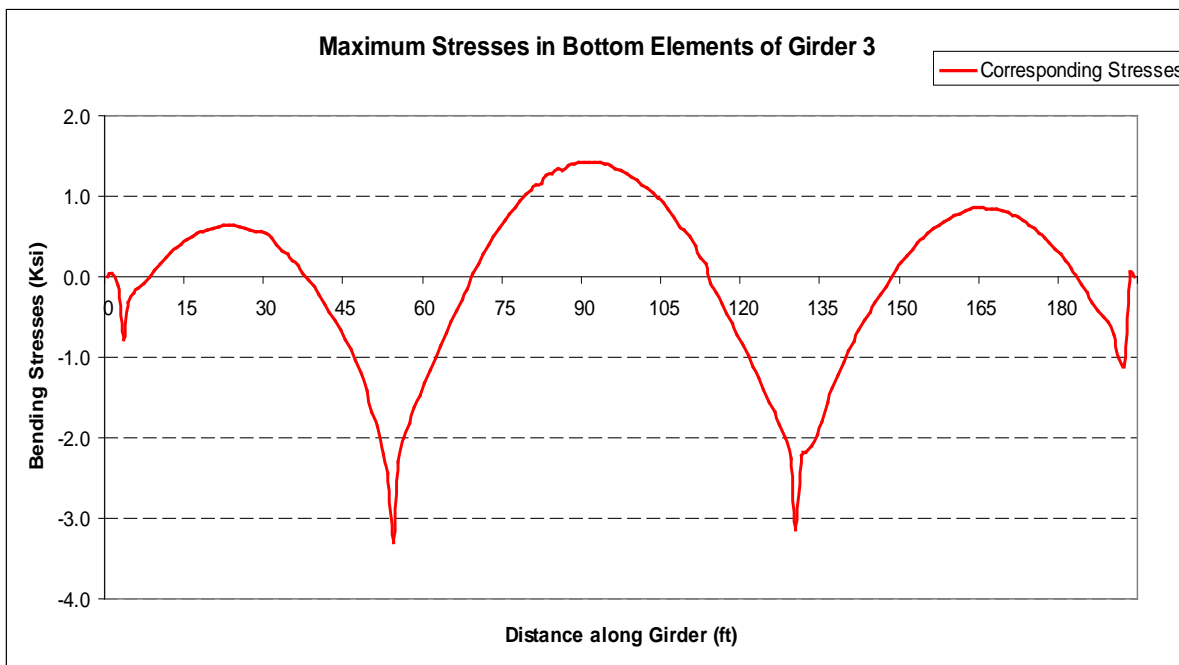


Figure 70
Bending stress distribution of bottom elements in Girder 3 of Case I

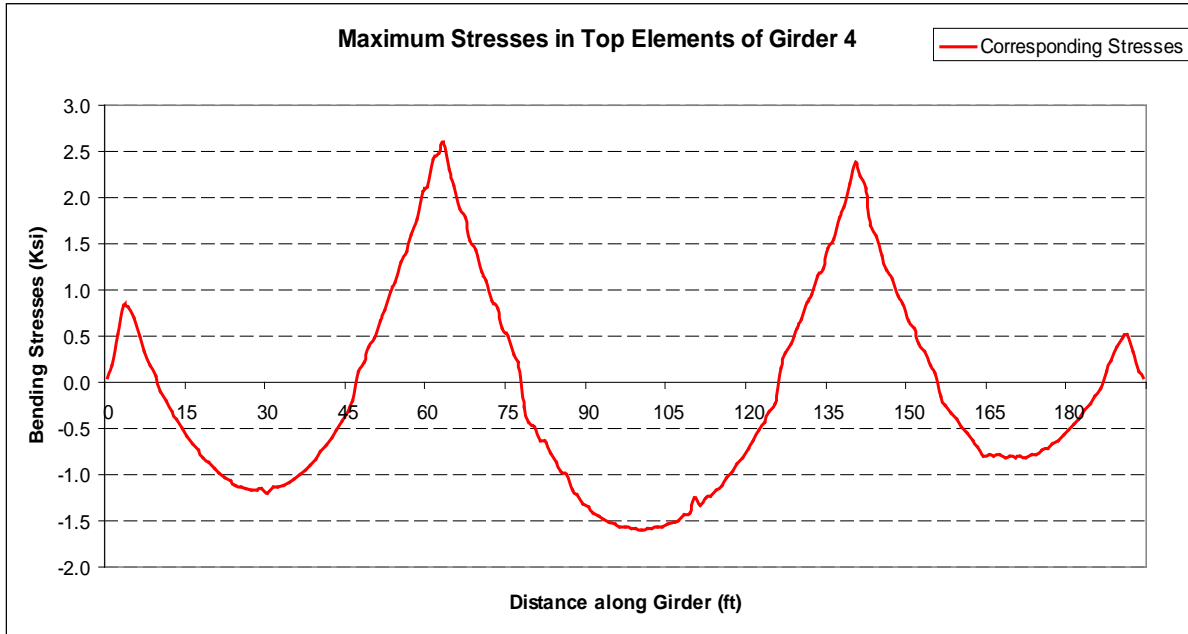


Figure 71
Bending stress distribution of top elements in Girder 4 of Case I

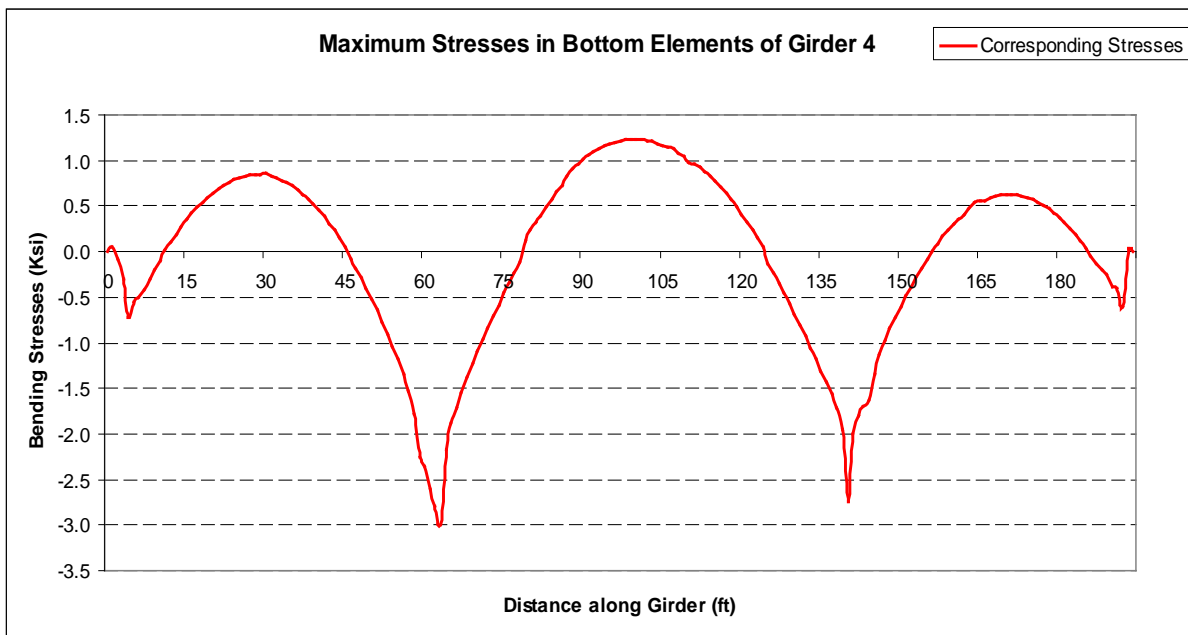


Figure 72
Bending stress distribution of bottom elements in Girder 4 of Case I

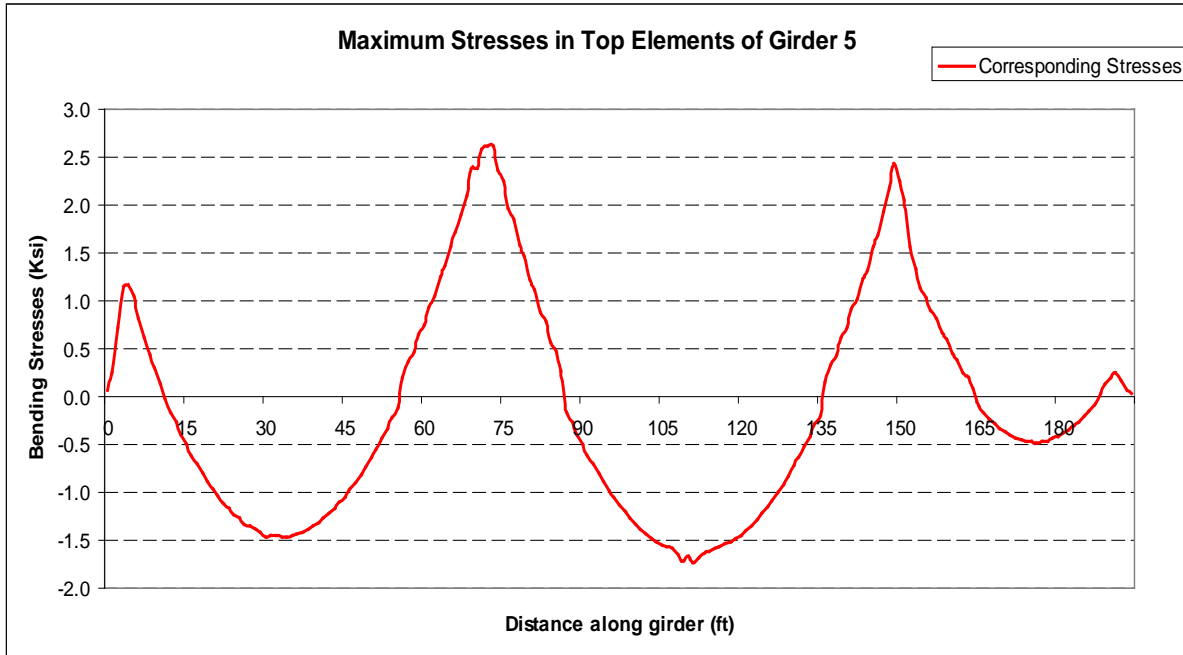


Figure 73
Bending stress distribution of top elements in Girder 5 of Case I

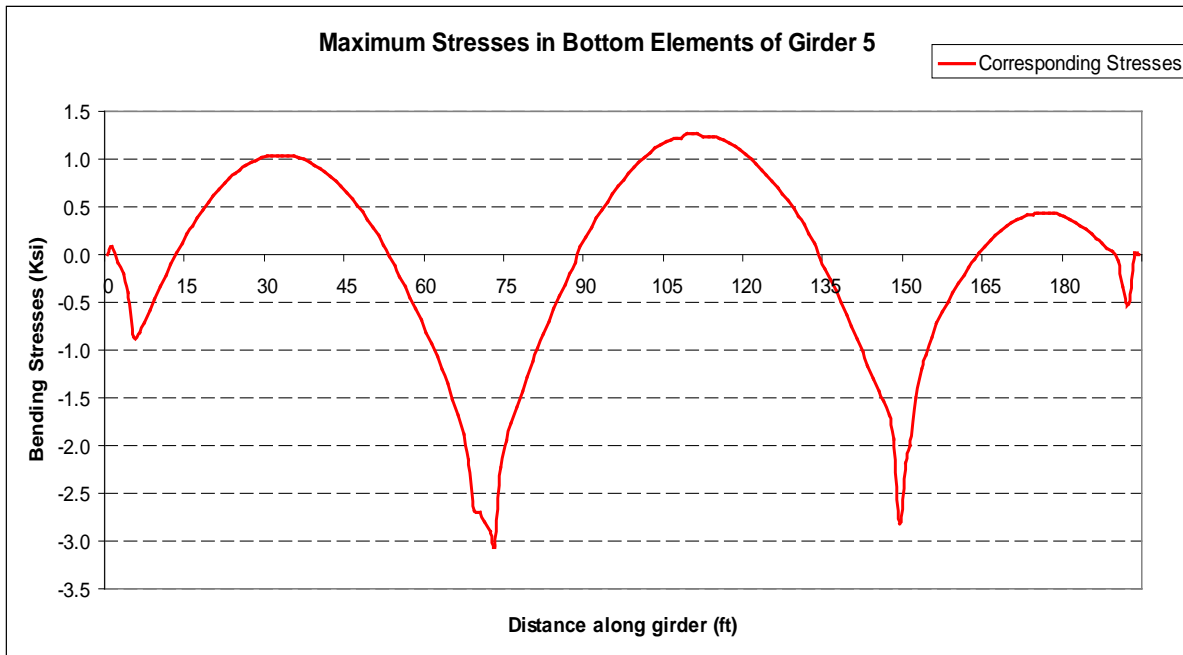


Figure 74
Bending stress distribution of bottom elements in Girder 5 of Case I

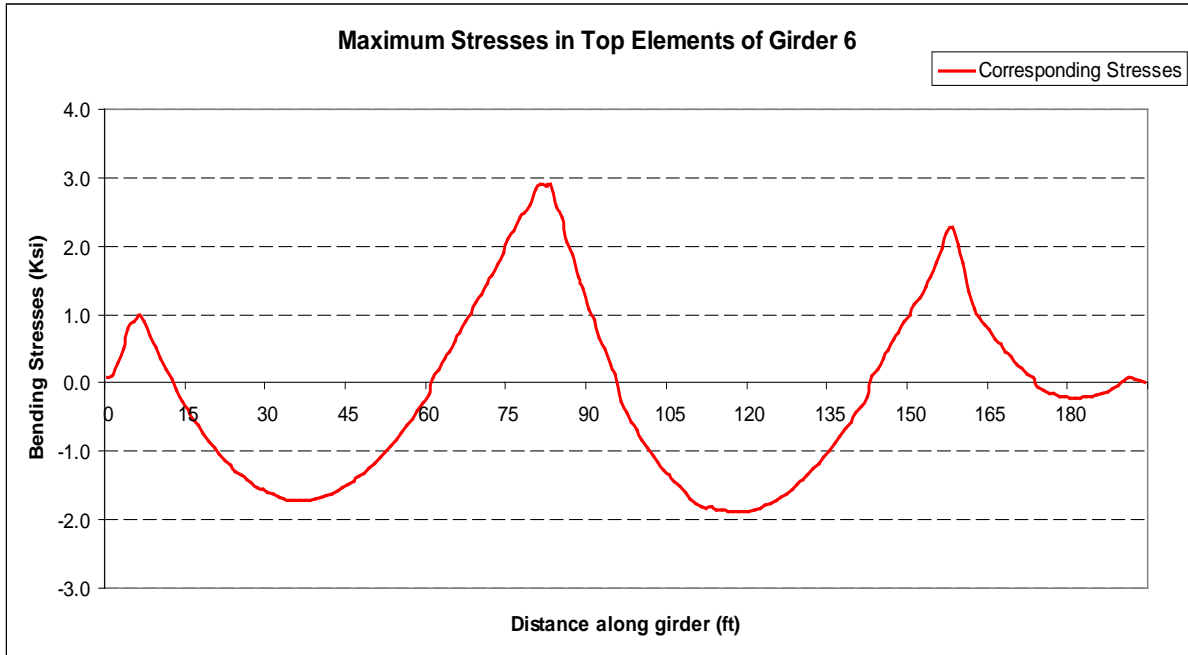


Figure 75
Bending stress distribution of top elements in Girder 6 of Case I

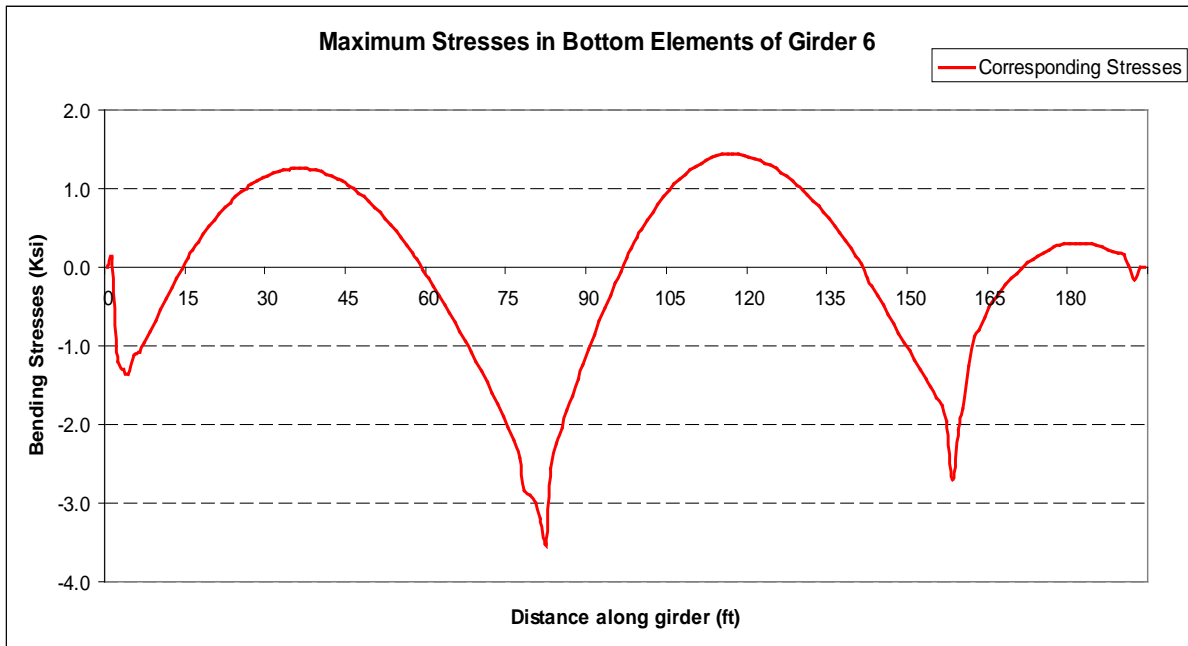


Figure 76
Bending stress distribution of bottom elements in Girder 6 of Case I

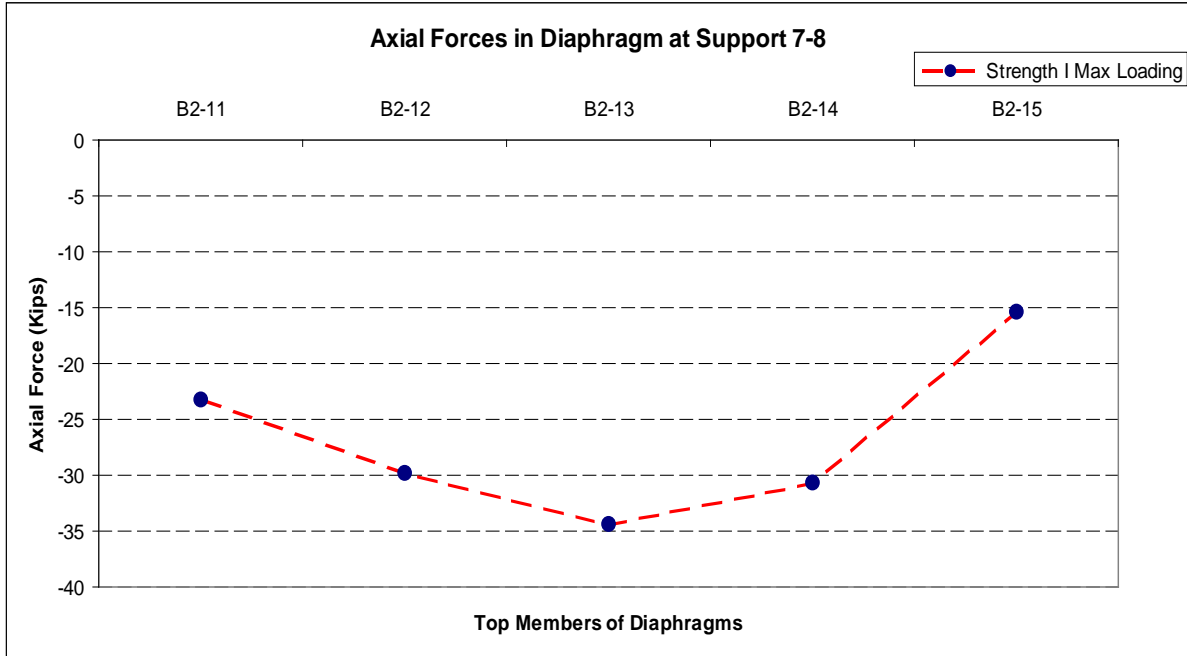


Figure 77
Bending stress distribution of bottom elements in Girder 6 of Case I

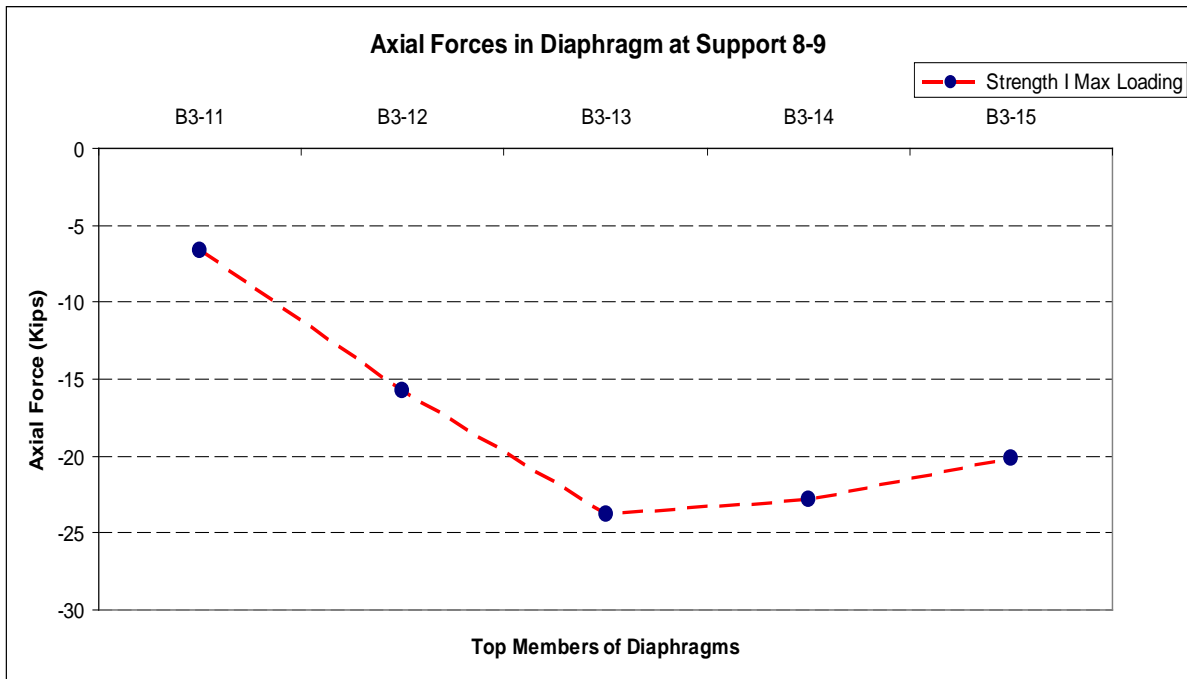


Figure 78
Axial force distribution in continuity diaphragm at support Span8-9 for Case I

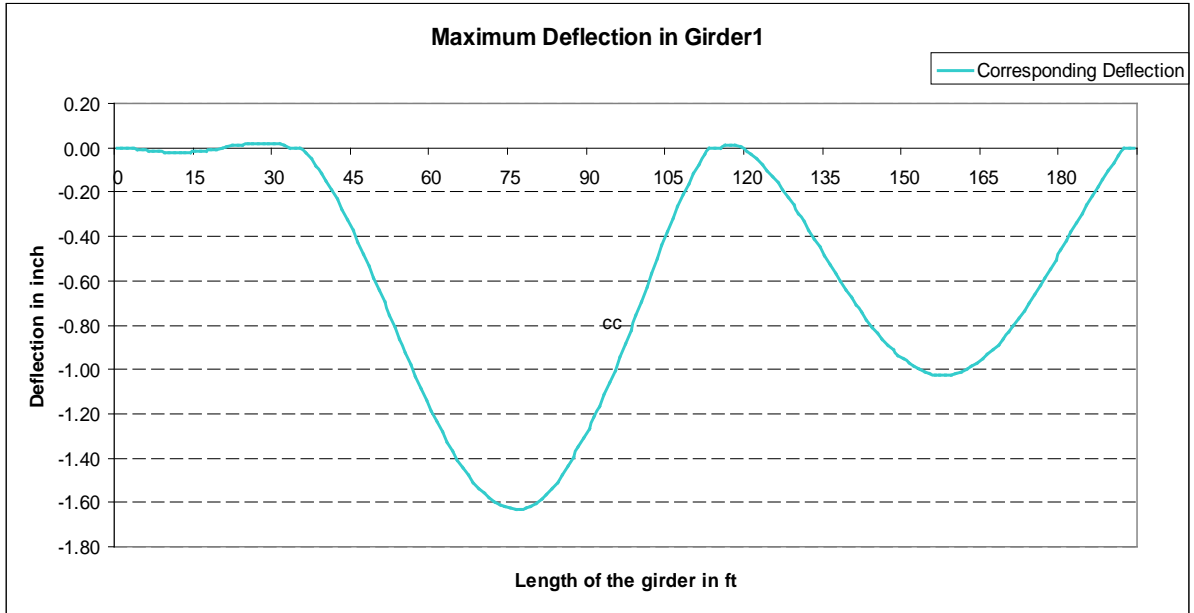


Figure 79
Maximum deflection in Girder 1 of Case I

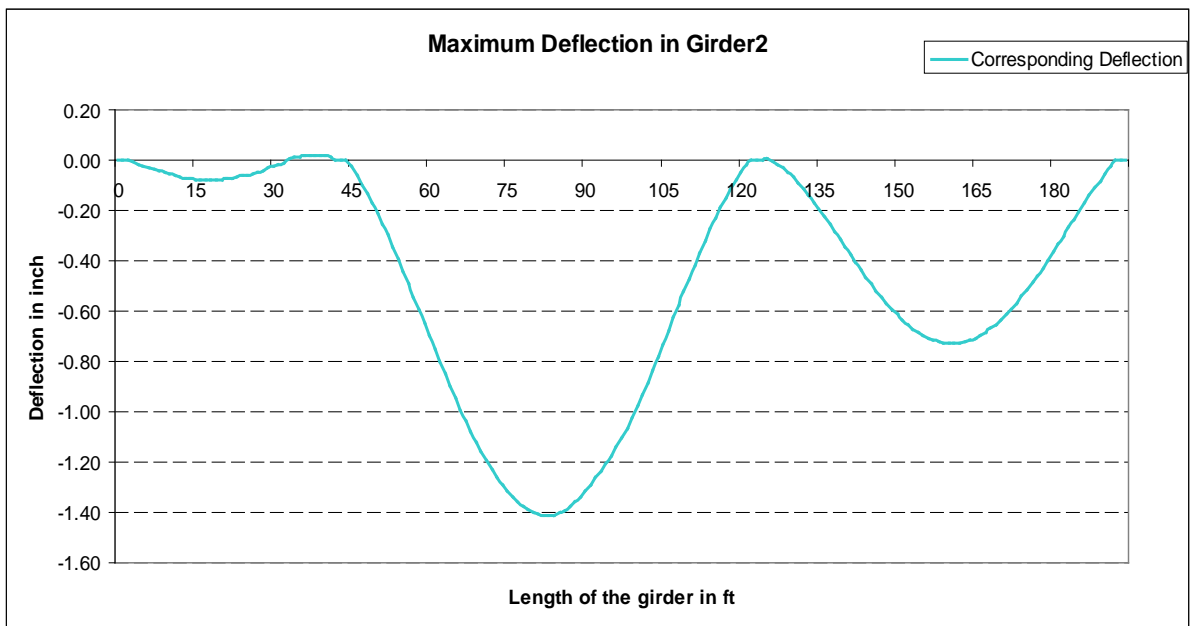


Figure 80
Maximum deflection in Girder 2 of Case I

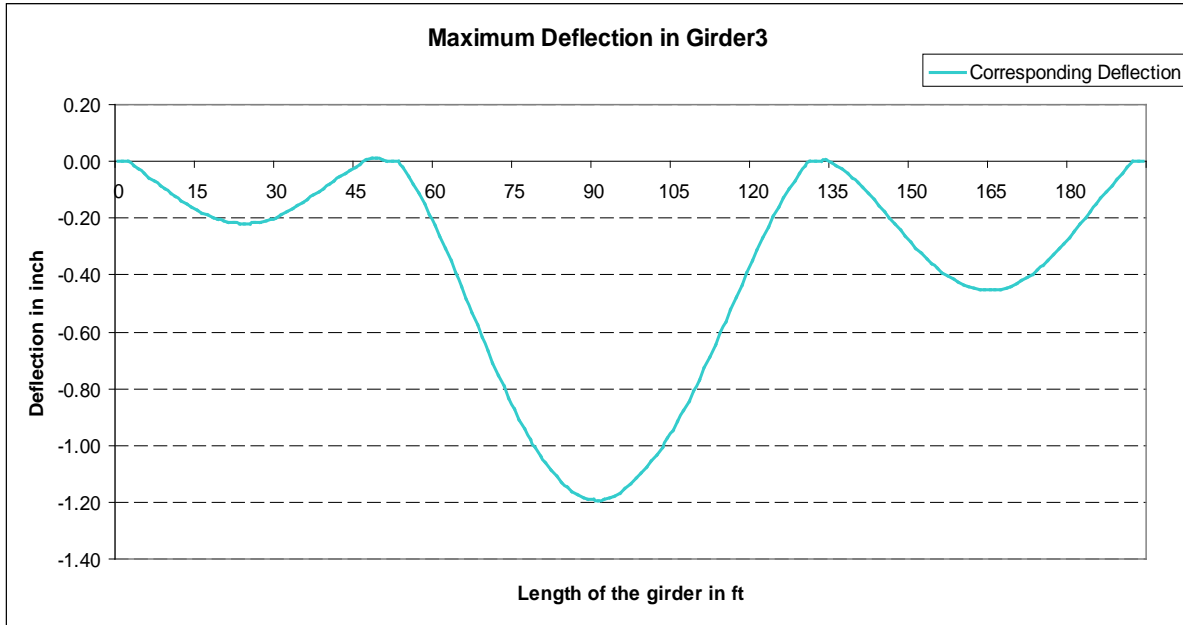


Figure 81
Maximum deflection in Girder 3 of Case I

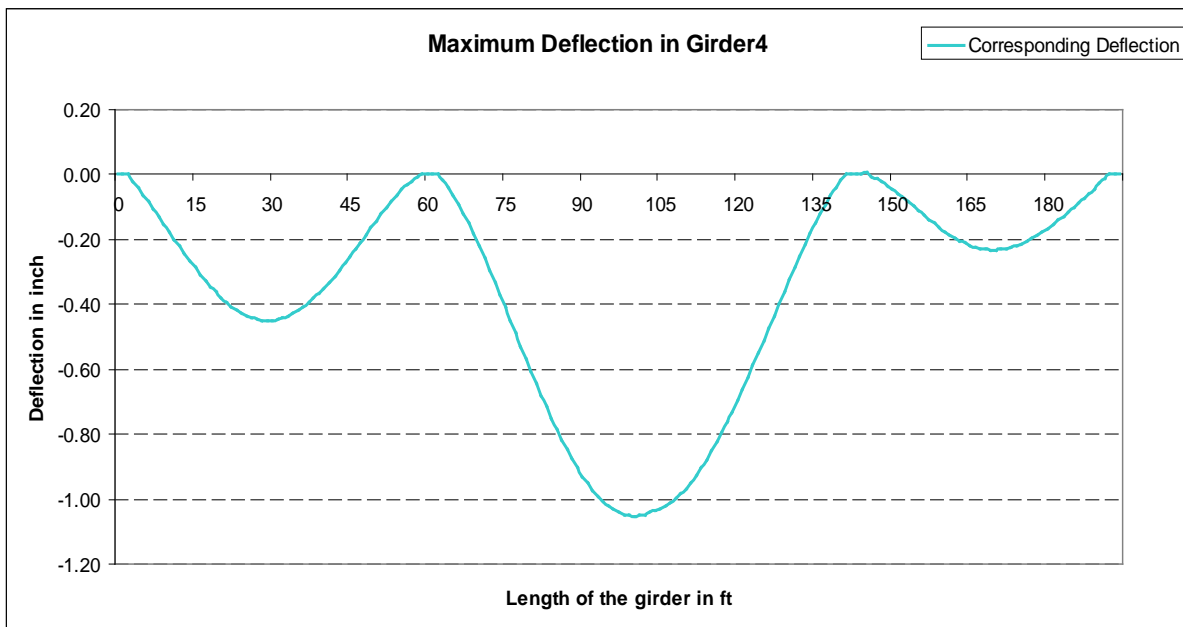


Figure 82
Maximum deflection in Girder 4 of Case I

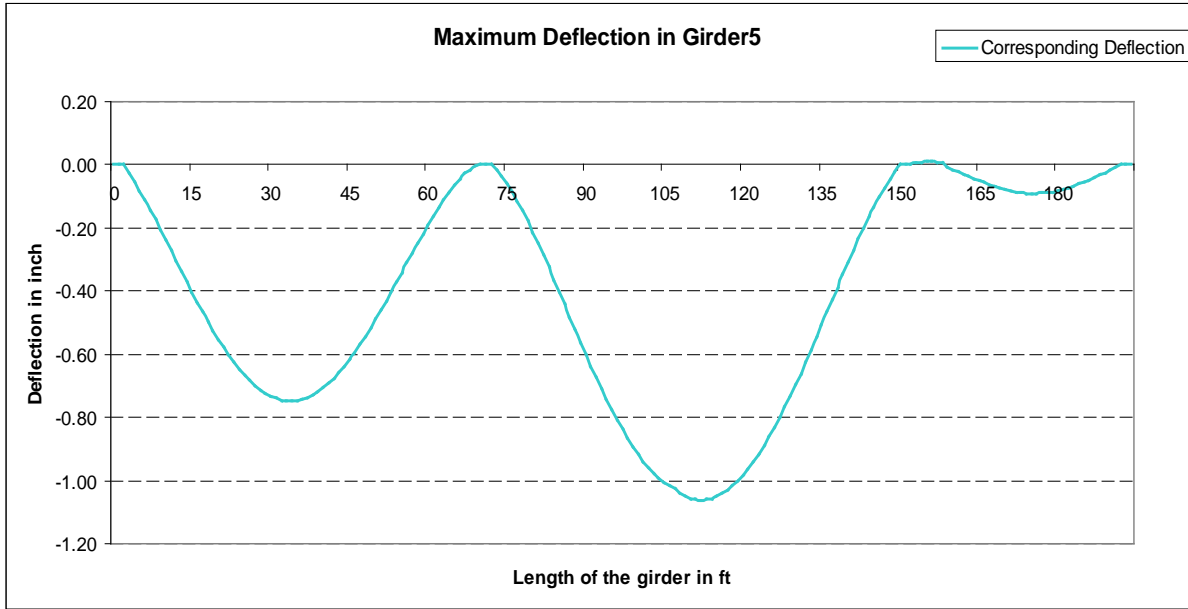


Figure 83
Maximum deflection in Girder 5 of Case I

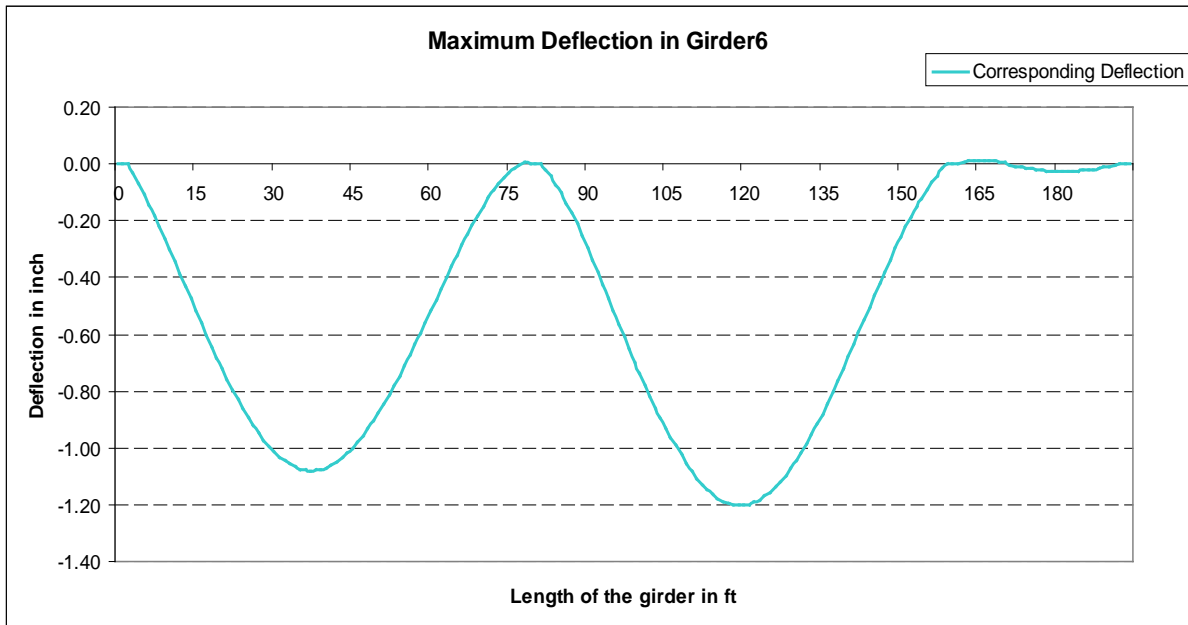


Figure 84
Maximum deflection in Girder 6 of Case I

Case II Truck Location for Maximum Negative Moment in the Girder

Table 16
Maximum stresses in deck top surface of Case II

Distance X , Z (ft)	Joint	Result	Result	Location		Stress (Mpa)	Stress (ksi)
16.25 , 53.15	308119	Sxx	Longitudinal	Top	Max	9.03	1.31
5.21 , 76.77	111722				Min	-6.89	-1.0
1.6 , 110.24	116820	Syy	Transverse	Top	Max	6.0	0.87
5.21 , 76.77	111722				Min	-6.83	-0.99
7.01 , 78.74	112023	Sxy	Shear	Top	Max	2.43	0.352
13.21 , 49.21	207522				Min	-3.38	0.49

Table 17
Maximum stresses in deck bottom surface of Case II

Distance X , Z (ft)	Joint	Result	Result	Location		Stress (Mpa)	Stress (ksi)
5.21 , 76.77	111722	Sxx	Longitudinal	Bottom	Max	6.89	1.0
16.25 , 53.15	308119				Min	-9.03	-1.31
5.206 , 76.77	111722	Syy	Transverse	Bottom	Max	6.77	0.983
1.6 , 110.24	116820				Min	-6.0	-0.87
13.21 , 49.21	207522	Sxy	Shear	Bottom	Max	3.38	0.49
7.02 , 78.74	112023				Min	-2.43	-0.352

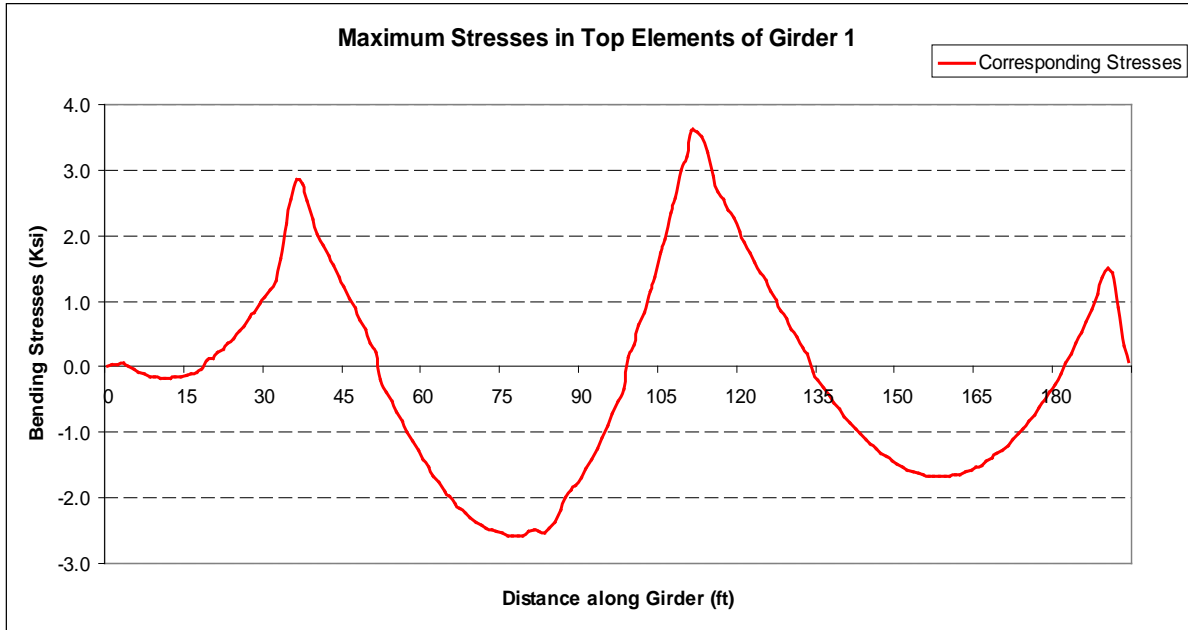


Figure 85
Bending stress distribution of top elements in Girder 1 of Case II

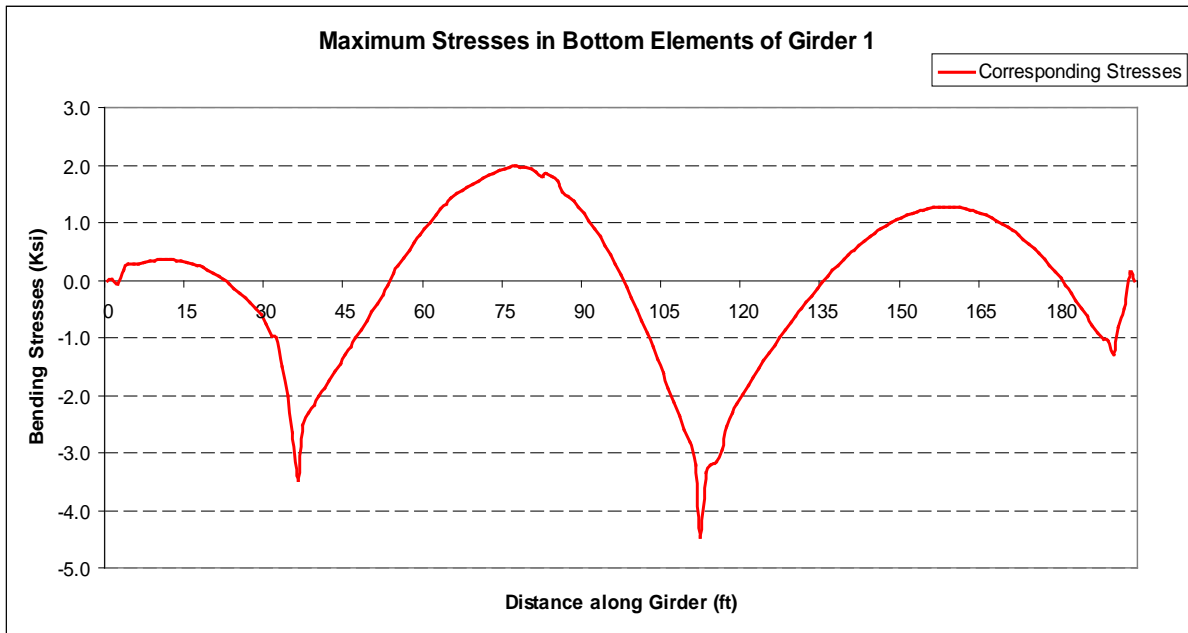


Figure 86
Bending stress distribution of bottom elements in Girder 1 of Case II

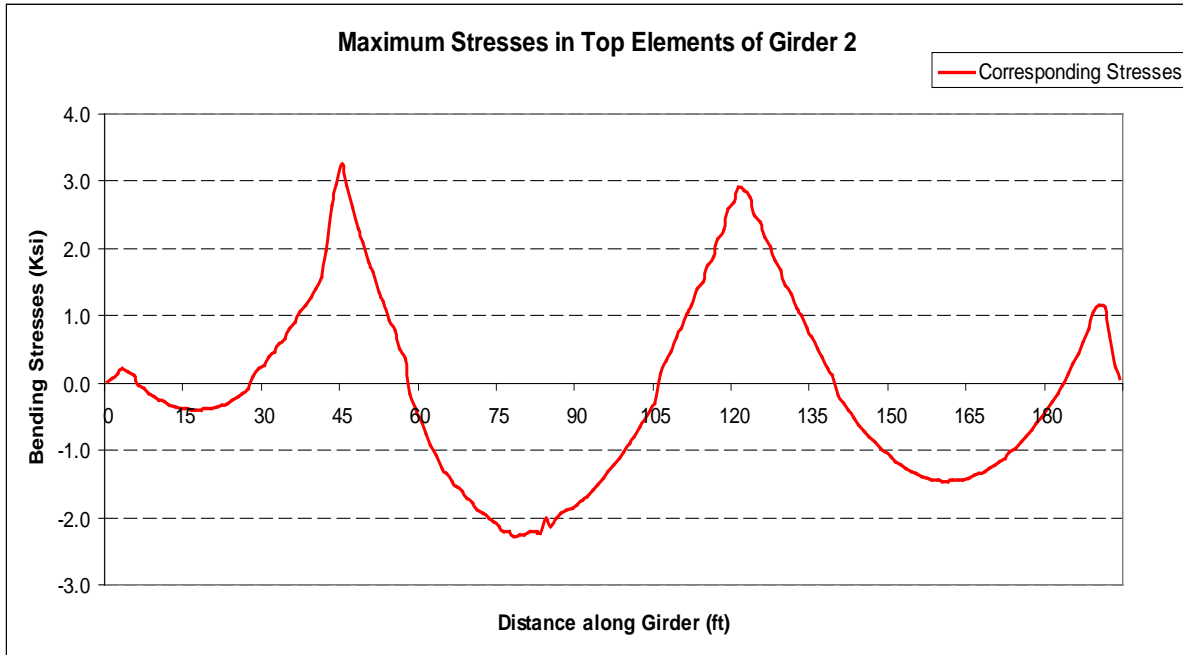


Figure 87
Bending stress distribution of top elements in Girder 2 of Case II

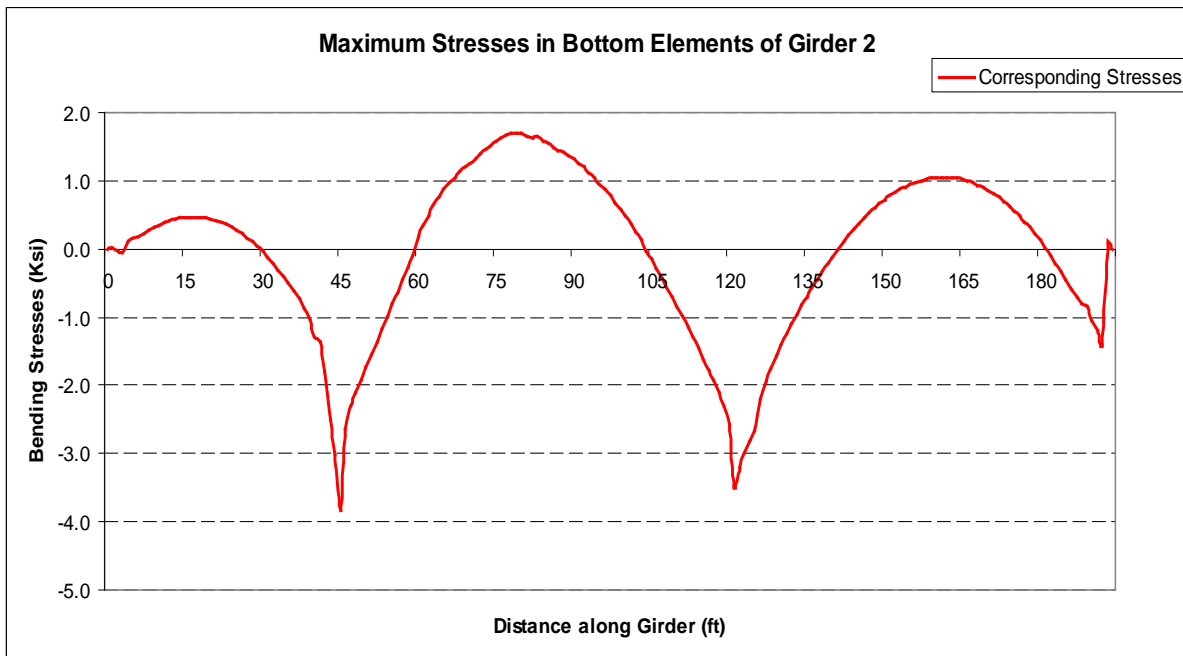


Figure 88
Bending stress distribution of bottom elements in Girder 2 of Case II

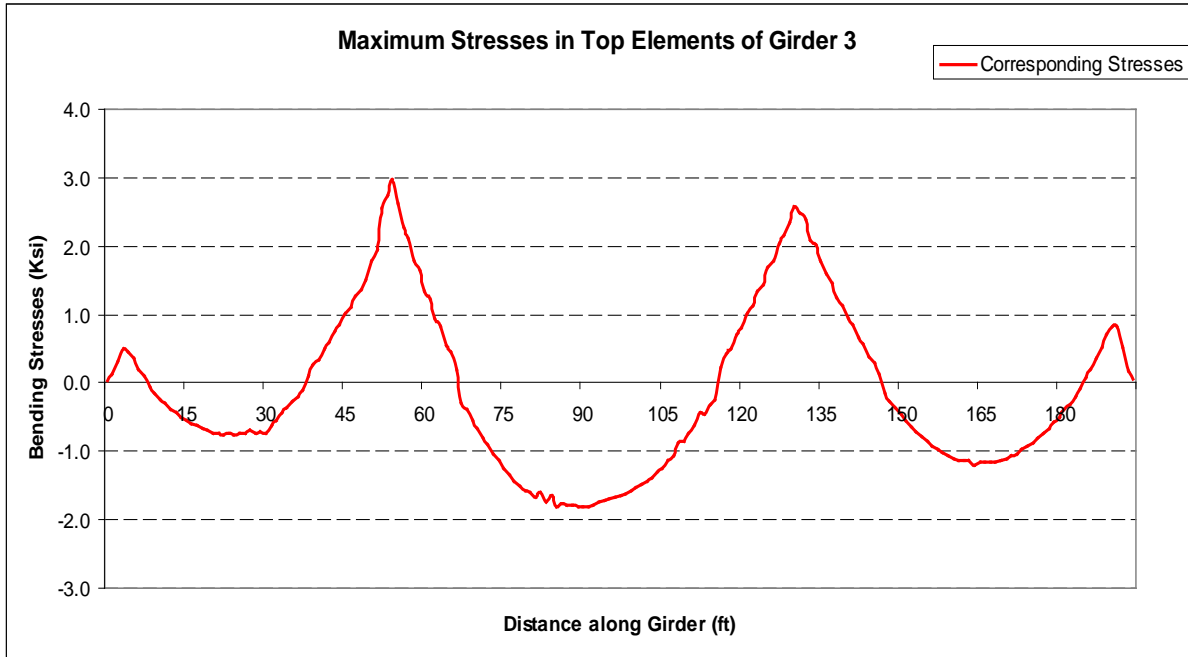


Figure 89
Bending stress distribution of top elements in Girder 3 of Case II

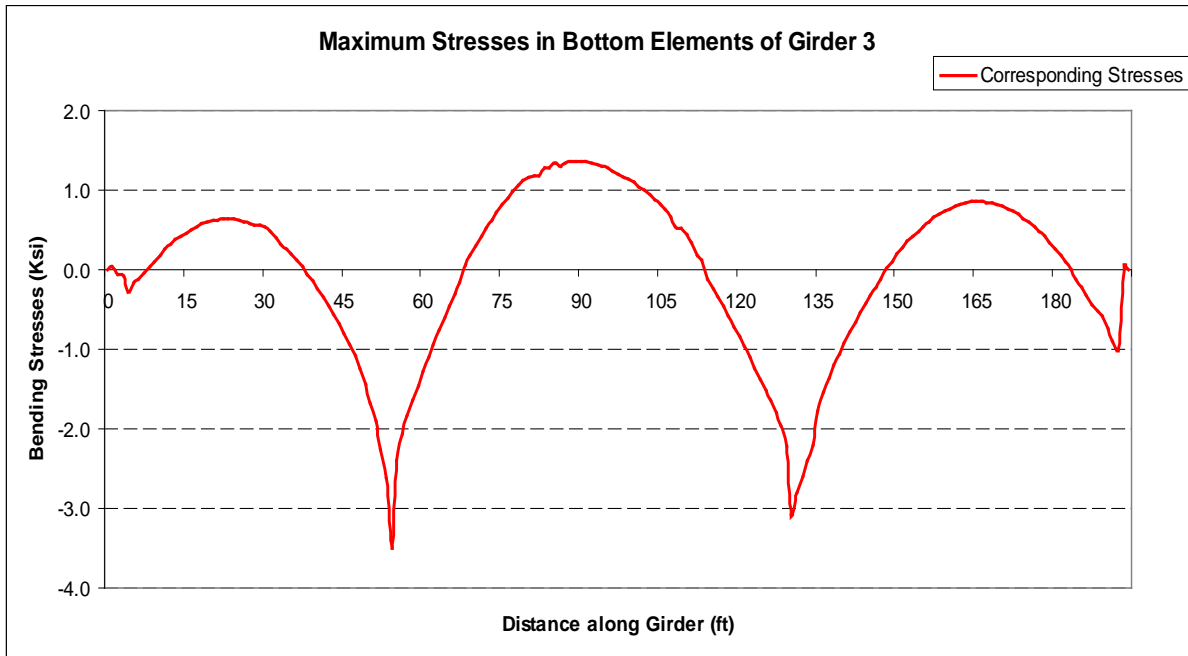


Figure 90
Bending stress distribution of bottom elements in Girder 3 of Case II

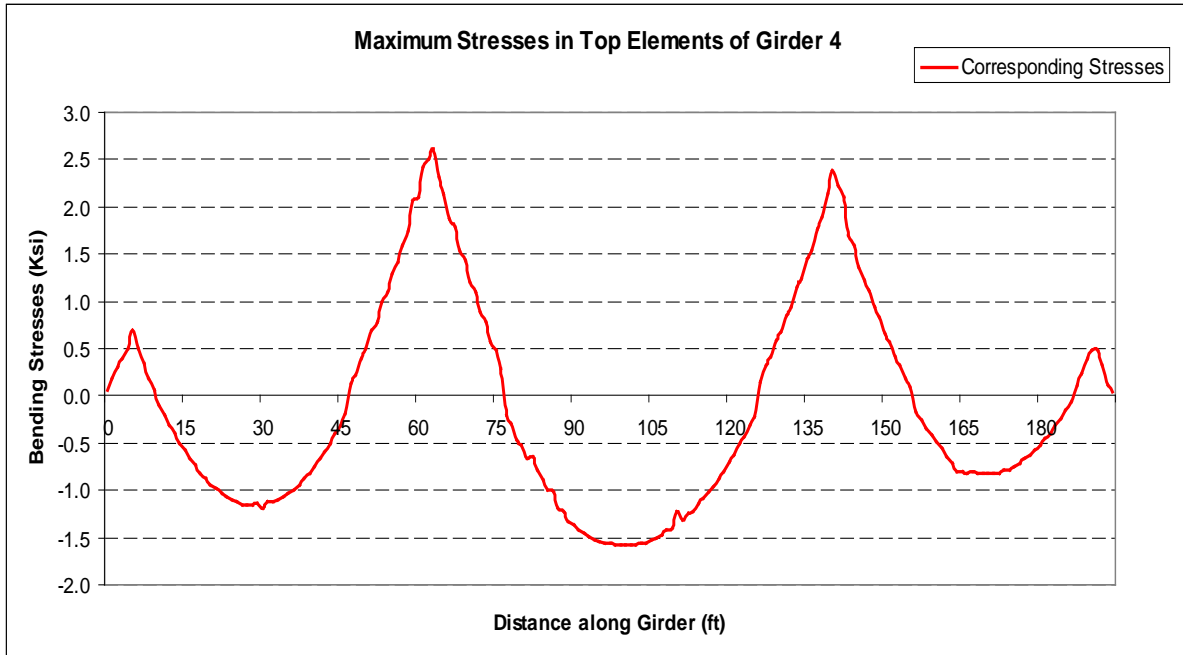


Figure 91
Bending stress distribution of top elements in Girder 4 of Case II

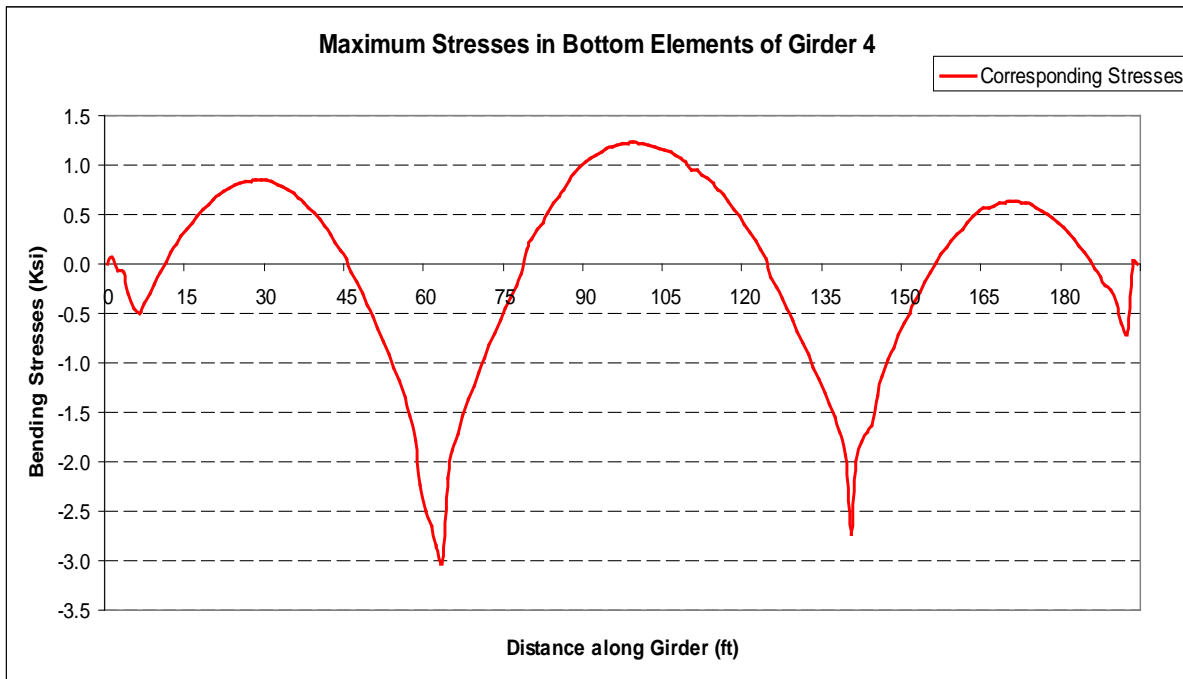


Figure 92
Bending stress distribution of bottom elements in Girder 4 of Case II

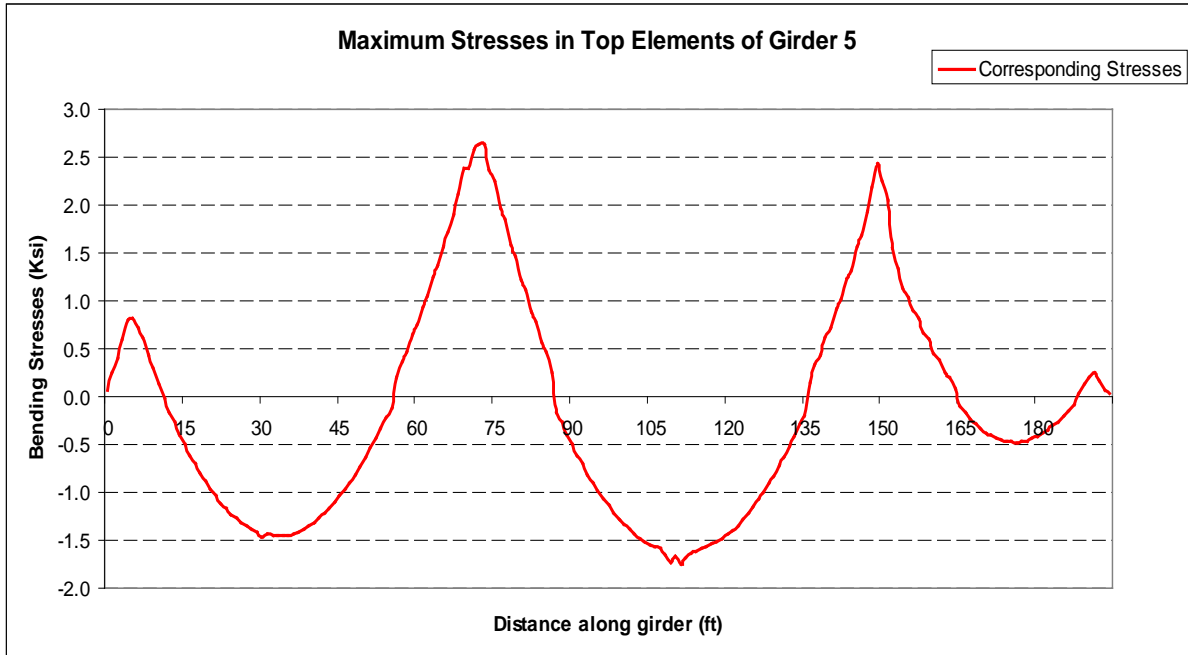


Figure 93
Bending stress distribution of top elements in Girder 5 of Case II

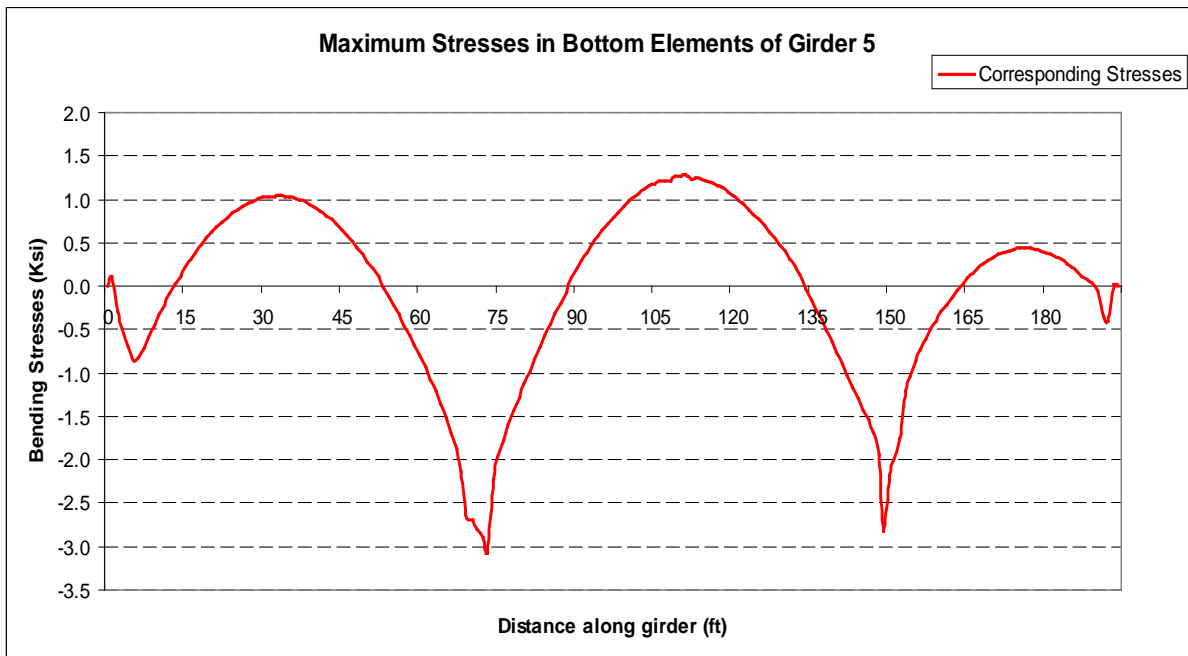


Figure 94
Bending stress distribution of bottom elements in Girder 5 of Case II

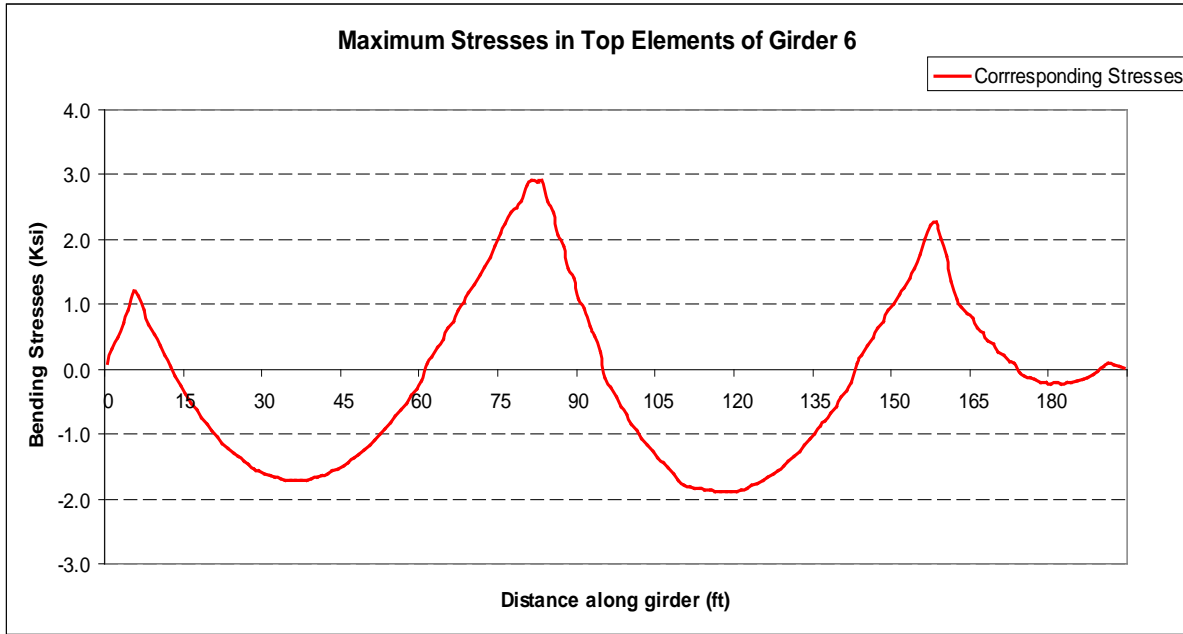


Figure 95
Bending stress distribution of top elements in Girder 6 of Case II

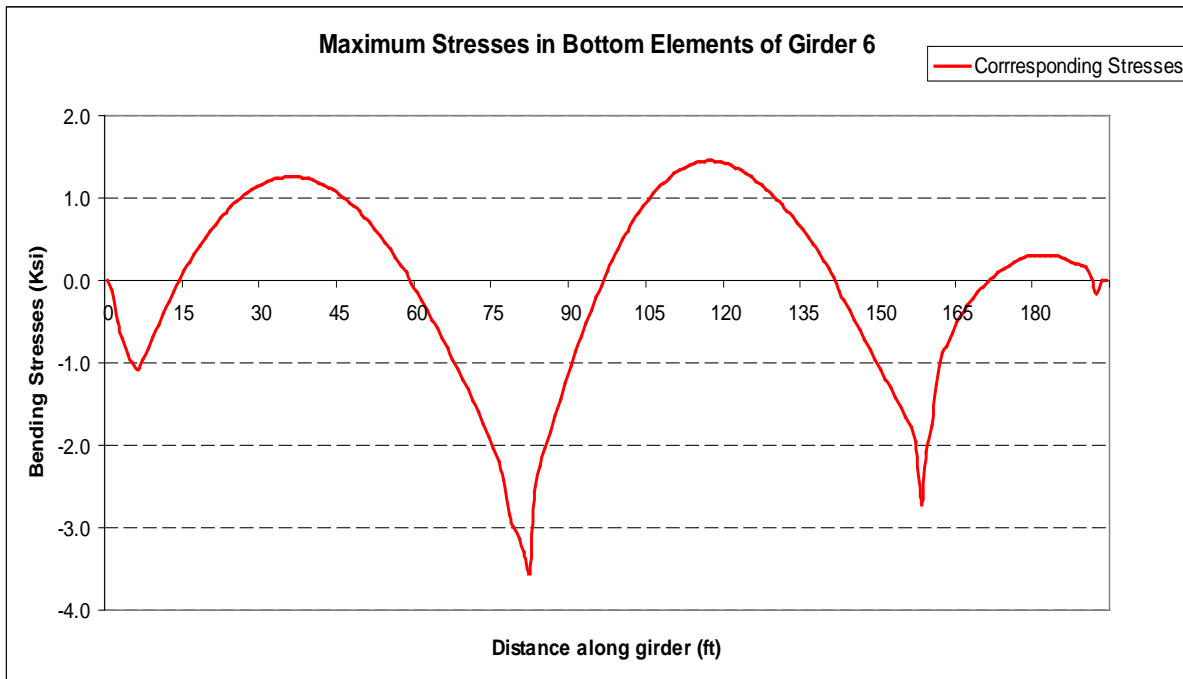


Figure 96
Bending stress distribution of bottom elements in Girder 6 of Case II

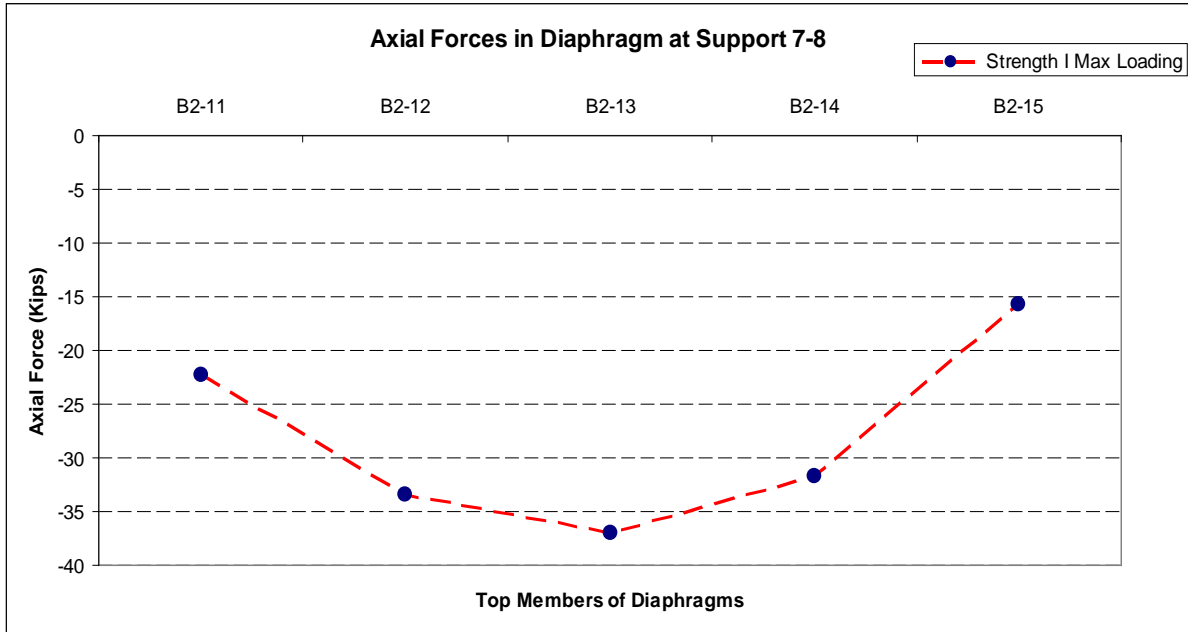


Figure 97
Axial force distribution in continuity diaphragm at support Span7-8 for Case II

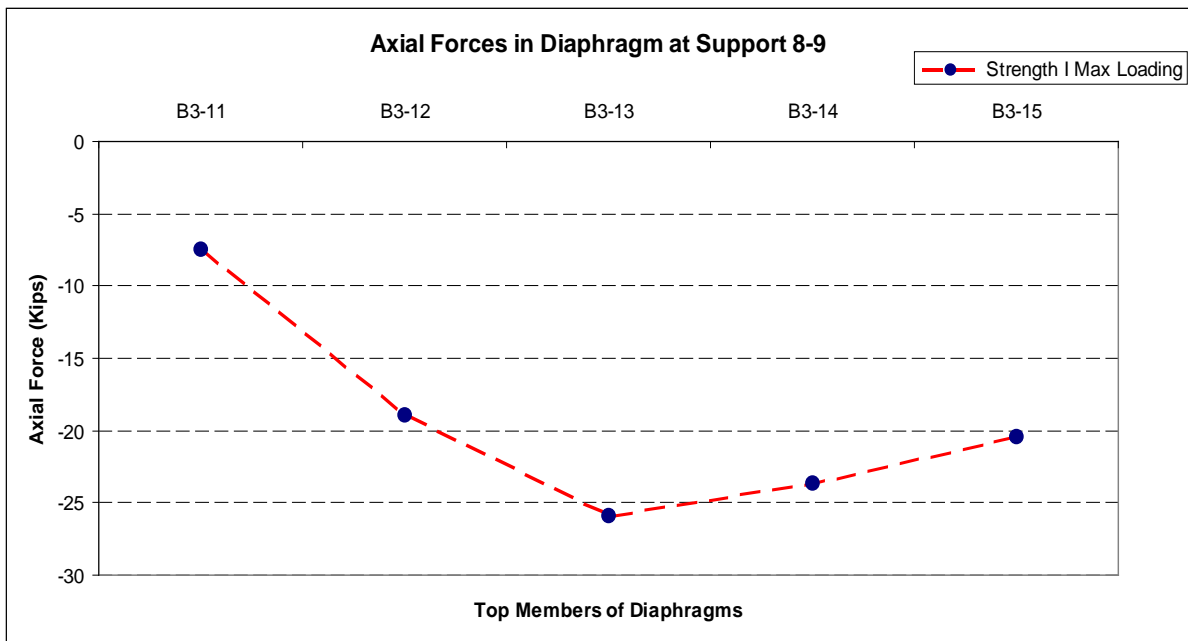


Figure 98
Axial force distribution in continuity diaphragm at support Span8-9 for Case II

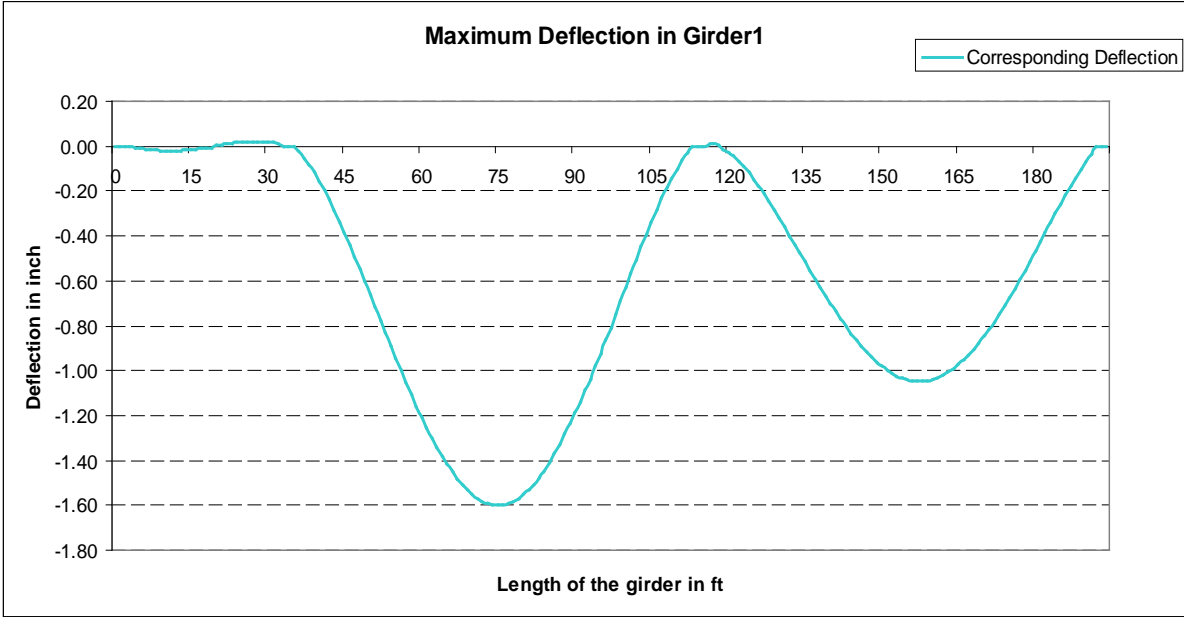


Figure 99
Maximum deflection in Girder 1 of Case II

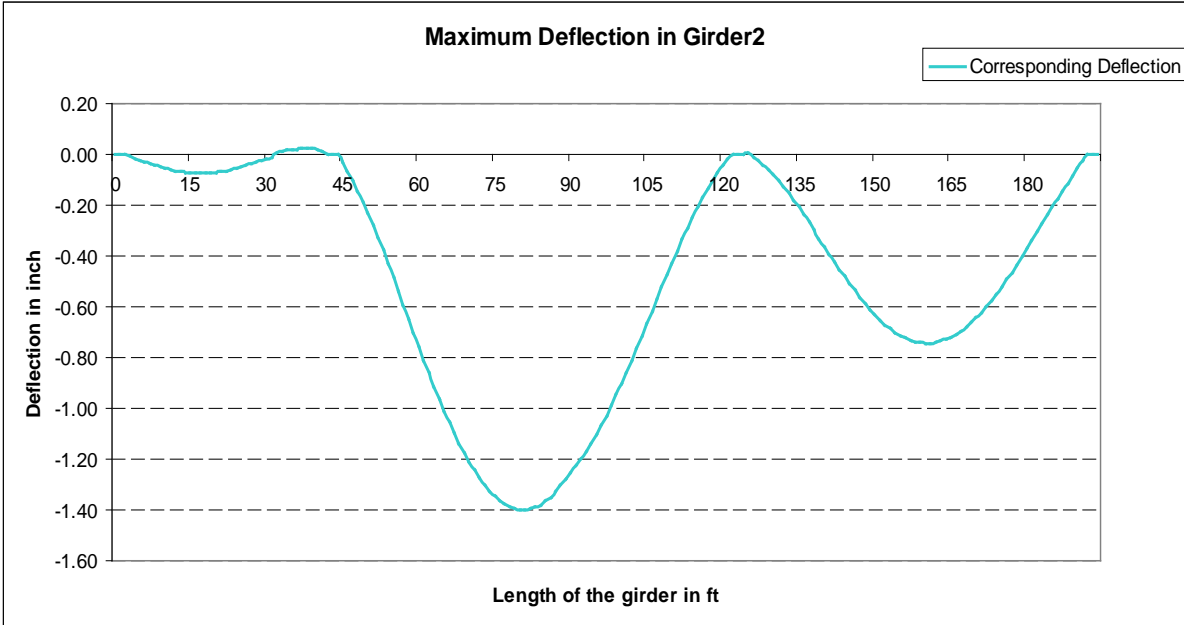


Figure 100
Maximum deflection in Girder 2 of Case II

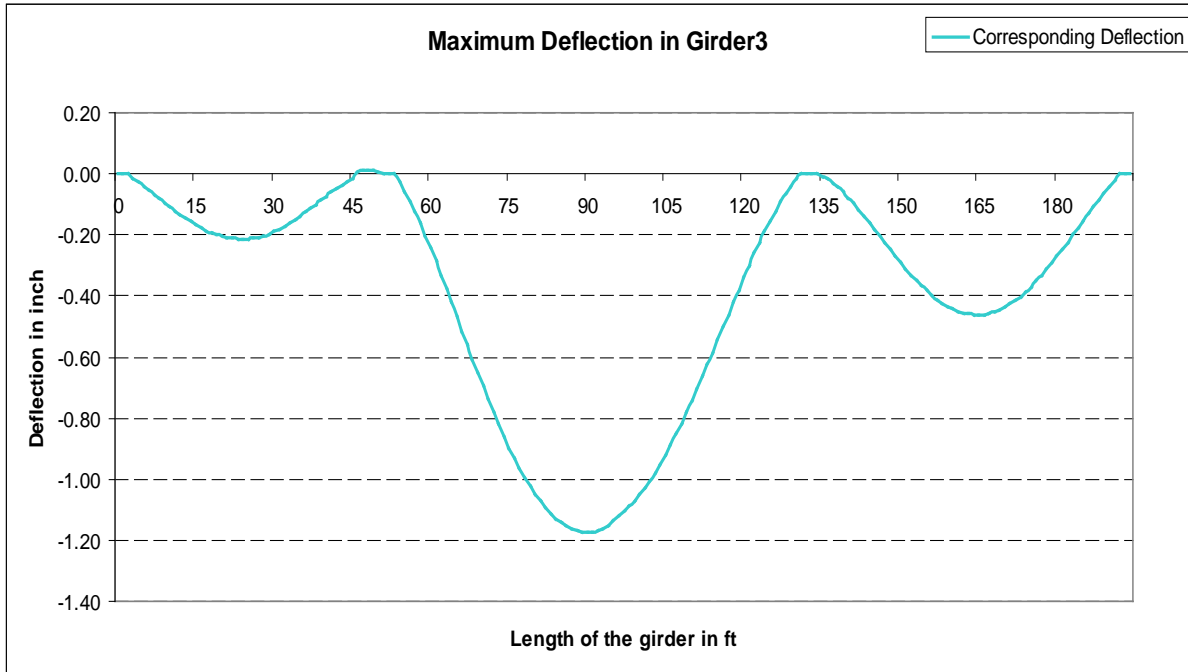


Figure 101
Maximum deflection in Girder 3 of Case II

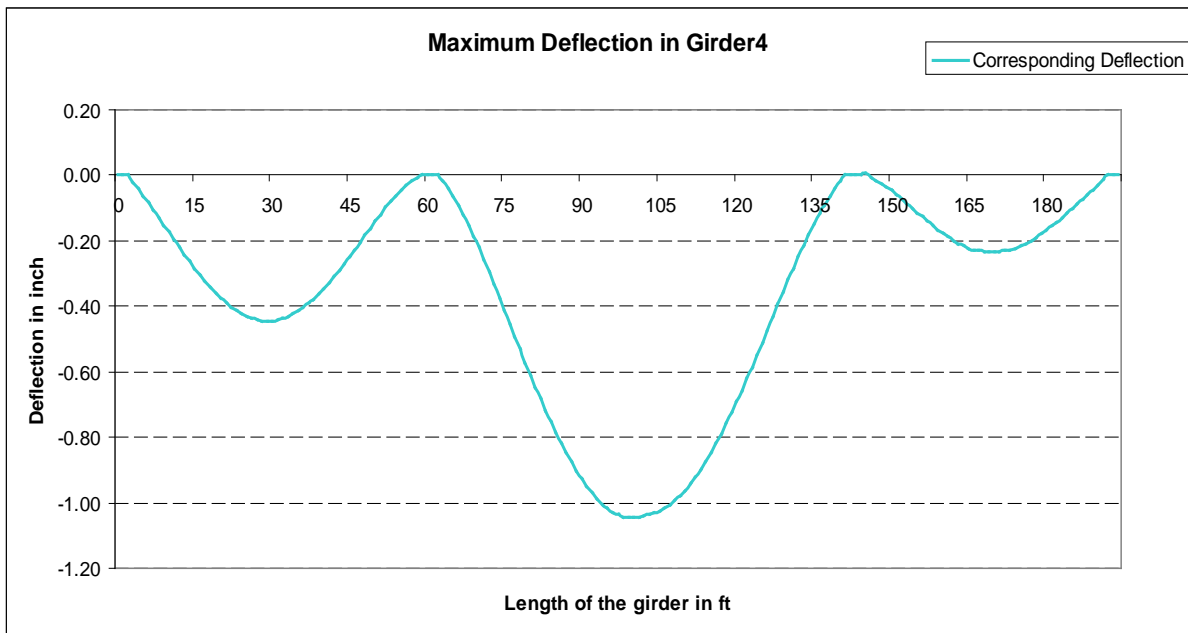


Figure 102
Maximum deflection in Girder 4 of Case II

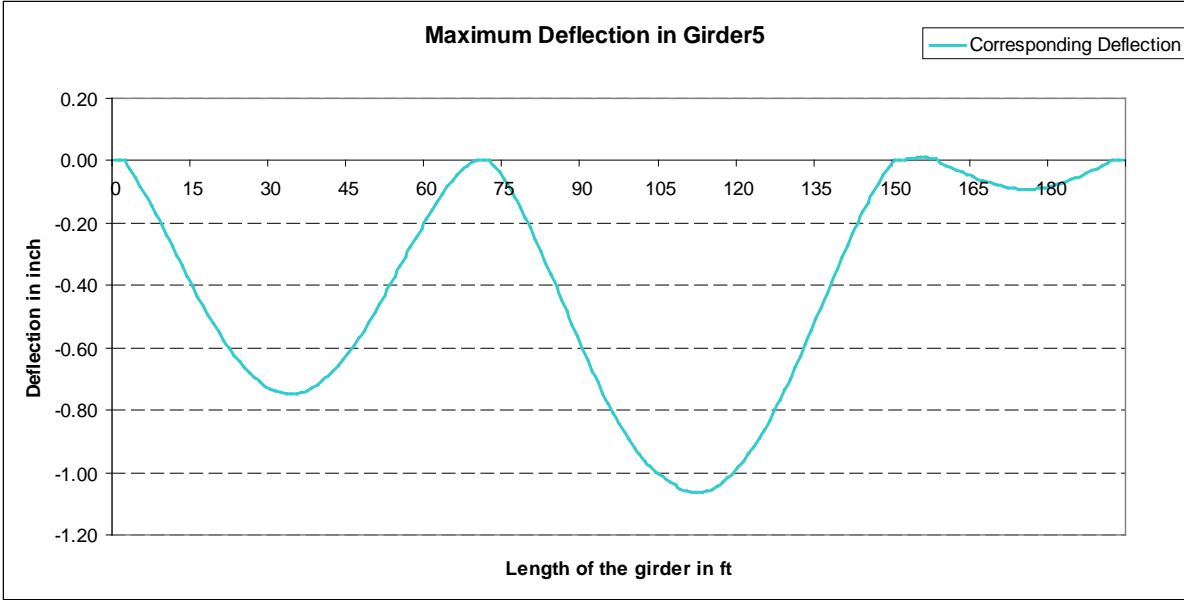


Figure 103
Maximum deflection in Girder 5 of Case II

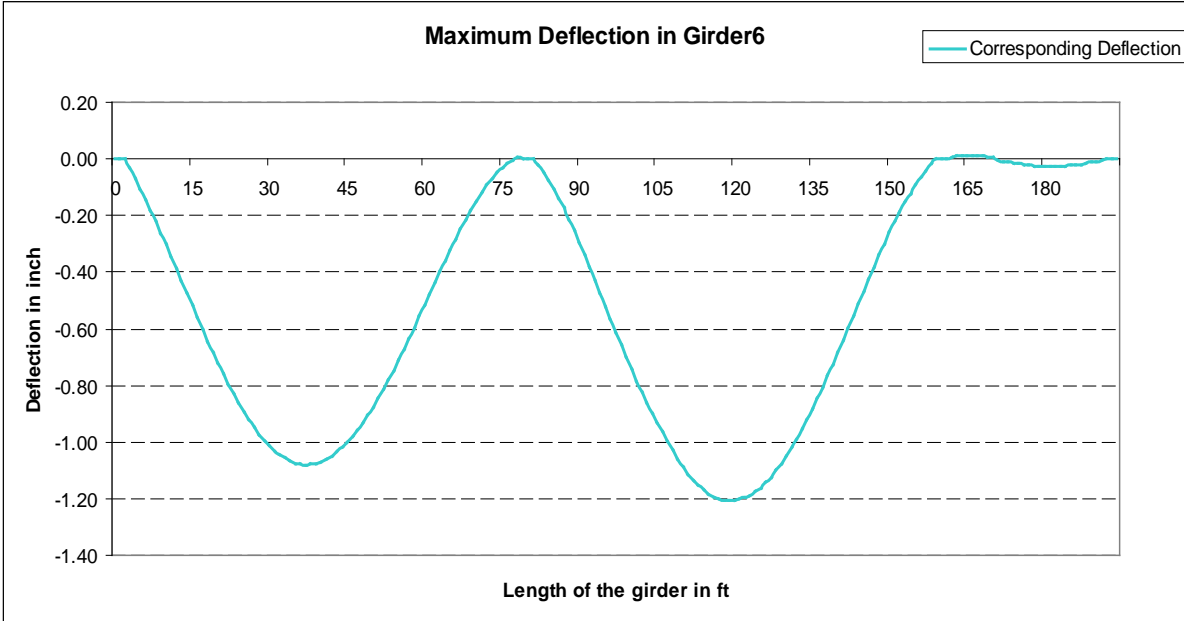


Figure 104
Maximum deflection in Girder 6 of Case II

APPENDIX E

GT STRUDL Input Files for Case III and Case IV

Case III Maximum Positive Moment in Girders without Continuity Diaphragms

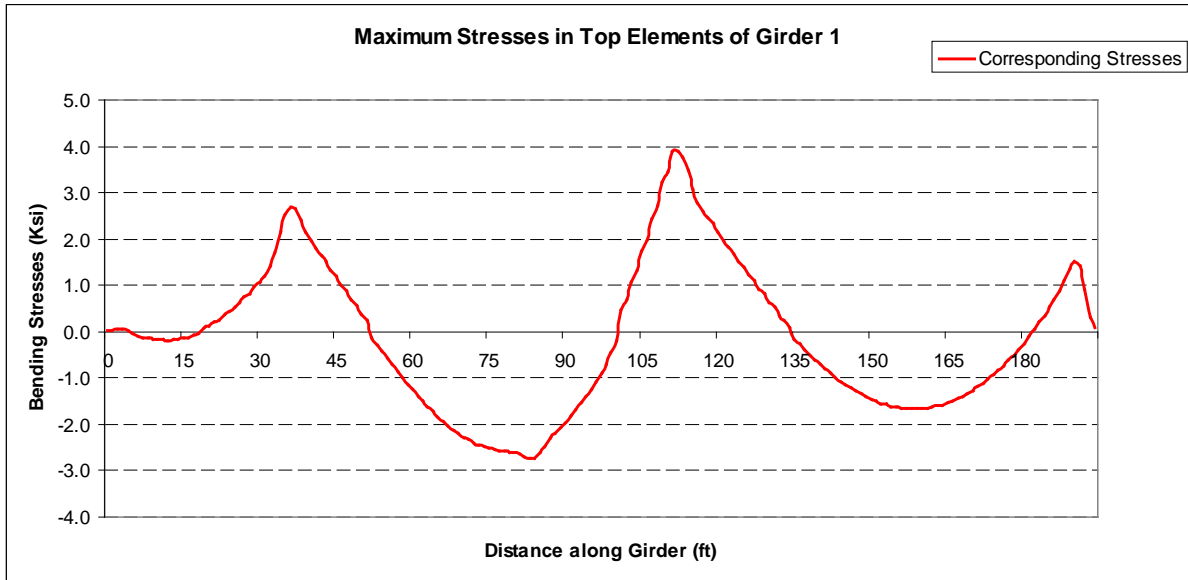


Figure 105
Bending stress distribution of top elements in Girder 1 of Case III

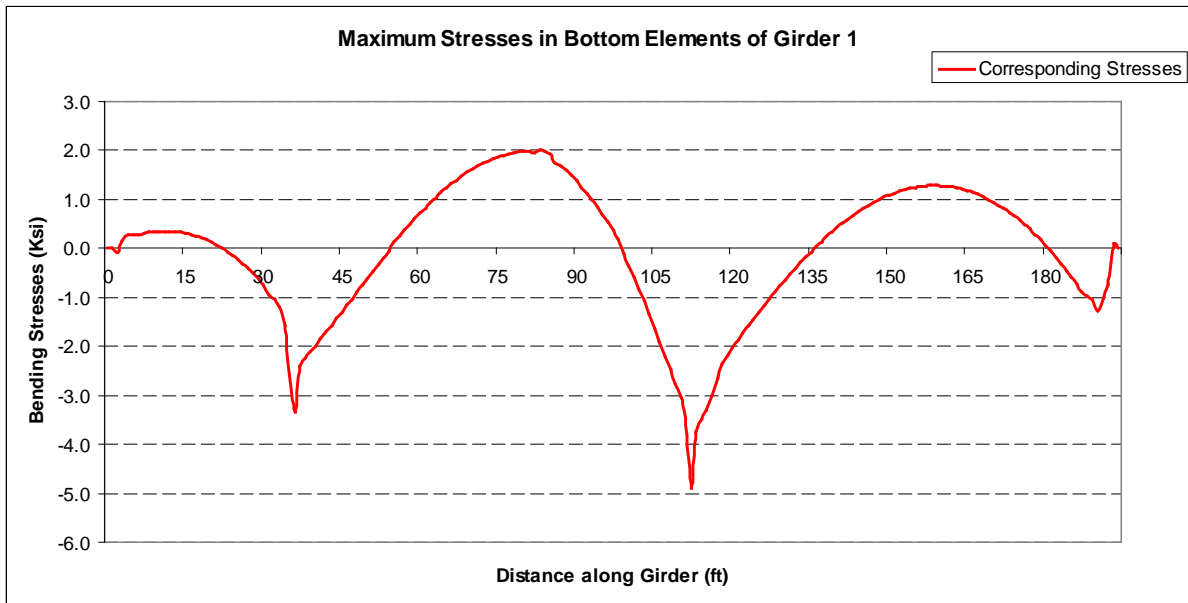


Figure 106
Bending stress distribution of bottom elements in Girder 1 of Case III

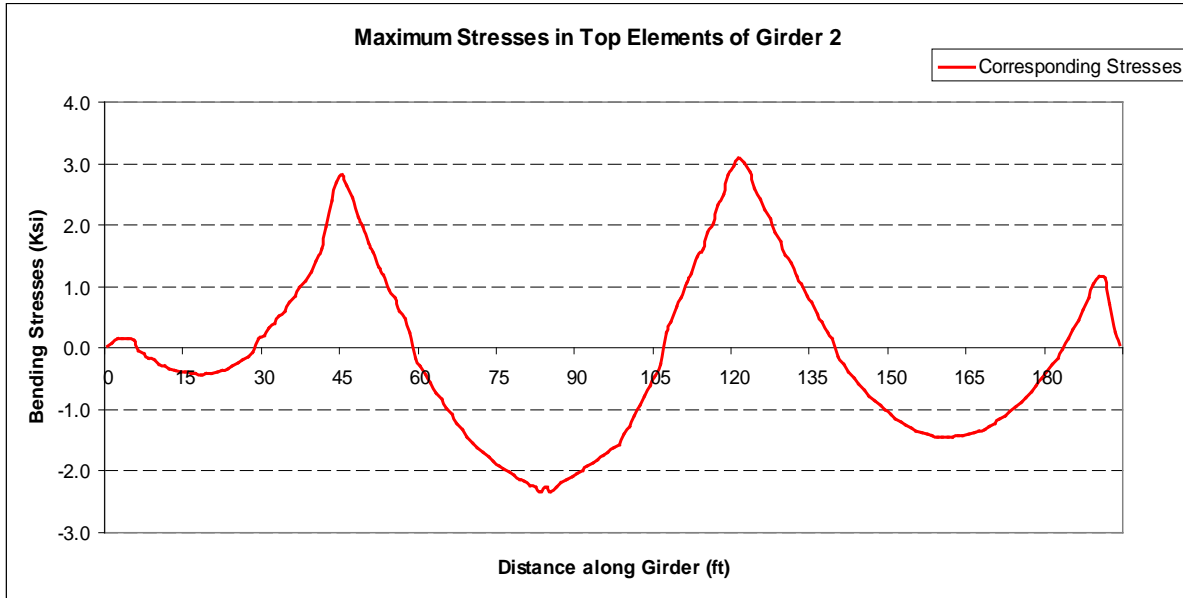


Figure 107
Bending stress distribution of top elements in Girder 2 of Case III

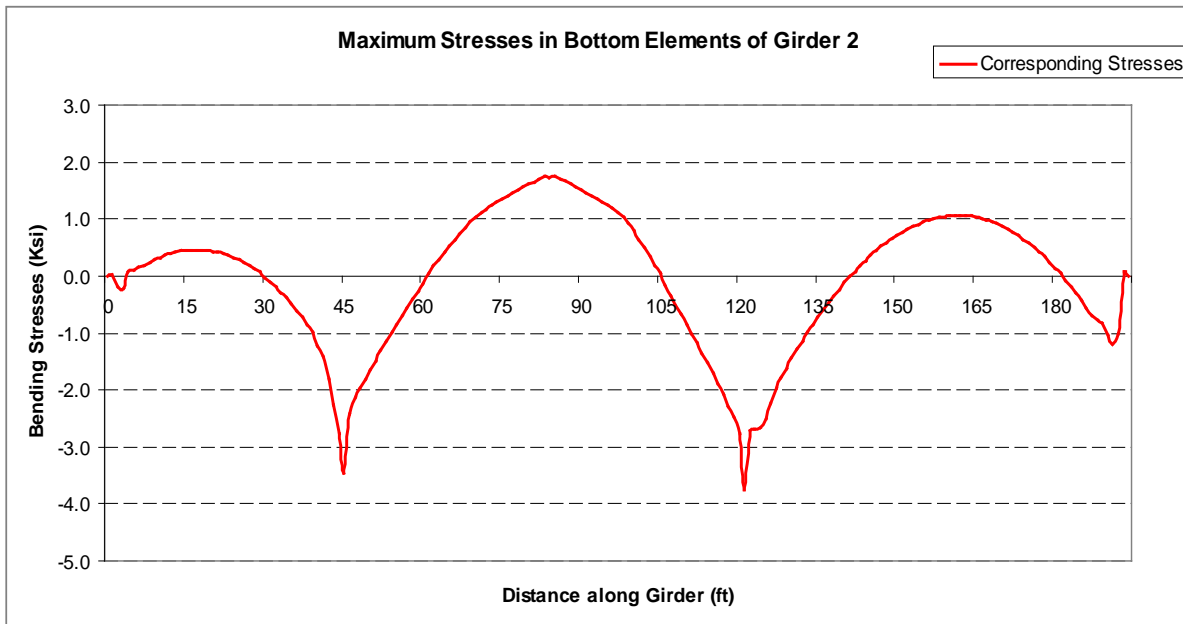


Figure 108
Bending stress distribution of bottom elements in Girder 2 of Case III

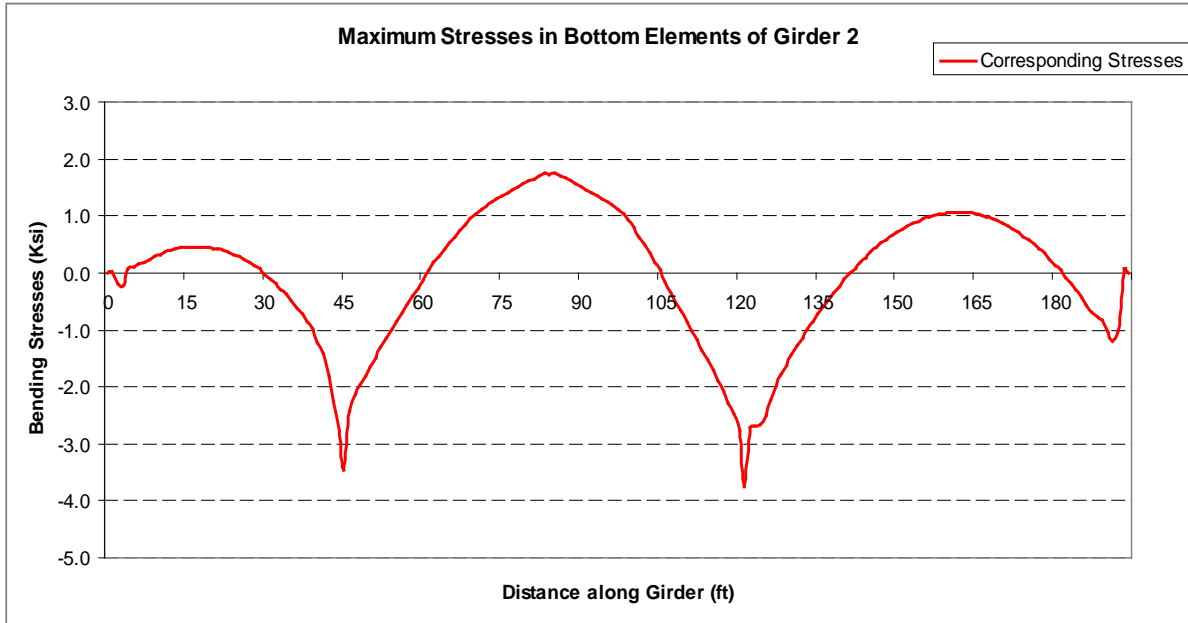


Figure 109
Bending stress distribution of top elements in Girder 3 of Case III

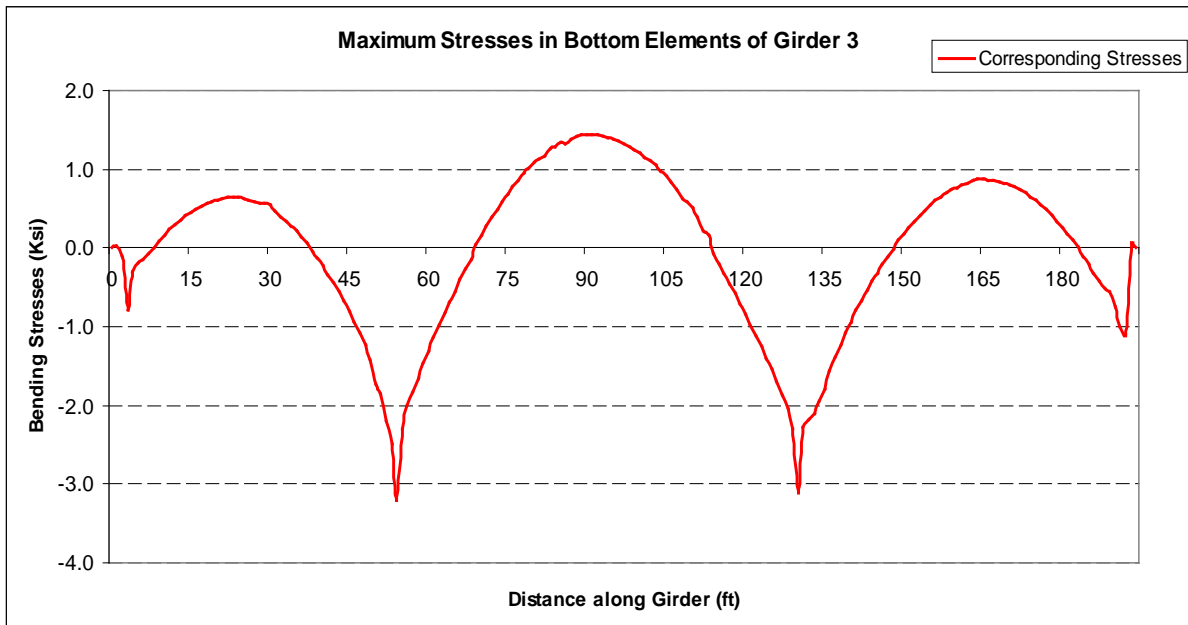


Figure 110
Bending stress distribution of bottom elements in Girder 3 of Case III

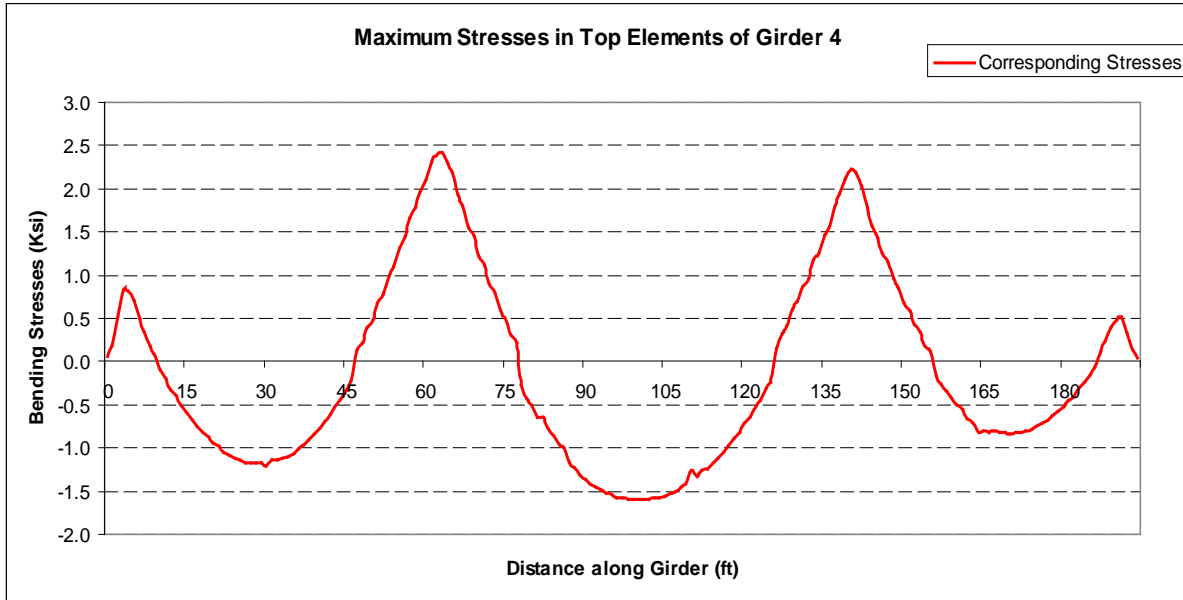


Figure 111
Bending stress distribution of top elements in Girder 4 of Case III

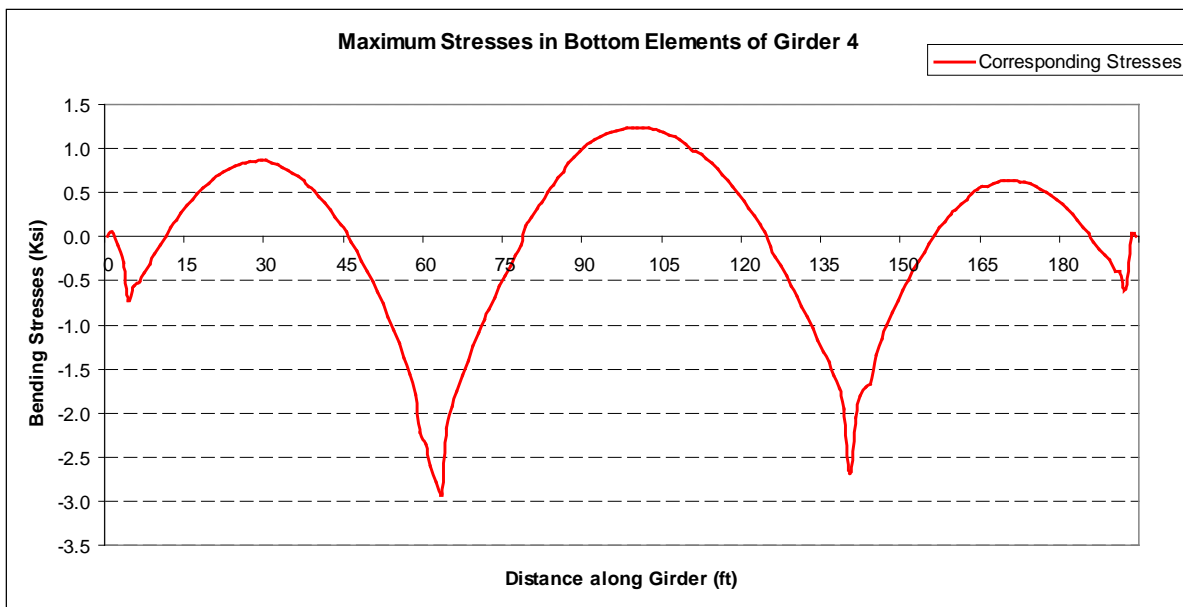


Figure 112
Bending stress distribution of bottom elements in Girder 4 of Case III

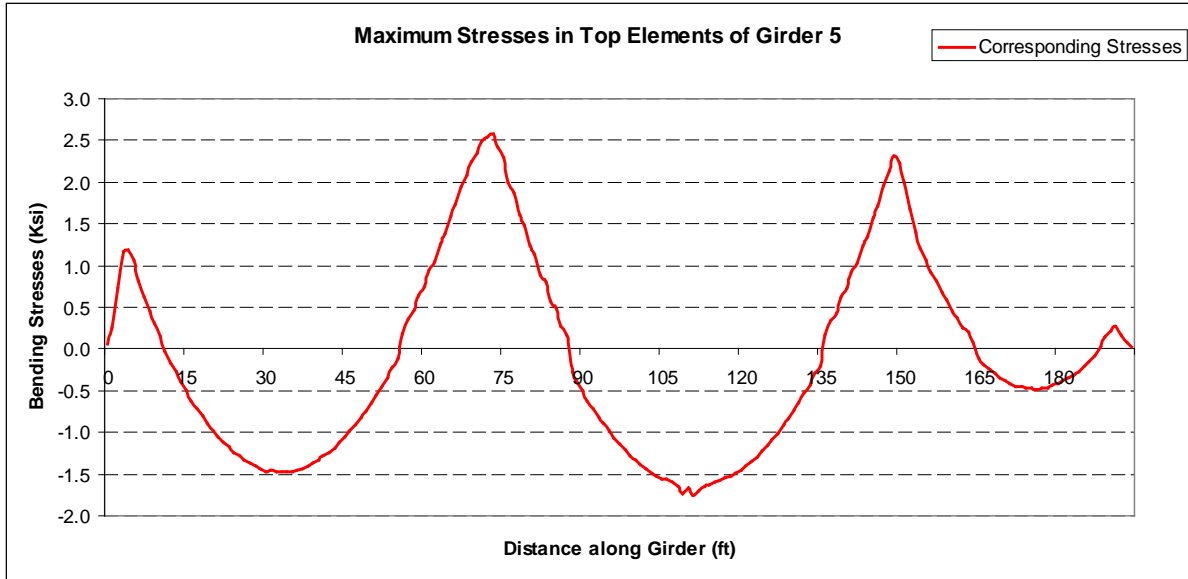


Figure 113
Bending stress distribution of top elements in Girder 5 of Case III

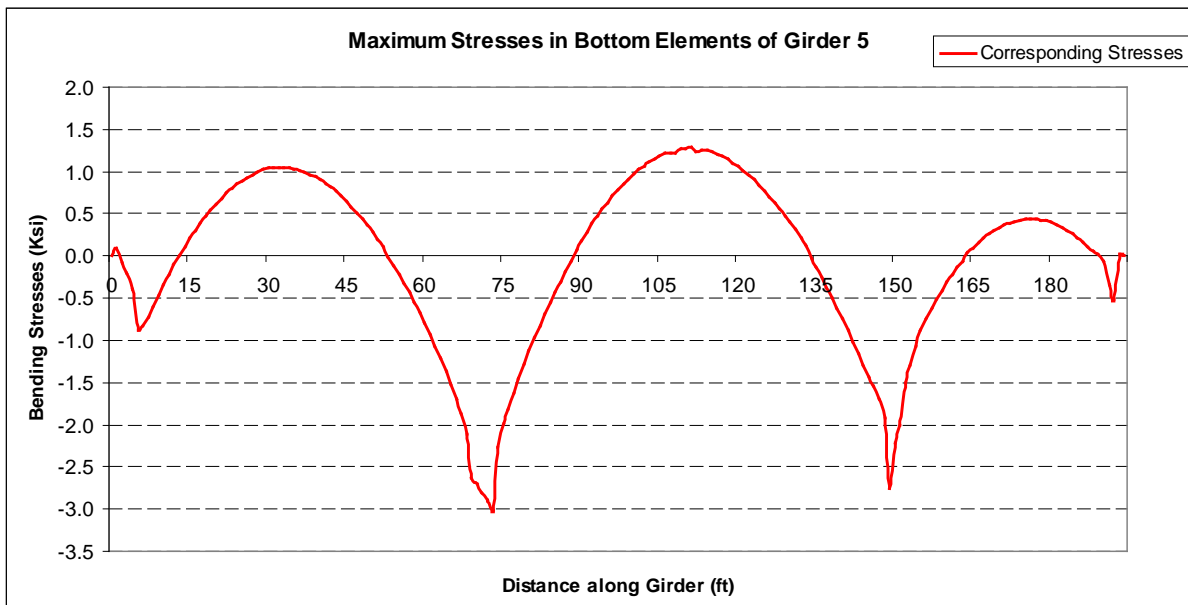


Figure 114
Bending stress distribution of bottom elements in Girder 5 of Case III

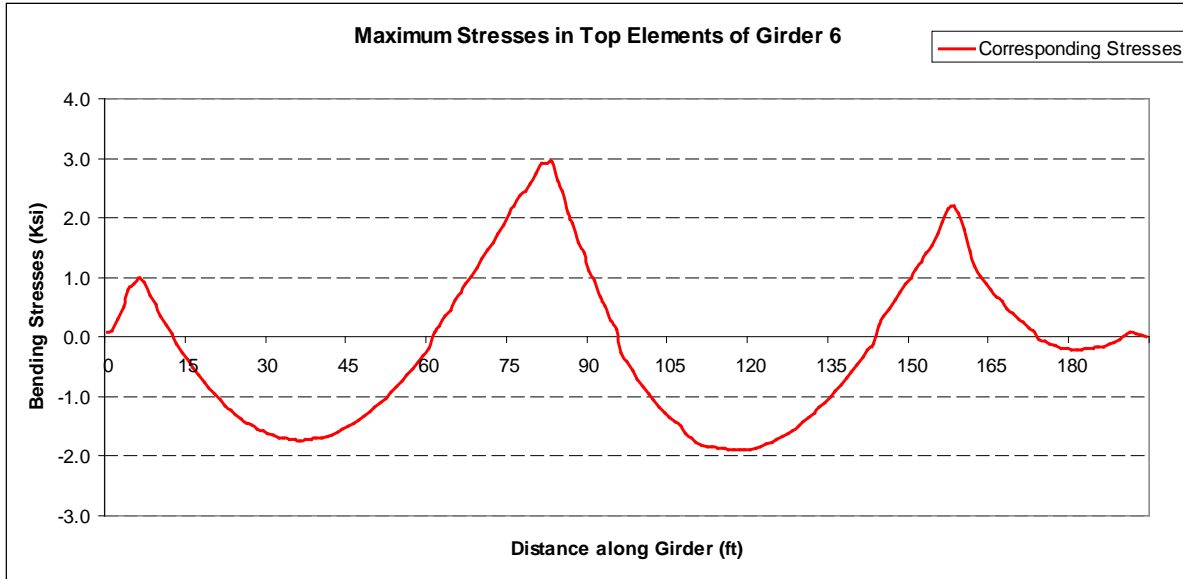


Figure 115
Bending stress distribution of top elements in Girder 6 of Case III

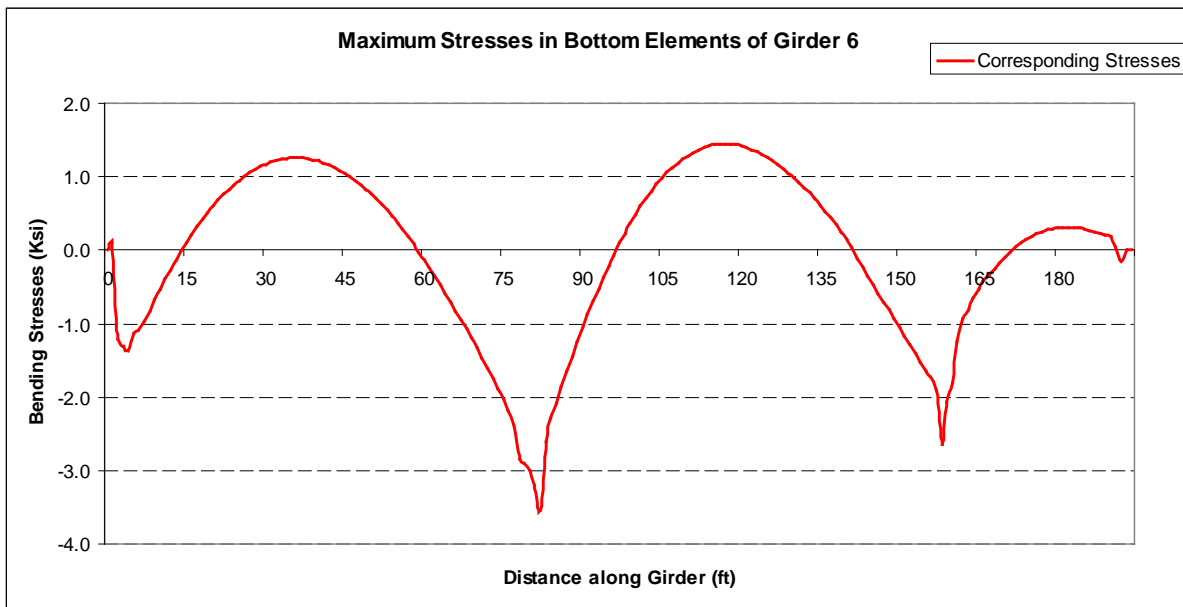


Figure 116
Bending stress distribution of bottom elements in Girder 6 of Case III

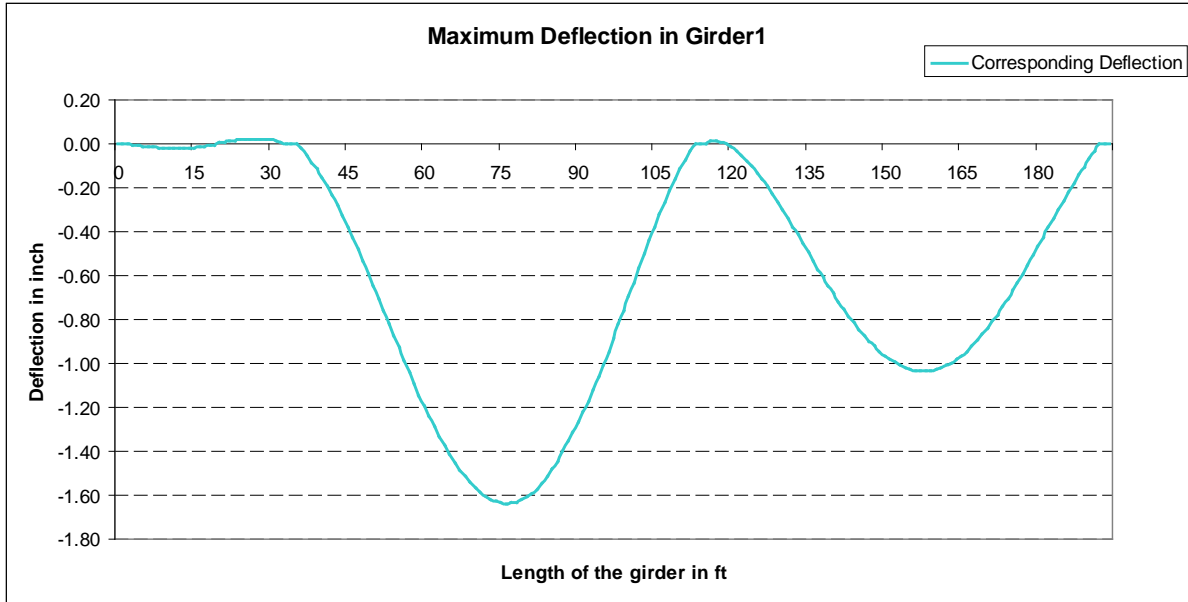


Figure 117
Maximum deflection in Girder 1 of Case III

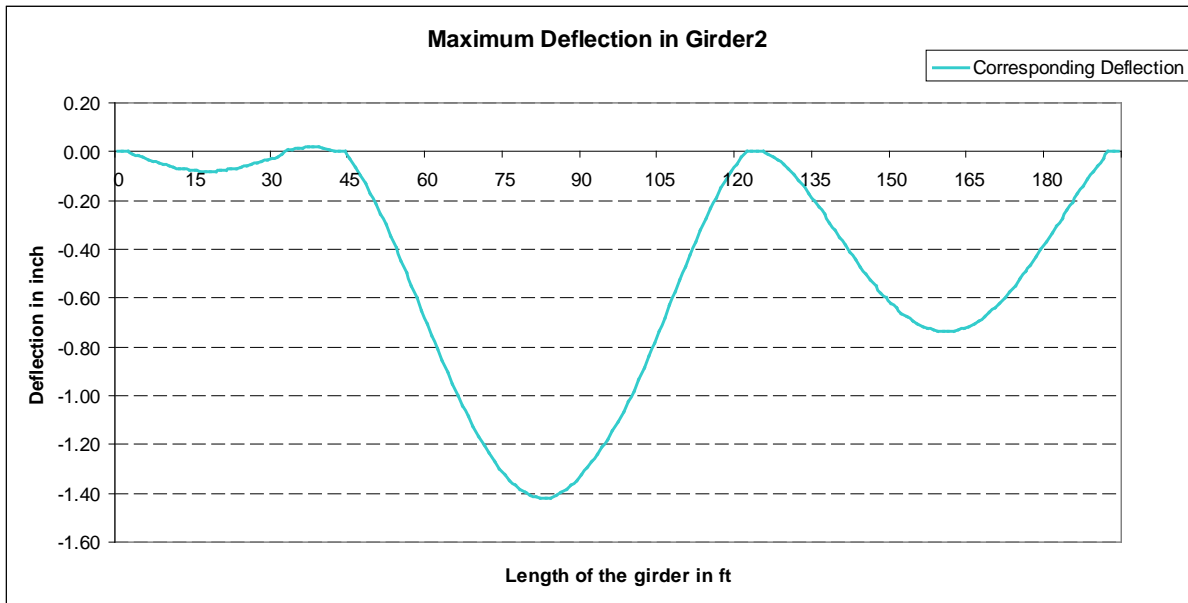


Figure 118
Maximum deflection in Girder 2 of Case III

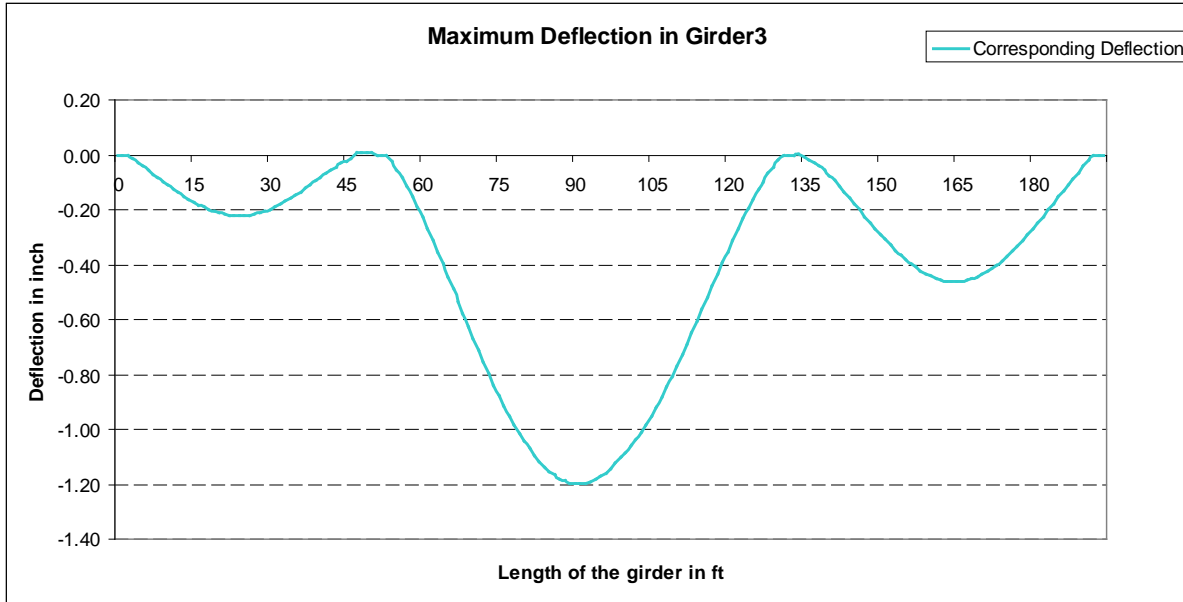


Figure 119
Maximum deflection in Girder 3 of Case III

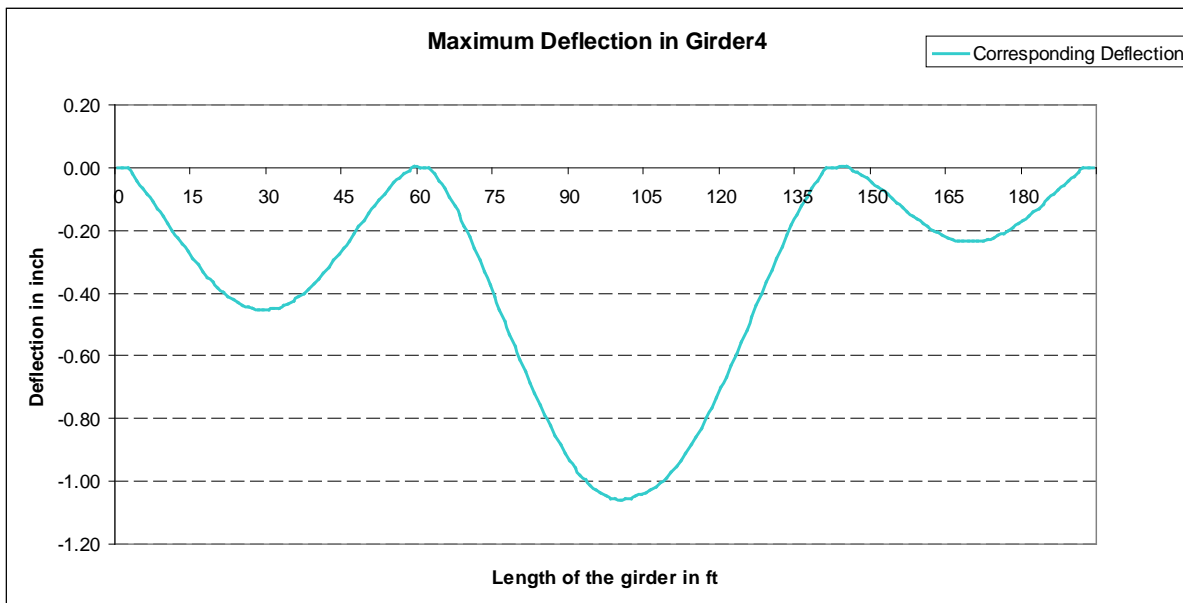


Figure 120
Maximum deflection in Girder 4 of Case III

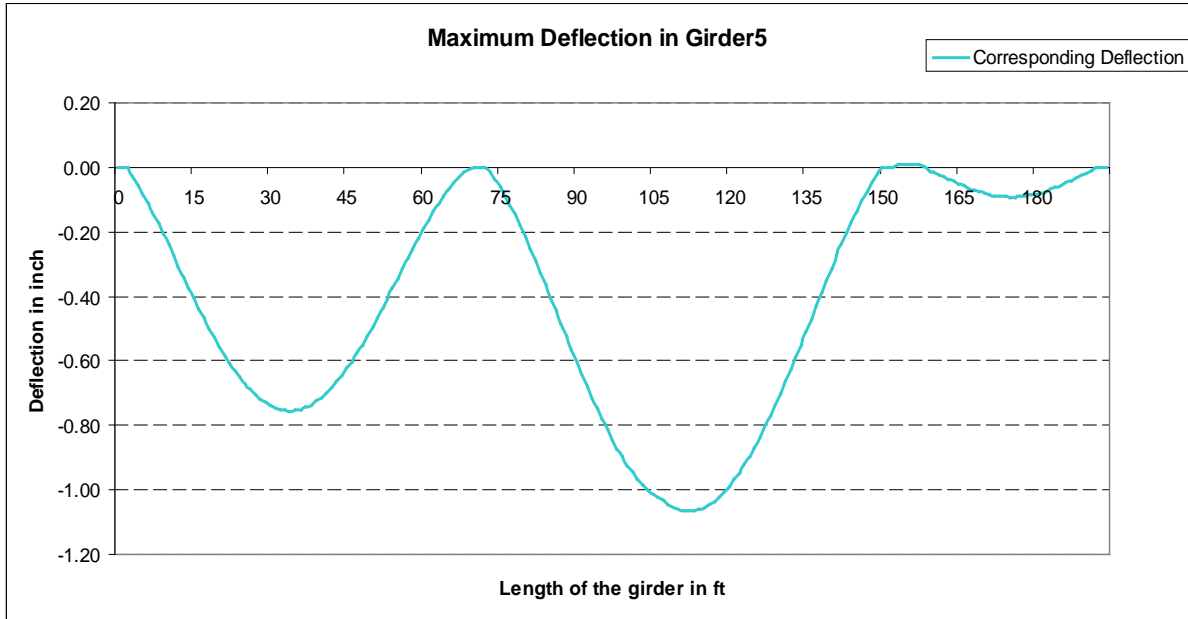


Figure 121
Maximum deflection in Girder 5 of Case III

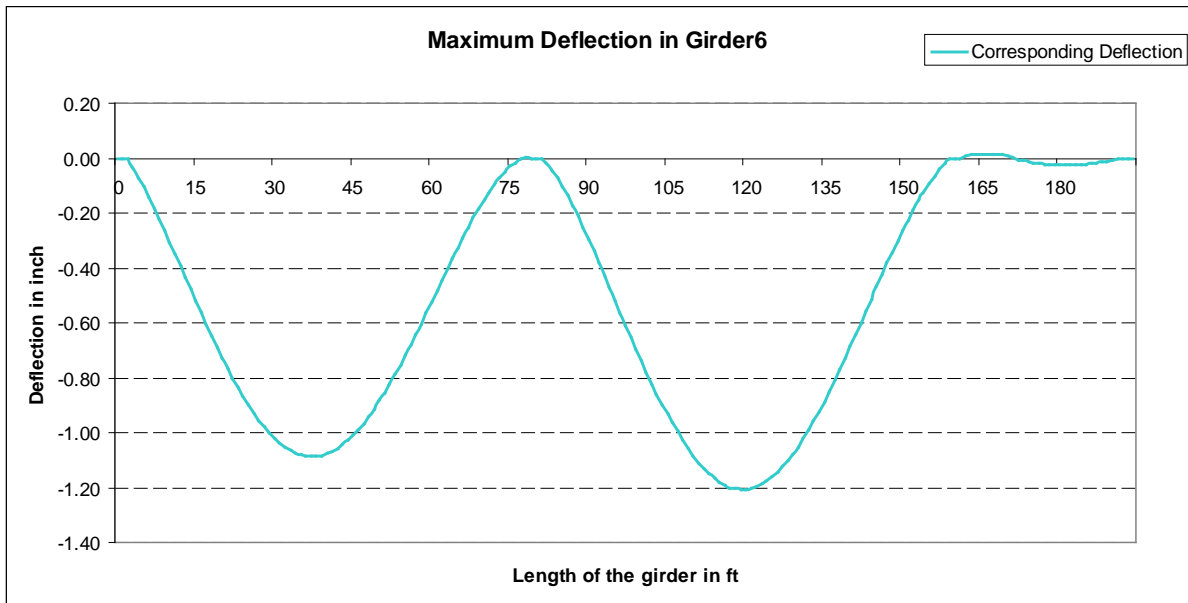


Figure 122
Maximum deflection in Girder 6 of Case III

Case IV Maximum Negative Moment in Girders without Continuity Diaphragms

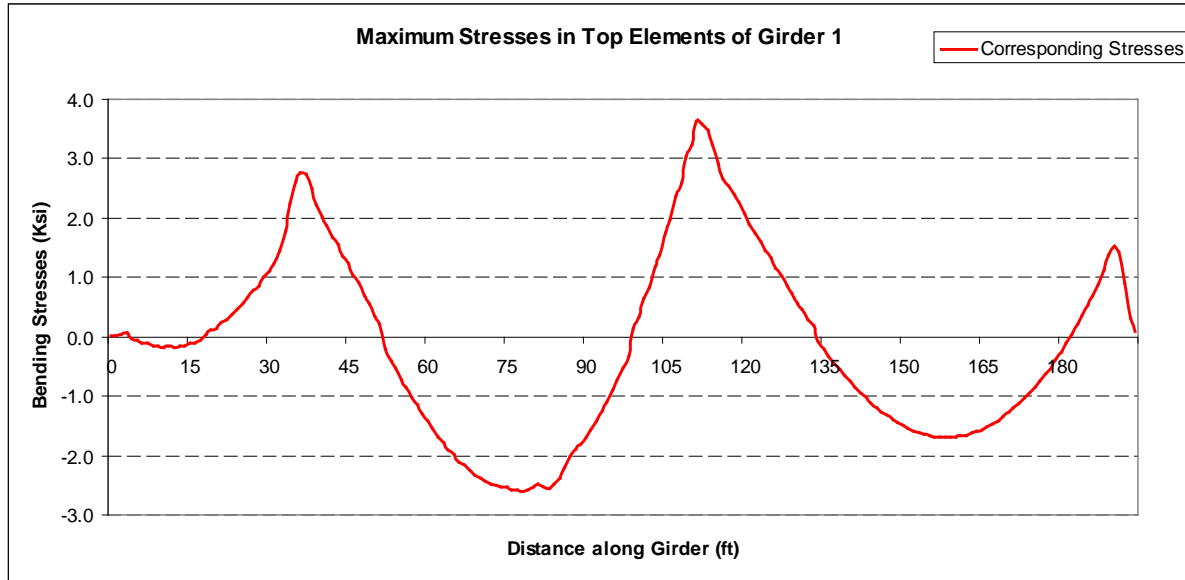


Figure 123
Bending stress distribution of top elements in Girder 1 of Case IV

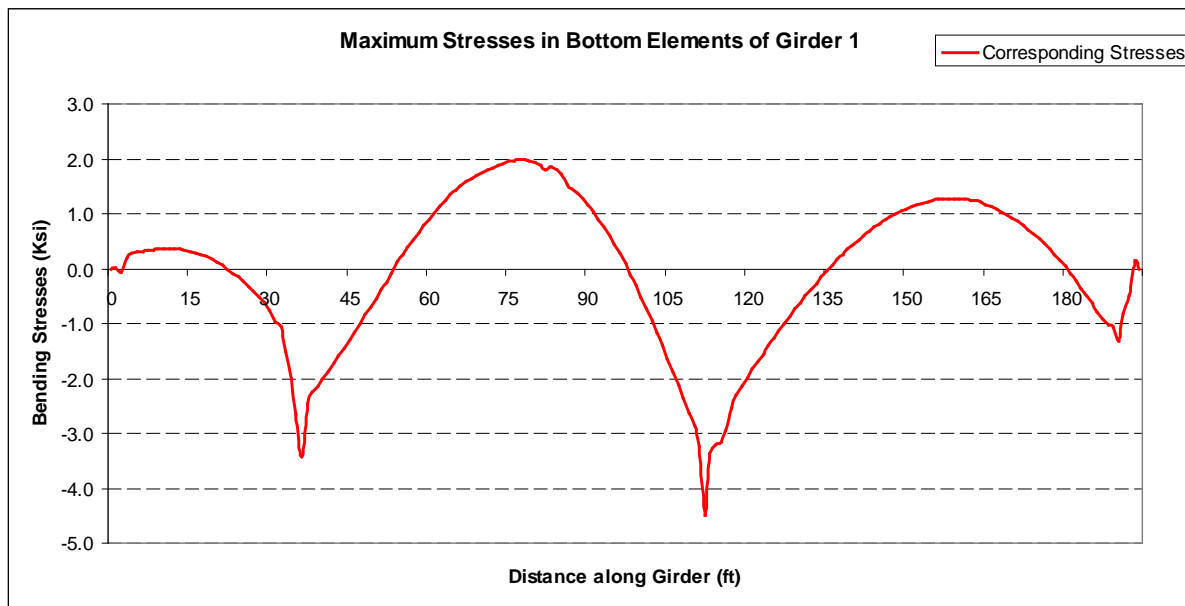


Figure 124
Bending stress distribution of bottom elements in Girder 1 of Case IV

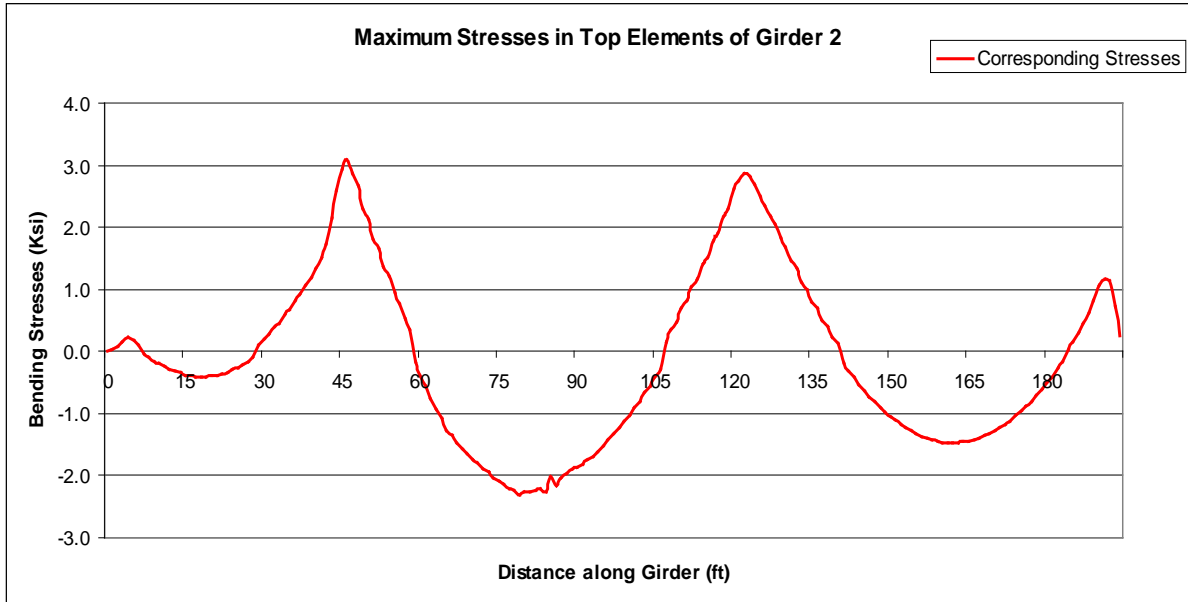


Figure 125
Bending stress distribution of top elements in Girder 2 of Case IV

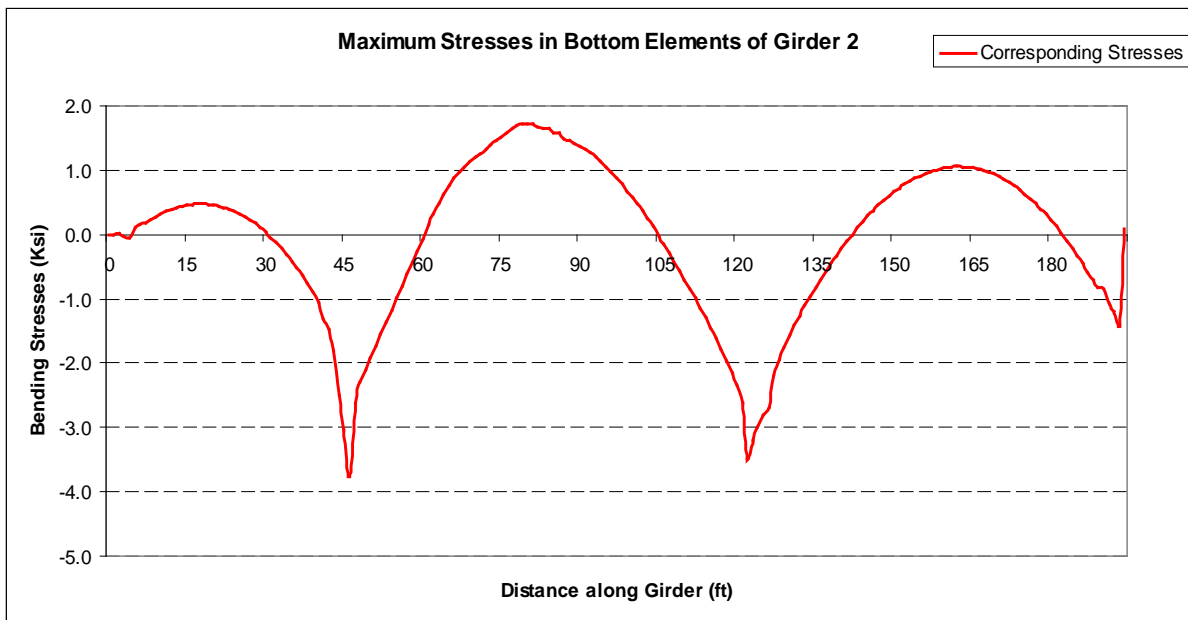


Figure 126
Bending stress distribution of bottom elements in Girder 2 of Case IV

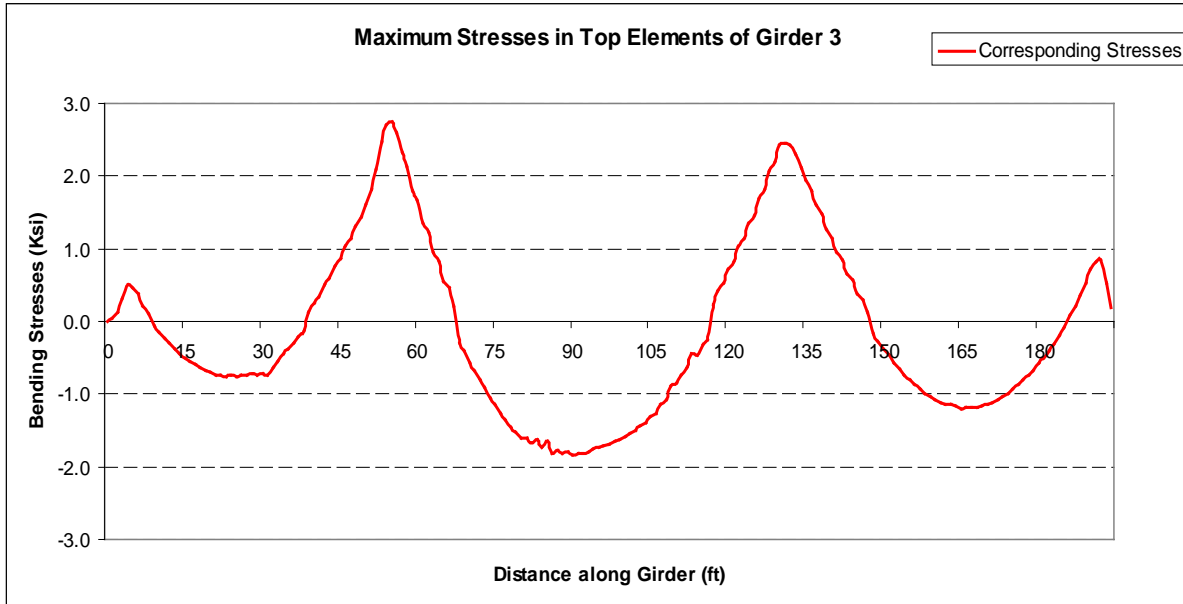


Figure 127
Bending stress distribution of top elements in Girder 3 of Case IV

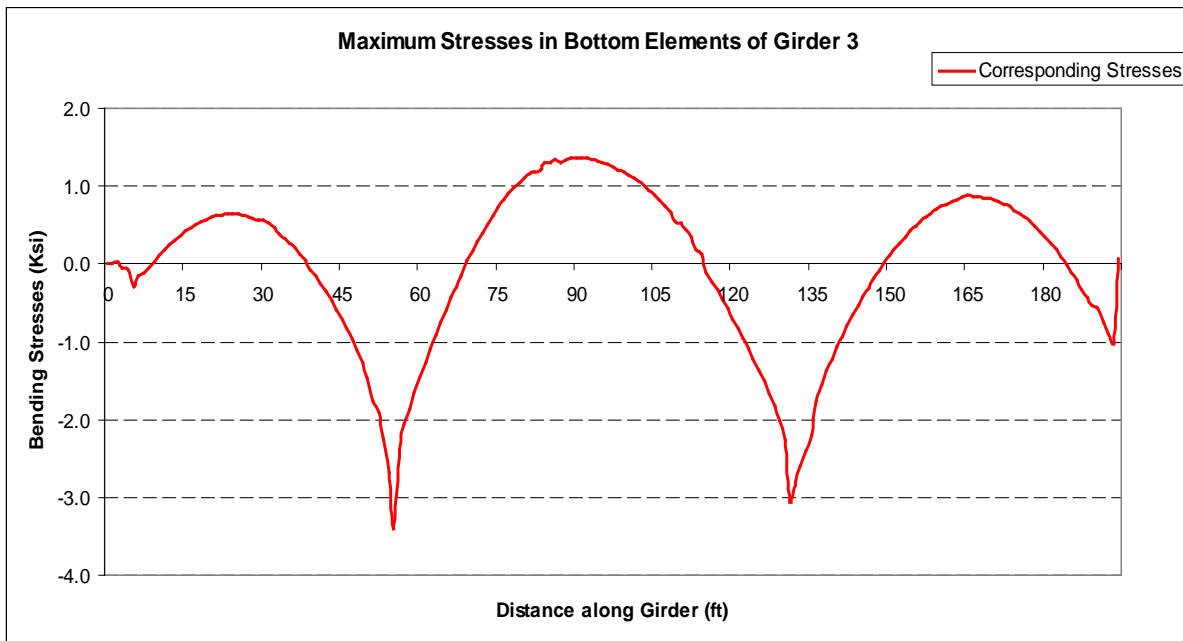


Figure 128
Bending stress distribution of bottom elements in Girder 3 of Case IV

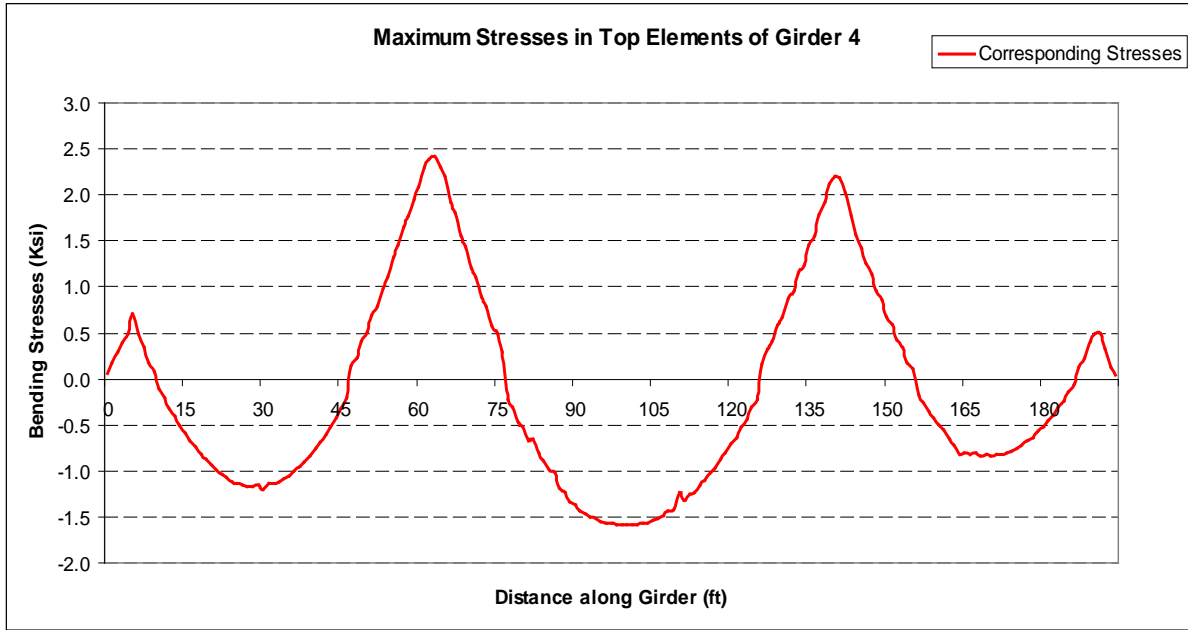


Figure 129
Bending stress distribution of top elements in Girder 4 of Case IV

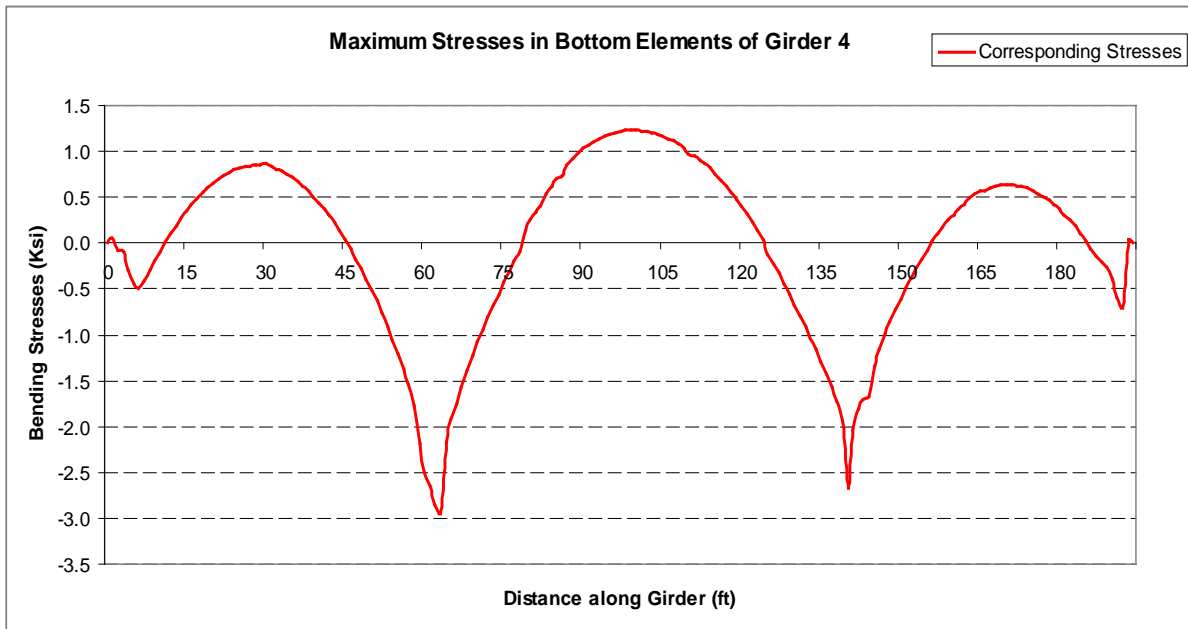


Figure 130
Bending stress distribution of bottom elements in Girder 4 of Case IV

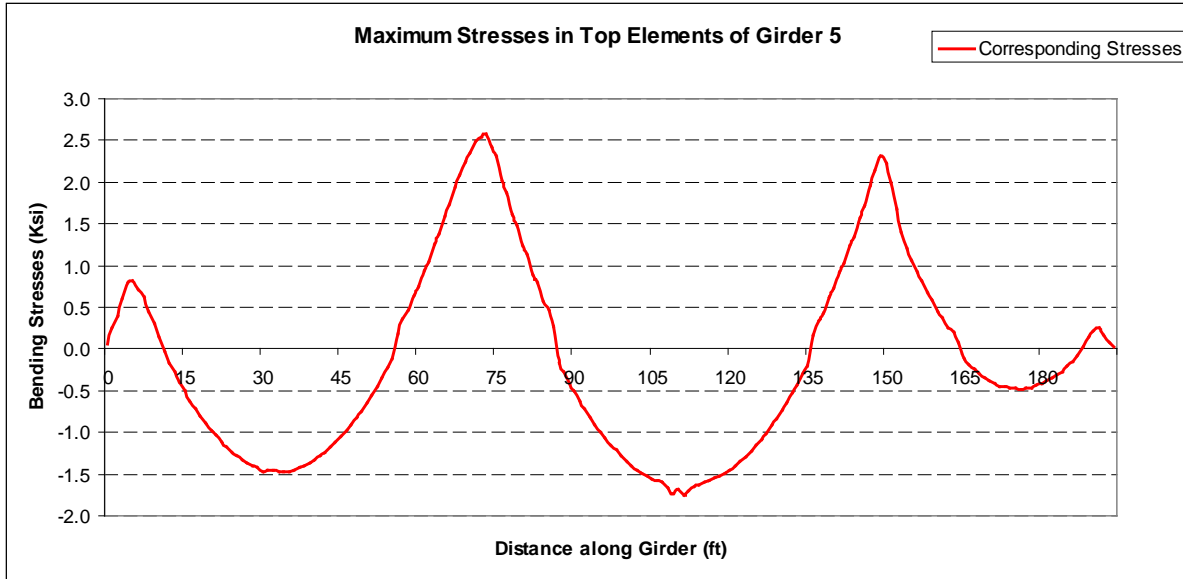


Figure 131
Bending stress distribution of top elements in Girder 5 of Case IV

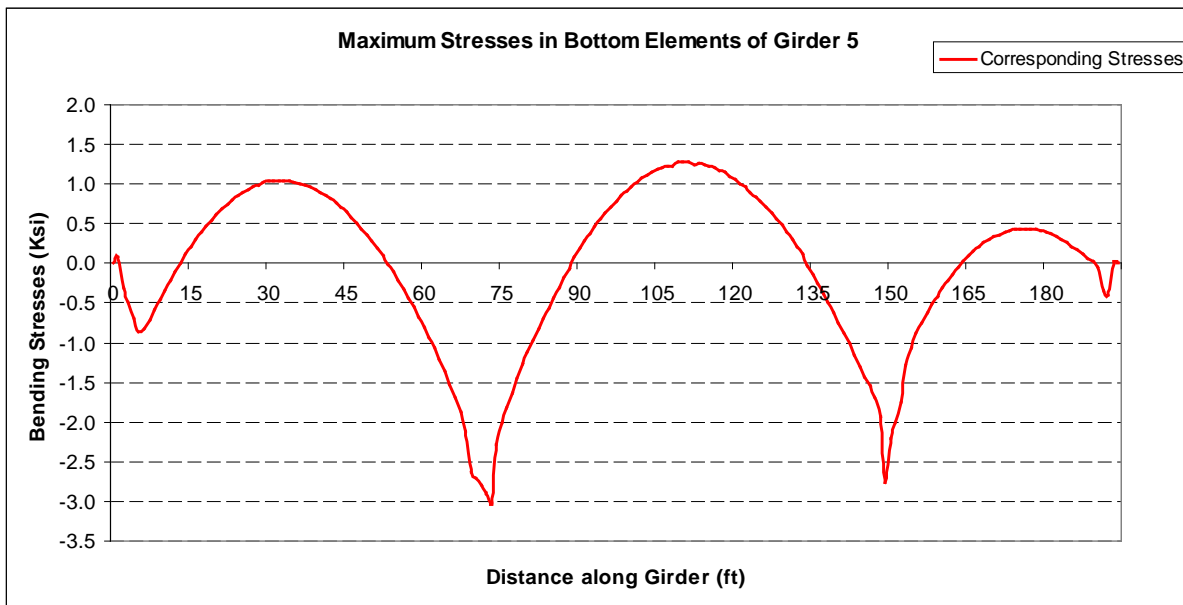


Figure 132
Bending stress distribution of bottom elements in Girder 5 of Case IV

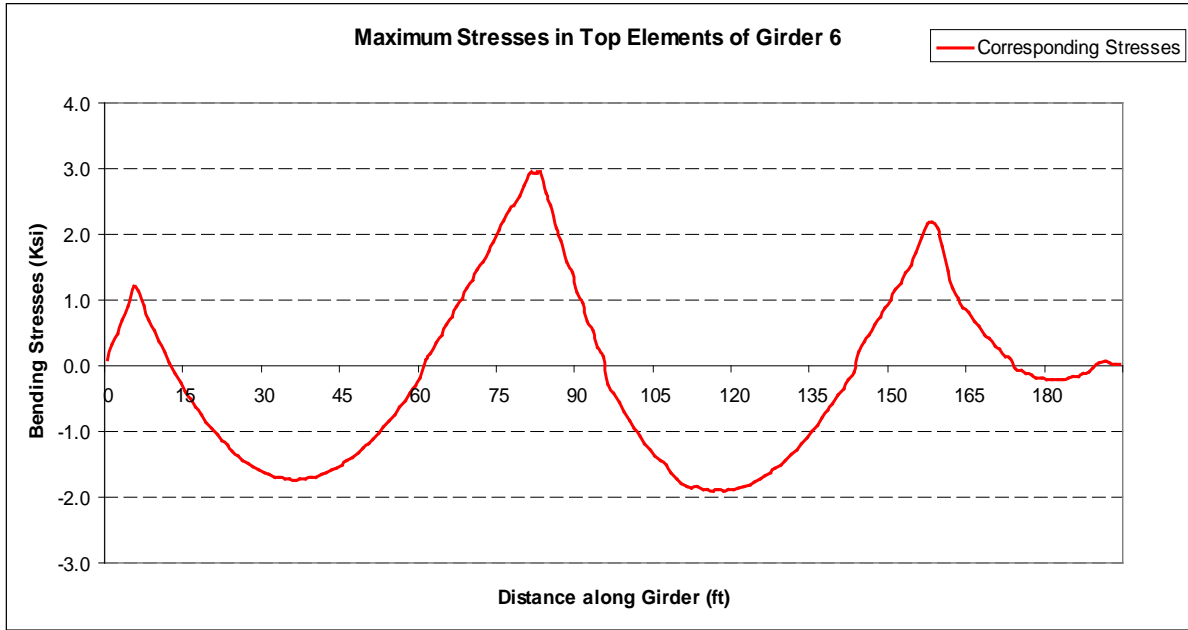


Figure 133
Bending stress distribution of top elements in Girder 6 of Case IV

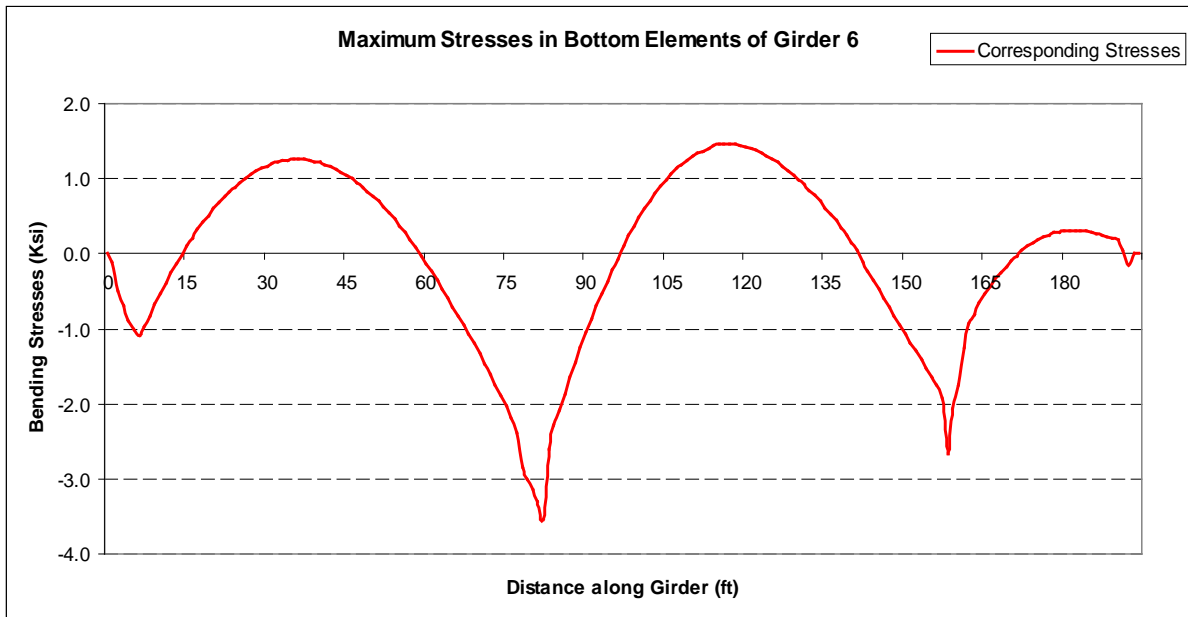


Figure 134
Bending stress distribution of bottom elements in Girder 6 of Case IV

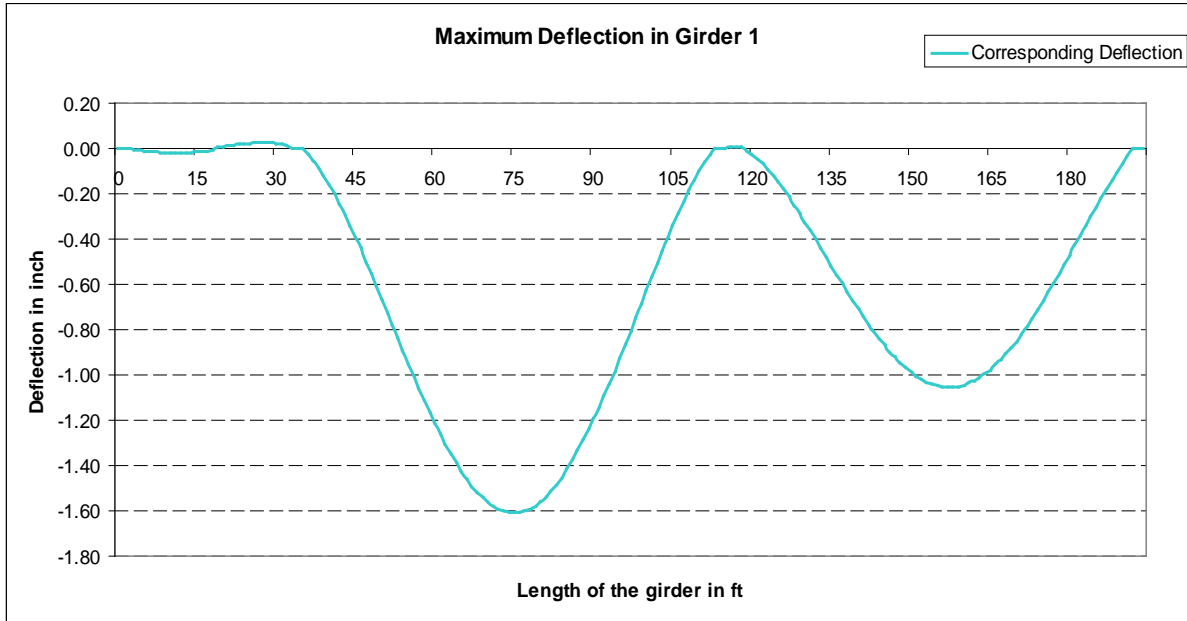


Figure 135
Maximum deflection in Girder 1 of Case IV

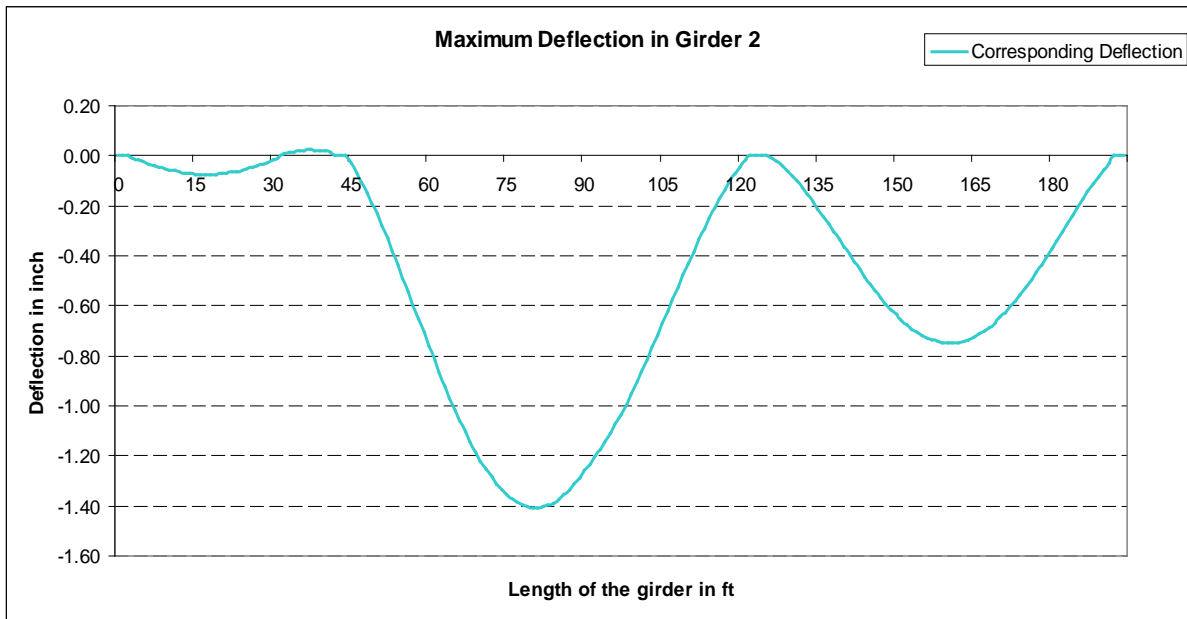


Figure 136
Maximum deflection in Girder 2 of Case IV

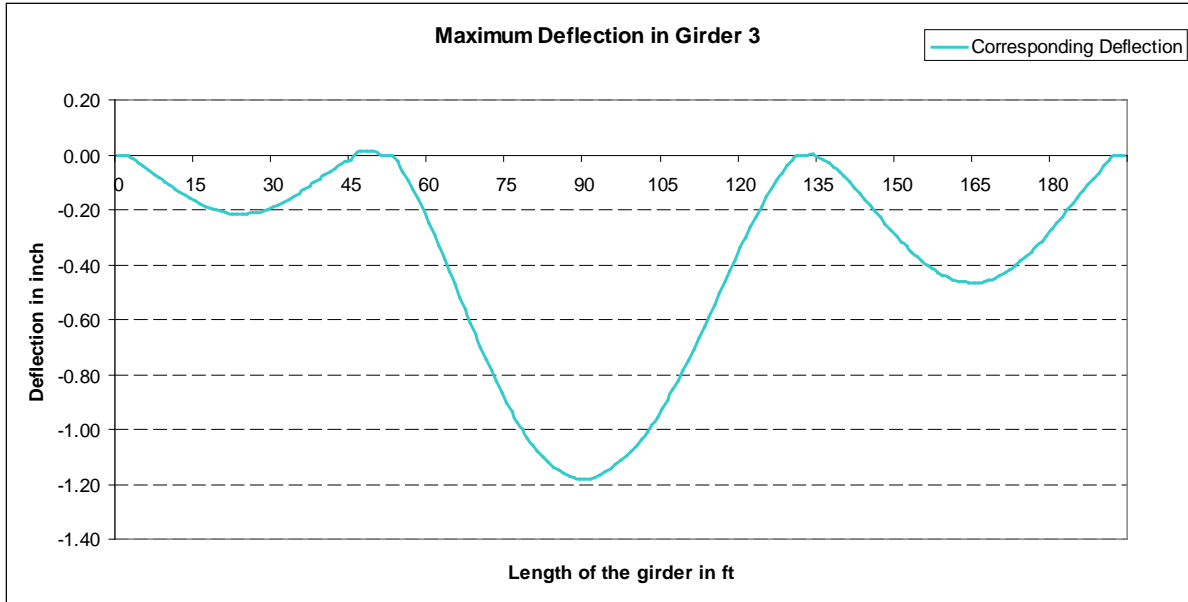


Figure 137
Maximum deflection in Girder 3 of Case IV

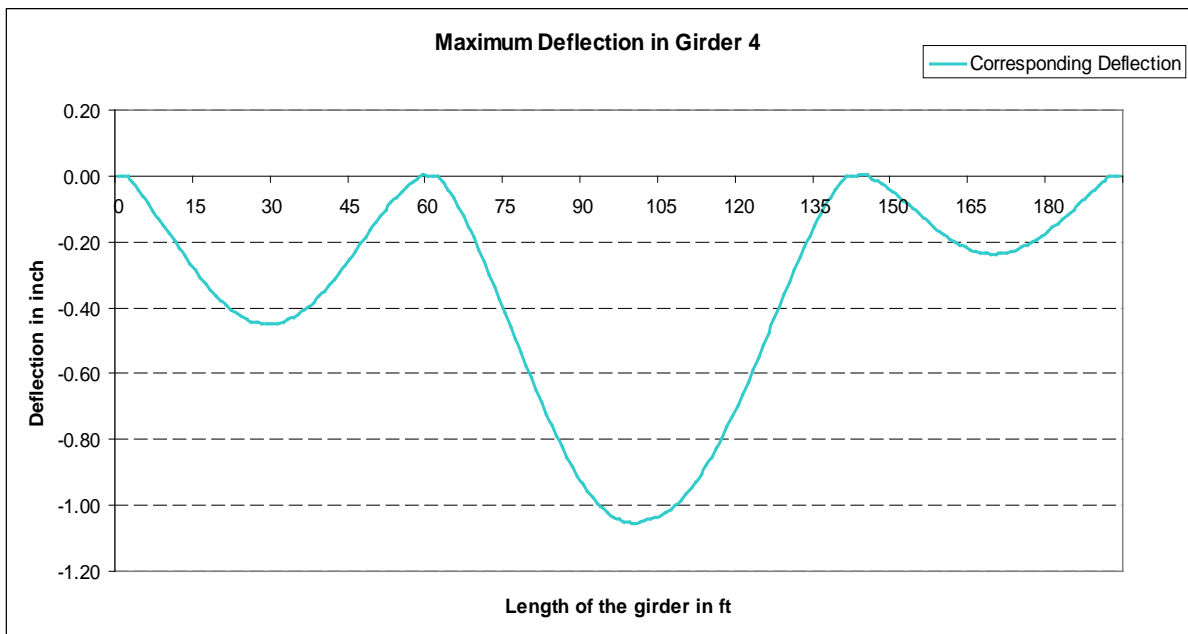


Figure 138
Maximum deflection in Girder 4 of Case IV

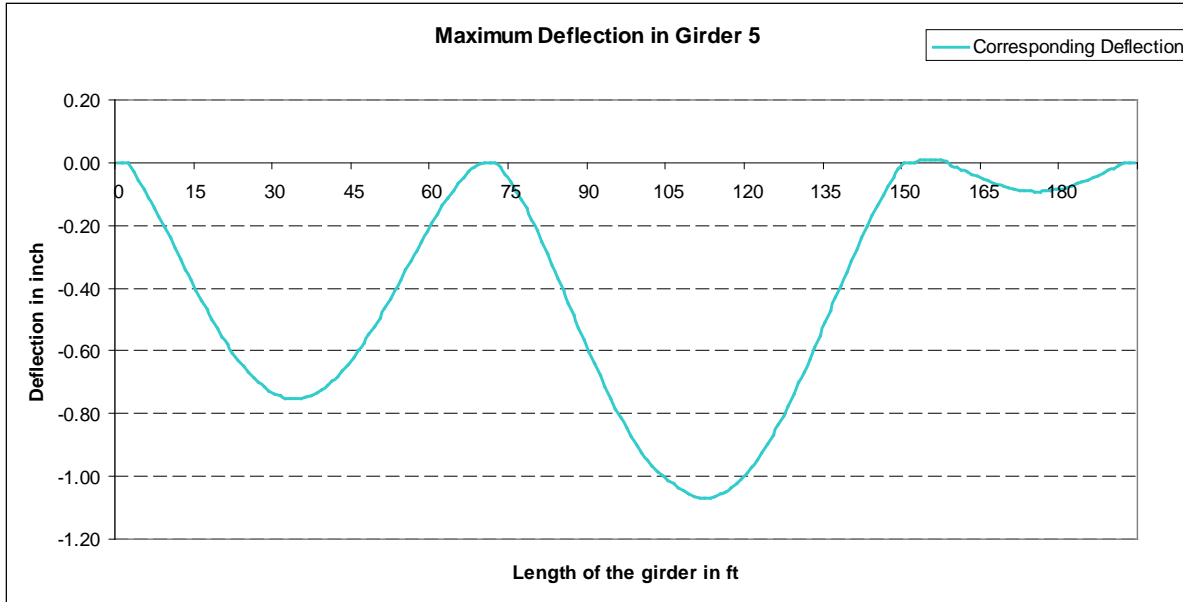


Figure 139
Maximum deflection in Girder 5 of Case IV

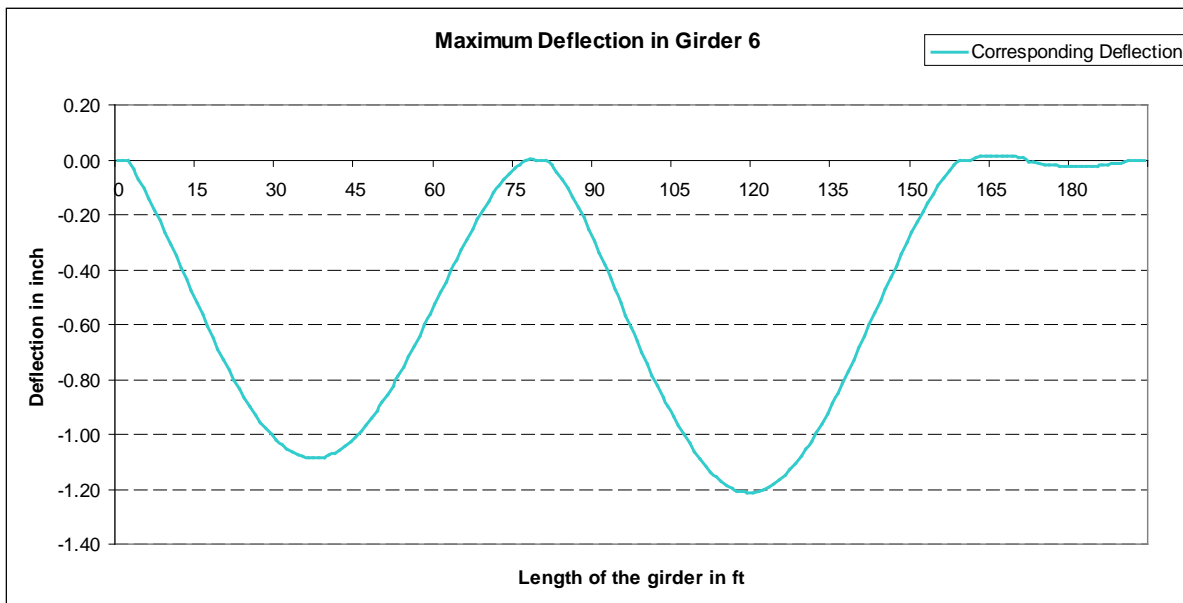


Figure 140
Maximum deflection in Girder 6 of Case IV

APPENDIX F

BNSF Overpass Field Testing Pictures



Figure 141
Gauge located at the bottom of the Girder 1

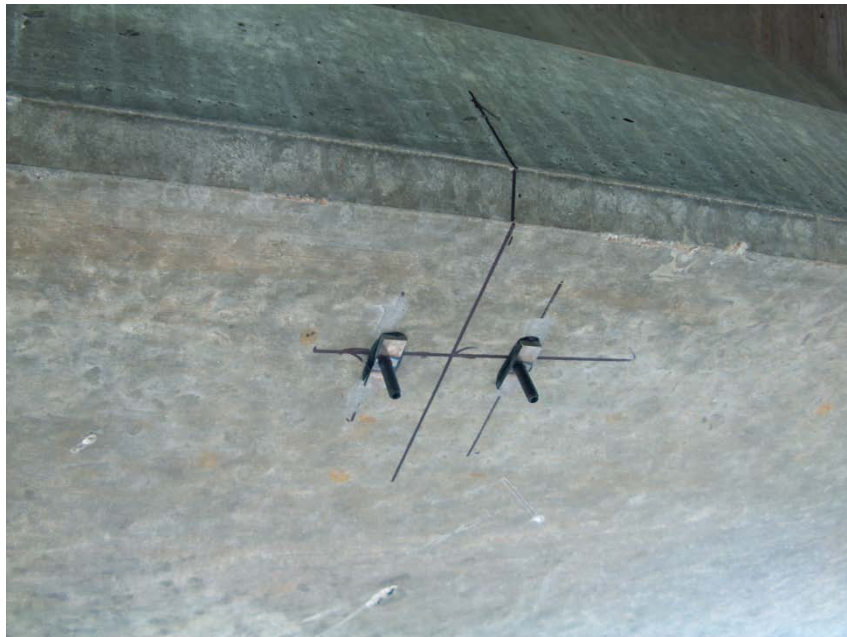


Figure 142
Tabs on the Girder 1 after removing the transducer



Figure 143
Initial marking on the girder for placing transducer



Figure 144
Gauge located at the top flange of the girder



Figure 145
Tabs on the Girder 1 after removing the transducer



Figure 146
Initial marking on the girder for placing transducer



Figure 147
Gauge located at the bottom of the Girder 1



Figure 148
Tabs on the Girder 1 after removing the transducer



Figure 149
Initial marking on the girder for placing transducer



Figure 150
Gauge located at the top flange of the Girder 1



Figure 151
Tabs on the Girder 1 after removing the transducer



Figure 152
Gauge located at the bottom of the Girder 1



Figure 153
Tabs on the Girder 1 after removing the transducer

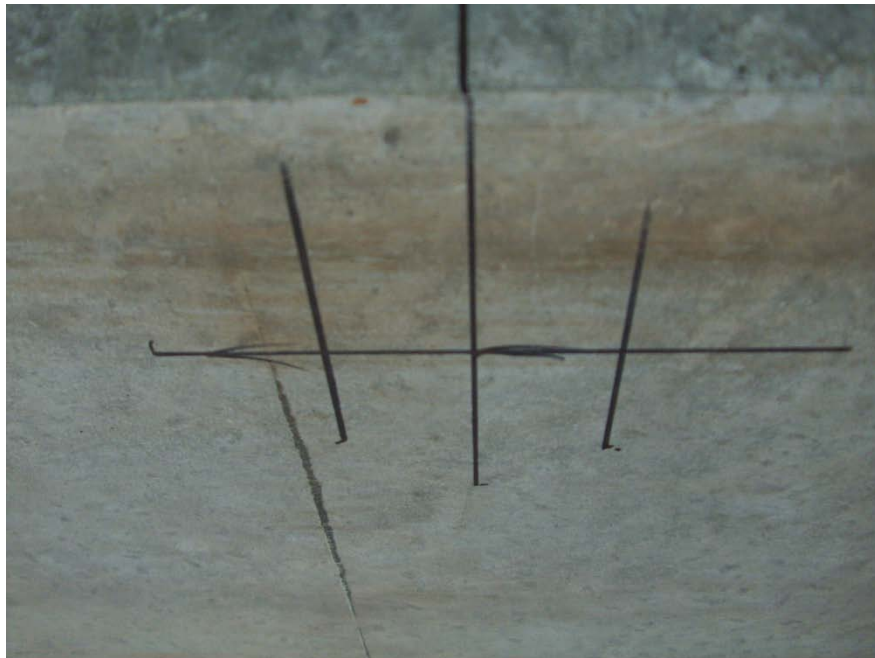


Figure 154
Initial marking on the girder for placing transducer



Figure 155
Gauge located at the bottom of the Girder 2



Figure 156
Gauge located at the top flange of the Girder 2



Figure 157
Tabs on the Girder 2 after removing the transducer



Figure 158
Gauge located at the bottom of the Girder 2



Figure 159
Tabs on the Girder 2 after removing the transducer

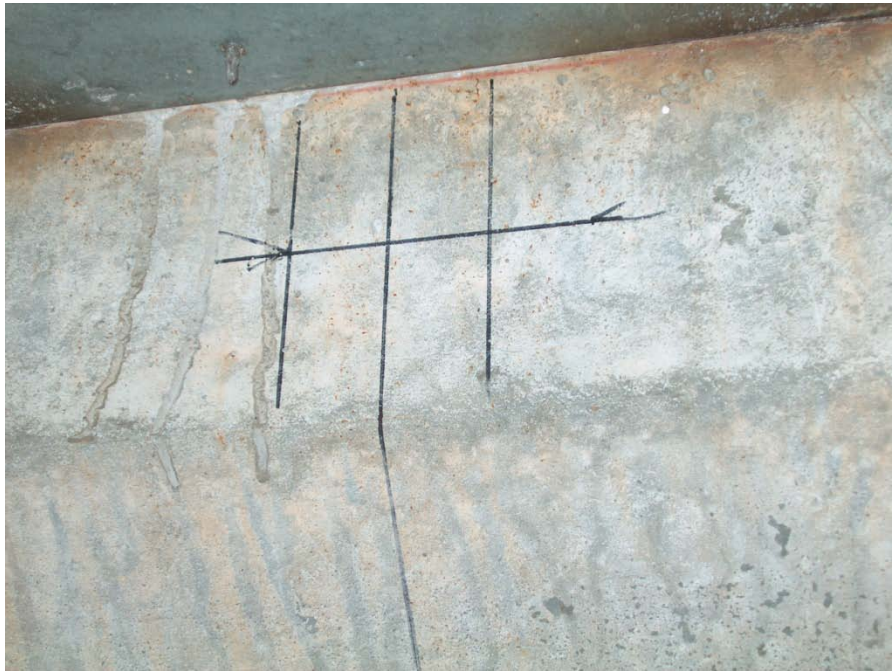


Figure 160
Initial marking on the girder for placing transducer



Figure 161
Tabs on the Girder 2 after removing the transducer



Figure 162
Gauge located at the top flange of the Girder 2



Figure 163
Gauge located at the bottom of the Girder 2



Figure 164
Tabs on the Girder 2 after removing the transducer

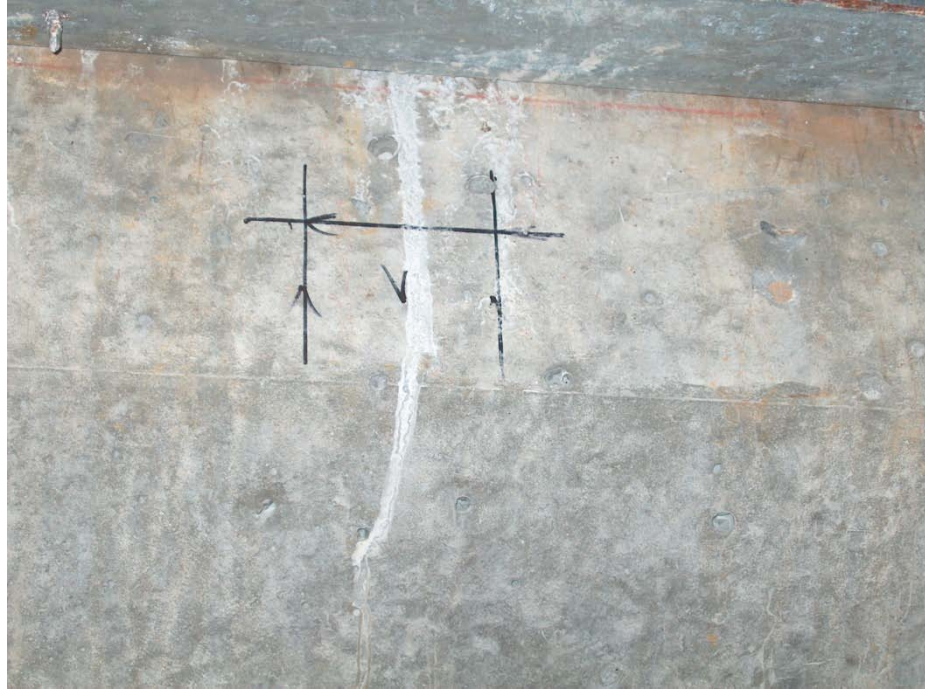


Figure 165
Initial marking on the girder for placing transducer



Figure 166
Gauge located at the top flange of the Girder 3



Figure 167
Tabs on the Girder 3 after removing the transducer



Figure 168
Initial marking on the girder for placing transducer



Figure 169
Gauge located at the bottom of the Girder 3



Figure 170
Tabs on the Girder 3 after removing the transducer



Figure 171
Initial marking on the girder for placing transducer



Figure 172
Gauge located at the top flange of the Girder 4



Figure 173
Tabs on the Girder 4 after removing the transducer



Figure 174
Initial marking on the girder for placing transducer



Figure 175
Gauge located at the bottom of the Girder 4



Figure 176
Tabs on the Girder 4 after removing the transducer



Figure 177
Initial marking on the girder for placing transducer



Figure 178
Gauge located at the top flange of the Girder 1



Figure 179
Tabs on the Girder 4 after removing the transducer



Figure 180
Initial marking on the girder for placing transducer



Figure 181
Gauge located at the bottom of the Girder 5

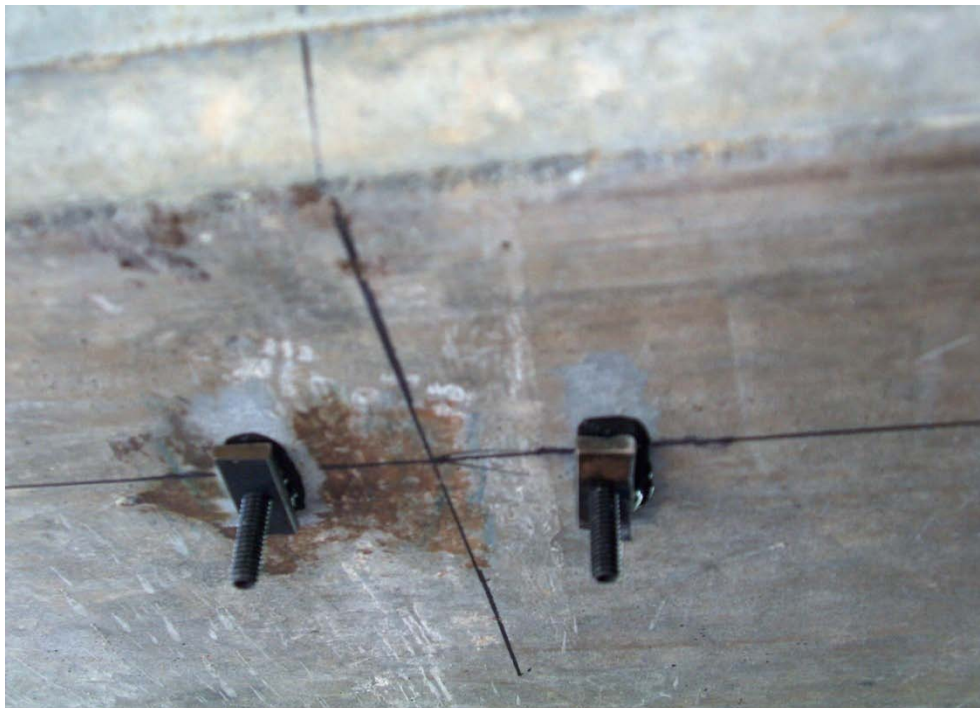


Figure 182
Tabs on the Girder 5 after removing the transducer



Figure 183
Gauge located at the top flange of the Girder 6



Figure 184
Tabs on the Girder 6 after removing the transducer



Figure 185
Gauge located at the bottom of the Girder 6



Figure 186
Tabs on the Girder 6 after removing the transducer



Figure 187
Initial marking on the continuity diaphragm for placing transducer



Figure 188
Gauge located on the continuity diaphragm of support Span 7-8



Figure 189
Initial marking on the continuity diaphragm for placing transducer



Figure 190
Gauge located on the continuity diaphragm of support Span 7-8



Figure 191
Gauge located on the continuity diaphragm of support Span 7-8

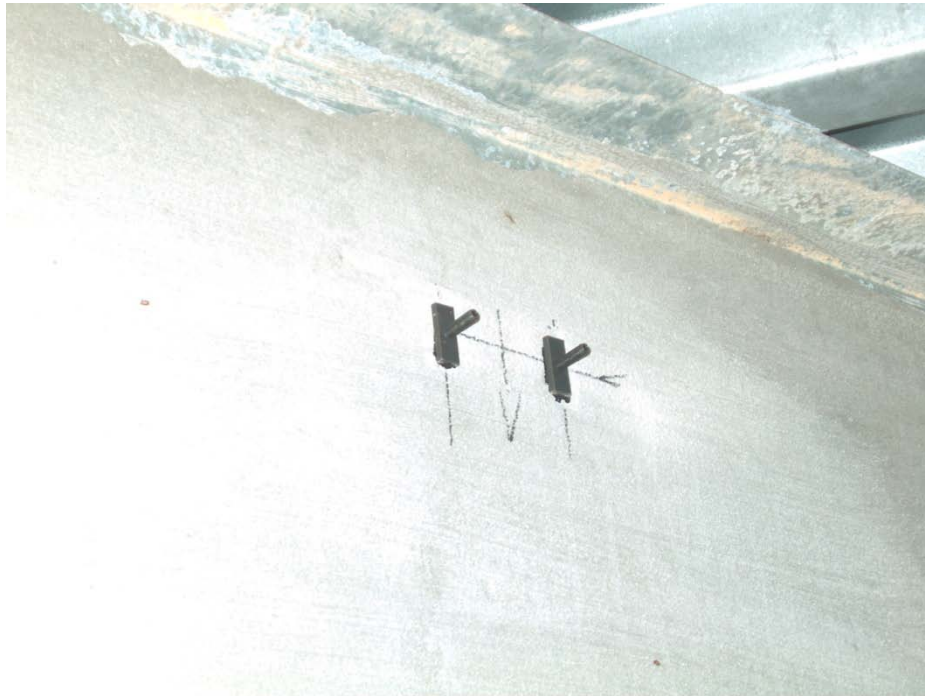


Figure 192
Tabs on the continuity diaphragm after removing the transducer



Figure 193
Gauge located on the continuity diaphragm of support Span 7-8



Figure 194
Tabs on the continuity diaphragm after removing the transducer



Figure 195
Initial marking on the continuity diaphragm for placing transducer



Figure 196
Gauge located on the continuity diaphragm of support Span 7-8



Figure 197
Gauge located on the continuity diaphragm of support Span 7-8



Figure 198
Gauge located on the continuity diaphragm of support Span 7-8